THE EFFECTS OF PHOTOPERIODISM ON MOLTING ACTIVITIES OF *PENAEUS MONODON* JUVENILES

WISA NAMWONG

A THESIS SUBMITTED IN PARTIAL FULFILLMENT
OF THE REQUIREMENTS FOR
THE DEGREE OF DOCTOR OF PHILOSOPHY (ANATOMY)
FACULTY OF GRADUATE STUDIES
MAHIDOL UNIVERSITY
2009

Thesis
entitled
**THE EFFECTS OF PHOTOPERIODISM ON MOLTING
ACTIVITIES OF *PENAEUS MONODON* JUVENILES**

....
Miss Wisa Namwong
Candidate

....
Prof. Boonsirm Withyachumnarnkul,
M.D., Ph.D.
Major-advisor

....
Prof. Timothy W. Flegel,
Ph.D.
Co-advisor

....
Assoc. Prof. Apinunt Udomkit,
Ph.D.
Co-advisor

....
Asst. Prof. Somluk Asuvapongpatana,
Ph.D.
Co-advisor

....
Miss Saengchan Senapin,
Ph.D.
Co-advisor

....
Asst. Prof. Auemphorn Mutchimwong,
Ph.D.
Acting Dean
Faculty of Graduate Studies
Mahidol University

....
Prof. Yindee Kitiyanant, D.V.M.,
M.Sc.
Program director
Doctor of Philosophy Programme in
Anatomy, Faculty of Science
Mahidol University

Thesis
entitled

THE EFFECTS OF PHOTOPERIODISM ON MOLTING
ACTIVITIES OF *PENAEUS MONODON* JUVENILES

was submitted to the Faculty of Graduate Studies, Mahidol University
for the degree of Doctor of Philosophy (Anatomy)
on
September 24, 2009

....
Wisa Namwong
Candidate

....
Prof. Timothy W. Flegel,
Ph.D.
Member

....
Prof. Paisarn Sithigorngul,
Ph.D.
Chair

....
Assoc. Prof. Apinunt Udomkit,
Ph.D.
Member

....
Asst. Prof. Somluk Asuvapongpatana,
Ph.D.
Member

....
Miss Saengchan Senapin,
Ph.D.
Member

....
Prof. Boonsirm Withyachumnarnkul,
M.D., Ph.D.
Member

....
Asst. Prof. Auemphorn Mutchimwong,
Ph.D.
Acting Dean
Faculty of Graduate Studies
Mahidol University

....
Prof. Skorn Mongkolsuk,
Ph.D.
Dean
Faculty of Science
Mahidol University

ACKNOWLEDGEMENTS

THE EFFECTS OF PHOTOPERIODISM ON MOLTING ACTIVITIES OF
PENAEUS MONODON JUVENILES

WISA NAMWONG   4637672   SCAN/D

Ph.D. (ANATOMY)

THESIS ADVISORY COMMITTEE : BOONSIRM WITHYACHUMNARNKUL,
M.D., Ph.D., TIMOTHY W. FLEGEL, Ph.D., APINUNT UDOMKIT, Ph.D.,
SOMLUK ASUVAPONGPATANA, Ph.D., SAENGCHAN SENAPIN, Ph.D.

ABSTRACT

         The purpose of this study is to elucidate if changes in normal light/dark
cycle or photoperiod affect the molt cycle and growth in juveniles *Penaeus monodon*,
and molt-related hormones. *P. monodon* were reared individually under normal
(12L:12D)-, long (18L:6D)- and short (6L:18D)-day, with light intensity at ~ 3000 lux.
Molt intervals, weight gain, survival rate, profiles of hemolymph ecdysteroids and
MIH-1 transcript in the optic lobe were determined. Anti-rMIH-1 polyclonal antibody
was raised in order to localize the MIH-1 immunoreactive cells in the optic lobe by
immunohistochemistry.
         Results showed no change in the molt intervals and durations of each molt
stage in the shrimp exposed to the three photoperiod regimes. There were no
differences in percentage of body weight gain or survival rate. The profiles of
hemolymph ecdysteroids were similar in all photoperiods: the basal levels were at
intermolt, gradually elevated during early premolt, and peaked significantly at the late
premolt, before rapidly declining to the basal level at the postmolt stage. In contrast,
the *MIH-1* transcript levels were markedly different among the three groups of
animals. In normal-day shrimp, the transcripts at postmolt gradually decreased from
the postmolt toward the late premolt stages. In the long-day shrimp, the transcript gene
was up-regulated at intermolt, whereas no differential levels among the molting stages
were observed in the short-day shrimp. The *MIH-1* transcripts at the late premolt stage
in the long- and short-day shrimp were up-regulated, compared to that of the normal-
day shrimp. The MIH-1 immunoreactivity was observed in the neurosecretory cells of
the medulla terminalis and in the sinus gland and other unidentified structures in the
eyestalk. In normal-day shrimp, MIH-1 staining intensity was variably high at
postmolt and low at late premolt, which corresponded to the pattern of MIH-1
transcript. The MIH-1 immunoreactivity in the neurosecretory cells of the long- and
short-day shrimp was variably low and high, respectively; high intensity was observed
in the late premolt stage of the short-day shrimp. In the sinus gland, MIH-1
immunoreactivity was similar in all molting stages, and in all groups of animals.

KEY WORDS: PHOTOPERIOD / *Pem-MIH-1* mRNA / ECDYSTEROIDS / MOLT
                      STAGE / ANTI-RECOMBINANT MIH-1 ANTIBODY / *PENAEUS
                      MONODON*

96 pages

ผลของช่วงความยาวของแสงสว่างในรอบวันต่อการลอกคราบของกุ้งกุลาดำวัยรุ่น

THE EFFECTS OF PHOTOPERIODISM ON MOLTING ACTIVITIES OF *PENAEUS MONODON* JUVENILES

วิสา นามวงค์   4637672   SCAN/D

ปร.ด. (กายวิภาคศาสตร์)

คณะกรรมการที่ปรึกษาวิทยานิพนธ์ : บุญเสริม วิทยชำนาญกุล, M.D., Ph.D., ทิมโมที วิลเลี่ยม เฟล-เกล, Ph.D., อภินันท์ อุดมกิจ, Ph.D., สมลักษณ์ อสุวพงษ์พัฒนา, Ph.D., แสงจันทร์ เสนาปิน, Ph.D.

บทคัดย่อ

การศึกษาในครั้งนี้มีวัตถุประสงค์เพื่อต้องการที่จะศึกษาผลของการเปลี่ยนแปลงช่วงความยาวของแสงสว่างในรอบวันที่มีต่อวงจรการลอกคราบ การเจริญเติบโตและฮอร์โมนที่เกี่ยวข้องในกุ้งกุลาดำวัยรุ่น กุ้งได้ถูกแยกเลี้ยงเดี่ยว ณ ช่วงความยาวของแสงสว่างในรอบวันในระยะต่างๆกัน แบ่งออกเป็น ระยะแสงสั้น (6L:18D) ระยะแสงปกติ (12L:12D) และระยะแสงยาว (18L:6D) โดยได้กระทำการวัดระยะวงจรการลอกคราบ ร้อยละการเพิ่มขึ้นของน้ำหนักตัว อัตราการรอดชีวิต รวมทั้งการวัดระดับฮอร์โมนที่เหนี่ยวนำการลอกคราบในเลือดและวัดระดับการแสดงออกของยีนที่ยับยั้งการลอกคราบจากเนื้อเยื่อประสาทก้านตา รวมทั้งการผลิตแอนตี้บอดี้ต่อโปรตีนของฮอร์โมนที่ยับยั้งการลอกคราบเพื่อที่จะดูว่าเซลล์หรือเนื้อเยื่อใดในก้านตาที่มีผลบวกต่อโปรตีนชนิดนี้บ้าง โดยใช้วิธีการย้อมดูเนื้อเยื่อด้วยอิมมูโนเทคนิค

ผลการทดลองจากการเปรียบเทียบข้อมูลโดยพิจารณาจากความแตกต่างกันอย่างมีนัยสำคัญทางสถิติ ระหว่างสามช่วงความยาวของแสงสว่างในรอบวัน พบว่าไม่มีความแตกต่างของระยะการลอกคราบในแต่ละวงจร อัตราการเพิ่มขึ้นของน้ำหนัก และอัตราการรอดชีวิต รวมทั้งระดับของฮอร์โมนที่เหนี่ยวนำการลอกคราบในเลือด แต่เมื่อเปรียบเทียบในแต่ละช่วงความยาวแสงสว่างในรอบวันพบว่ามีการหลั่งของฮอร์โมนสูงสุดที่ระยะสุดท้ายก่อนการลอกคราบสูงกว่าระยะอื่นๆอย่างมีนัยสำคัญทางสถิติ (P<0.001) ในทางตรงกันข้าม ระดับการแสดงออกของยีนที่ยับยั้งการลอกคราบพบว่ามีความแตกต่างกันอย่างมีนัยสำคัญทางสถิติ (P<0.05) ทั้งระหว่างวงจรการลอกคราบ และภายในวงจรการลอกคราบเดียวกัน ณ ช่วงความยาวของแสงสว่างในรอบวันระยะแสงปกติพบว่าการแสดงออกของยีนสูงสุดและต่ำสุดในระยะหลังและก่อนการลอกคราบ ตามลำดับและมีความแตกต่างกันอย่างมีนัยสำคัญทางสถิติ (P<0.05) ณ ช่วงความยาวของแสงสว่างในรอบวันระยะแสงยาวพบว่าการแสดงออกของยีนสูงสุดช่วงกลางของการลอกคราบ (intermolt stage) สูงกว่าระยะอื่นๆในวงจรลอกคราบอย่างมีนัยสำคัญทางสถิติ (P<0.05) นอกจากนี้ยังพบว่าการแสดงออกของยีน ณ ระยะสุดท้ายก่อนการลอกคราบ (late premolt stage) เพิ่มขึ้นอย่างมีนัยสำคัญทางสถิติในช่วงความยาวของแสงสว่างทั้งระยะแสงสั้นและระยะแสงยาว เปรียบเทียบกับระยะแสงปกติ (P<0.001) สำหรับผลการย้อมเนื้อเยื่อในก้านตาด้วยแอนติบอดี้ของฮอร์โมนที่ยับยั้งการลอกคราบพบว่ามีผลบวกที่ต่อมไซนัส (sinus gland) ต่อมเอ็กซออร์แกน (X-organ) ต่อมบางชนิดที่ยังจำแนกไม่ได้และเซลล์ขนาดเล็ก ผลบวกในต่อมเอ็กซออร์แกน ณ ช่วงความยาวของแสงสว่างในรอบวันระยะแสงปกติพบว่ามีความเข้มข้นไปในทิศทางเดียวกับปริมาณการการแสดงออกของยีน กล่าวคือเข้มข้นมากในระยะหลังการลอกคราบและเจือจางลง ณ ระยะสุดท้ายก่อนการลอกคราบ ผลบวก ณ ช่วงความยาวของแสงสว่างในรอบวันระยะแสงสั้นและแสงยาว มีความเข้มข้นมากและน้อยลงตามลำดับ สำหรับผลบวกในต่อมไซนัสพบว่ามีความเข้มข้นสูงและไม่แตกต่างกันมากนักในกุ้งแต่ละตัว

96 หน้า

CONTENTS

CONTENTS (cont.)

LIST OF TABLES

LIST OF FIGURES

LIST OF FIGURES (cont.)

LIST OF ABBREVIATIONS

20E	=	20-hydroxyecdysone
AEC	=	Aminoethyl carbazole , an alcohol soluble chromogen
D	=	Day
DNA	=	Deoxyribonucleic acid
D	=	Hour of darkness, or scotophase
L	=	Hour of light, or photophase
EF-1α	=	Elongation factor
H	=	Hour
kDa	=	Kilodalton
MIH	=	molt-inhibiting hormone
MTXO	=	Medulla terminalis X-organ
mRNA	=	Messenger ribonucleic acid
mL	=	Mililiter
ng	=	Nanogram
nt	=	Nucleotide
PAGE	=	Polyacrylamide gel electrophoresis
PCR	=	Polymerase chain reaction
qRT PCR	=	Quantitative real-time polymerase chain reaction
pg	=	Picogram
rMIH	=	Recombinant molt-inhibiting hormone
RIA	=	Radioimmunoassay
RT–PCR	=	Reverse transcriptase polymerase chain reaction
SDS	=	Sodium dodecyl sulfate
SG	=	Sinus gland
μg	=	Microgram
μL	=	Microliter
μm	=	Micrometer

LIST OF ABBREVIATIONS (CONT.)

TG	=	Tegumental gland
TBS	=	Tris-buffer saline
TBST	=	Tris-buffer saline in Tween-20
YO	=	Y-organ

CHAPTER I

INTRODUCTION

Shrimp Culture in Thailand

Because of its largest size and fastest growth rate, the black tiger shrimp *Penaeus monodon* is the major species cultured in the shrimp culture industry constituting more than 50% in 1999, followed by several others (Rönnbäck, 2001). Since 1990, Thailand was leader of shrimp production, export and processing. Shrimp industry gave income value of more 2 billion baht and export value of 75,000-85,000 million baht/year (http://www.aseanshrimpalliance.net/news01.html). In last year, shrimp from Thailand was exported to Japan in the third ranging, lower than only Indonesia and Vietnam, about 10,412 metric tons (http://www.shrimpnews.com/FreeNewsBackIssues/FreeNewsOctober200803.html). According to information released by the National Marine Fisheries Service, USA, shrimp imports from Thailand, by far the number one supplier to the USA, reached 182.4 million kilograms in 2008, down 3.2 percent from the previous year (http://www.shrimpnews.com/FreeNews.html). During 1995-2000, farmed shrimp producers in Thailand were mainly small-scale farmers, and wild broodstocks were used to produce postlarvae (PL). The pattern of production in 2004 has been changed. Because of trade regulations, such as the prohibition of the use of chemicals, especially antibiotics, and the requirement of ability to trace the source of the shrimp (its production process, source, etc), shrimp culture industry has become more integrated. The integration includes activities from upstream to downstream production, i.e. the production of broodstock, PL, harvest-sized shrimp, shrimp feed, processing plant and quality control lab. The integration therefore requires operations of medium- to large-sized company; the process causes a fading away of the small-scale shrimp farming in Thailand.

Nowadays organic shrimp have been produced by the private company in Chanthaburi, Thailand and exported into Europe (http://www.thaishrimp.info/index.php?topic=General), and to meet the growing demand for food safety, the private company have been developed the biosecure shrimp farming system in Trat province (http://www.thaishrimp.info/article.php/CPF_set_to_expand_biosecure_shrimp_farm). The knowledge of rearing environments are accordingly important, in order to avoid contaminants and safe costs, becomes a great benefit for the industrial cultivation.

Domestication and Selective Breeding Program of *P. monodon* in Thailand

The technology for controlling shrimp reproduction is under constant refinement by commercial and academics. Disease-resistant, hatchery-reared PLs are becoming more popular for pond stocking. Comparisons of grow-out results among ponds stocking with PLs from different sources have been made; and it is documented that domestication and the high health genetically improved animals concept (with added bio-security measures practiced) have benefits over wild-caught stocks. The USDA funded US Marine Shrimp Farming Program, the Oceanic Institute (OI), and a number of other organizations, have made progress in domesticating and selecting faster-growing, disease-resistant families of shrimp and have brought them forth in their breeding programs (Treece, 2000).

Domestication of *P. monodon* in Thailand was started 1996, with founding populations from wild broodstocks caught from Andaman Sea. Starting from F0 generation, which was the offspring of the wild broodstocks being reared for one year to sexually mature adults, the present (2004) F7 generation has been commercialized. The breeding program is aimed at producing broodstocks being free of white-spot syndrome virus (WSSV), yellowhead virus (YHV), Taura syndrome virus (TSV), infectious hypodermal and hematopoietic necrosis virus (IHHNV), monodon baculovirus (MBV), hepatopancreatic parvovirus (HPV), gill-associate virus (GAV), and monodon slow-growth virus (MSGV). Most of the viruses mentioned have been eliminated from the stock to make them specific pathogen-free (SPF). The genetic traits being selected for are fast growing, disease resistance and high fecundity. With a

stocking density of 25-30 pieces per square meter in earthen ponds, and under standard pond management, the growth rate of domesticated *P. monodon* has been at least at 0.2 g per day at four month of culture. To avoid inbreeding, as well as to expand their genetic bases, some domesticated shrimp have been mated with wild broodstocks caught from various places. Domesticated shrimp from different families are identified by a DNA based microsatellite marking, as well as by physical tagging. Families of different genetics are shown to have different growth rate, and selection on growth is based not only on family but also on individuals (Withyachumnarnkul, personal communication). To avoid inbreeding, selection of mating pairs is employed in the breeding program; and this is accomplished through artificial insemination (AI). With AI, one could improve quality and select traits of the PLs, such as those that are tolerant to a low salinity environment, those that exhibit rapid growth, and those that are resistant to diseases (Arce et al, 2001). In *P. vannamei*, the AI technique is carried out by removal of both spermatophores (right and left sides) from a single male and placing them over the thelycum of a sexually mature female. In *P. monodon*, the AI could be accomplished by a similar manner. But *P. monodon* is a closed thelycum species, the male spermatophores are thus placed into the sperm receptacle of the thelycum; and it requires at least three days for the sperm to be capacitated by the female thelycal fluid (Vanichviriyakit et al., 2004).

In order to perform AI in *P. monodon*, the female's molting stage has to be in post-molt, since the thelycum would be soft and insertion of spermatophores is made possible. In the selective breeding program, it is desirable to perform AI as many times as possible, with spermatophores from different males; the reason is to increase genetic base of the offspring within a short period of time. Therefore, induction of molting in the female broodstock could help facilitate the breeding program.

This experiment in *P. monodon* proposes to induce molting in juveniles as the preliminary study, since it costs less expense than handling in the broodstock. Accordingly the molt interval in juvenile is shorter than adult, so it anticipates that if photoperiods induce molting in juvenile then it could be more successful in adult shrimp. The response of shrimp could be the developmental stages-specific, however these need further clarification.

Photoperiod Effects Molt and Growth in Crustaceans

In previous reports, photoperiods affected the molt cycle of crustaceans in different manners. The induction of molting by modification of daily photoperiod was earlier taken in juvenile crayfish *Cambarus* (*Orconectes*) *virilis* (Stephen, 1955), animals were kept in continuous darkness, ambient photoperiod (10-13 h of light), and 20:4 (L-D). The increase daily illumination tended to stimulate the molt and also led to the high mortality. The long-day photoperiod, 15:9 (L-D) increased the molting rate in adult crayfish *Orconectes nais* (Armitage et al., 1973), and crab *Hemigraphsus nudus* (Kurup, 1970) than the shorter light regimes. The long-day photoperiods also influenced the molting frequency in larvae of crab *Pseudocarcinus gigae*, the development from zoeal phases to megalopa was more rapidly with the longer hours of light exposure, and the molt intervals were correspondingly decrease from long to short as follows: 0>6>12>18>24 (h of light) (Garner and Maguire, 1998). Similarly in the juvenile freshwater prawn *Palaemonetes argentinus* reared under three different light/dark conditions: 0:24, 10:14 and 13:11 (L-D), molting rate and mortality was significantly highest in a long-day photoperiod. However there were no significant differences in the percentage increment in mean weight in this specie (Díaz et al., 2003).

On the contrary, short day at 8:16 (L-D) instead of long-day, 16:8 (L-D) photoperiods induced molt in sub-adult lobster *Panuilrus argus* (Quackenbush and Herrnkind, 1983). Whereas in juvenile prawn *Fenneropenaeus chinensis* exposed to four light/dark cycles; 0:24, 24:0, 10:14 and 14:10 (L-D), the molt frequency was significantly higher in the latter two groups than the continuous light or darkness. However the growth rate was not different in any photoperiod (Wang et al., 2004a). Beside the molt frequency, growth and survival are considered the essential factors. Since crustaceans do molt in order to grow; in the mass production increase molt frequency without growth may not benefit. The constant darkness promoted molt and limb growth in crab *Gecarcinus lateralis* (Bliss, 1964), whereas this regime stimulated the body growth and survival in juvenile freshwater prawn *Macrobrachium rosenbergii* (Withyachumnarnkul et al., 1990). However absence of light led to the

highest mortality rate in juvenile crayfish *Procambarus clarkii* (Castañon-Cervantes et al., 1995). Photoperiod sometime promoted the growth without influenced the molt frequency. As had been found in juvenile prawn *Penaues merguiensis*, imposing two light/dark cycles at 7:5 (L-D) in 24 h resulted in a significantly higher of the percentage of mean body weight gain than the normal photoperiod at 12:12 (L-D) ($P<0.05$) (Hoang et al., 2003).

In *P. monodon*, only two light regimes at 0:24 and 24:0 (L-D) with the light intensity at 500-800 lux at water surface had been examined on post-larvae. Shrimp significantly survived at higher rates in the light condition than the darkness; in contrast, body weight gains in individual shrimp were slightly higher in the darkness than the light (Pan et al., 2001). From the previous experiment, it implies that photoperiod may influence the molt and growth in this penaeid shrimp. Therefore this study proposes to examine whether variation of photoperiods can induce molt and growth in juvenile *P. monodon* under the laboratory conditions. The outcomes of the studies may be beneficial for applying in the massive culture in the pond, if any photoperiod promotes molt and growth.

CHAPTER II
OBJECTIVES

The general objective of this study is to induce molting in juveniles *P. monodon* by subject to various photoperiods. To achieve the goal, certain knowledge must be known. Therefore the following specific objectives are set forth.

1. To examine the affects of different photoperiods; short (6L:18D), normal (12L:12D), and long (18L:6D) daylengths, how they influence the molting in *P. monodon* juveniles, in the aspects of the molt intervals, the growth rate (mean percentage of body weight gain), and the survival rate

2. To determine the *Pem-MIH-1* mRNA expression profiles during the molt cycle according to the molting stages and the photoperiods

3. To determine the profiles of hemolymph ecdysteroids during the molt cycle according to the molting stages and the photoperiods

4. To produce the anti-recombinant MIH-1 polyclonal antibody

5. To localize the distribution of MIH-1 in the eyestalk by Immunohistochemical detection during the molt cycles according to the molting stages and the photoperiods

6. To localize the distribution of MIH-1 receptor in the Y-organ during the molt cycles by Immunohistochemical detection

CHAPTER III
LITERATURE REVIEW

The soft body of crustaceans is protected by exoskeleton. In order to grow, the exoskeleton have to be shed off, followed by DNA and protein synthesis in the muscle and other tissues, with accumulation of fat, carbohydrate and other materials, followed by water absorption; all these result in the expansion of the body. The process of exoskeleton or exuviae shedding is called "molting", which is controlled by several factors. Molting is composed of four main stages; postmolt, intermolt, premolt and ecdysis (Guyselman, 1953), and each stage can be divided into sub-stages.

3.1 The Integument and Molt Cycle

The integumentary system of crustaceans (Fig. 3-1) is composed of the exoskeleton, epidermis and subepidermis (Skinner, 1962). The exoskeleton is composed of, from the most outward layer, the epicuticle, exocuticle, endocuticle and a membranous layer (Fig. 3-1a). The epidermis is single-layered epithelium, pseudostratified cuboidal or squamous type, underneath the cuticle. In the case of branchial lamellae, underneath of the epithelium is the collagen basal lamina that separates the epidermis from the subepidermis. The subepidermis contains several types of cells (e.g., chromatophores, trichrogenic cells, reserve cells, etc.) and tegumental glands. As its name implies, the reserve cell accumulates lipid, polysaccharide, calcium and sterol in its cytoplasm, and may provide nutrients under conditions when food is scarce.

Growth of crustacean requires molting process. Basically, the molting process is a shedding out of the old exoskeleton, from the membranous layer outward, and replaced by a new exoskeleton. Coupling with the molting process is the production of DNA and proteins by the shrimp body, especially the muscle, and water absorption into the body, causing a rapid expansion and thus growth. Molting has at least two purposes, one is for growth and another is for reproduction. Several crustacean

species, including penaeid shrimp, the females need to molt before mating. Therefore crustaceans have to molt periodically, either to grow or to reproduce.

a
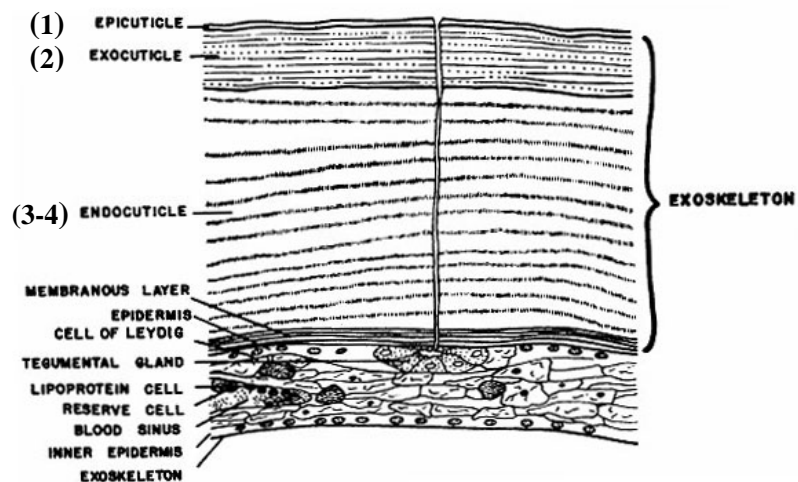
b
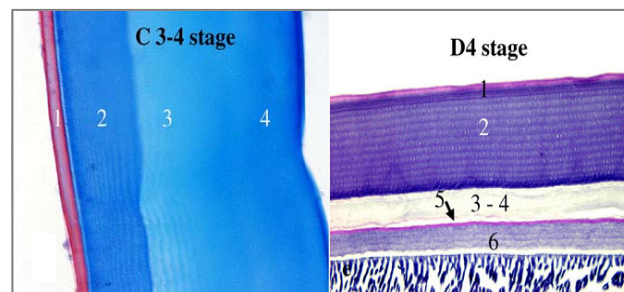
Figure 3-1   Histology of the integumentary system in crustacean. **a**. Schematic diagram showing of the integumentary system of crustacean at intermolt stage (Skinner, 1962) **b**. Histology of the cuticle in *P. monodon* staining with Masson's trichrome at intermolt (left panel) or PAS and hematoxylin at late premolt (right panel) (Promwikorn et al., 2007)

Numbers inside parenthesis of **a** are corresponding to those in **b**, new cuticle, the epicuticle (5), and exocuticle (6) completely forming during the late premolt.

The degree of growth increment depends on species and sex of the crustaceans. In American lobster *Homarus americanus*, the male is larger than the female (Comeau and Savoie, 2001), but the contrary is true for the black tiger shrimp *P. monodon*; whether the difference in growth rate is due to the difference in molting frequency or the degree of growth increment following molting has not been advocated. In general, at younger age, crustaceans molt frequently, with higher growth increment and the molting frequency is less when they grow older (Lytle, 2001; Chockley and Mary, 2003). The periods between each molt, called "molt intervals", are variable among crustacean species; for instances, it is 9-15 days in *P. monodon* juveniles (~15 g body weight) (Promwikorn et al., 2007), 120 days in the crab *Cancer magister* (Miller, 2004), and one month in *Penaeus vannamei* juveniles (Chan et al, 1988).

The molt cycle is roughly classified into postmolt (further sub-divided into stage A and B), intermolt (or stage C), premolt (further sub-divided into stages D_{0-4}), and ecdysis (or stage E) (Buchholz, 1982; Chan et al, 1988). In practice, the determination of molt stages is based on morphological changes observed under light microscope, which includes, not only the separation of the old and new exoskeleton, but also the formation of setae or hairs of the integument (Kuo and Lin, 1996; Promwikorn et al, 2007).

During molting, the animal pulls itself out of the exuviae, usually the cephalothorax first, then the abdomen (Chan et al, 1988). Immediately after molting, the shrimp body is usually soft and vulnerable to injury, especially being victim of cannibalism, and it takes a few hours to days for the new exoskeleton to become harden; it took 1-2 days for *P. vannamei*, (Buchholz, 1982; Chan et al., 1988) and *P. monodon* (Promwikorn et al., 2007).

The molting process begins after molting or ecdysis stage; this stage is termed postmolt. During this stage, the endocuticle, which is the principal layer of the cuticle, begins to develop, in association with chitin and protein synthesis from the epidermis (Stevenson, 1972). DNA contents, several genes and the enzymes Ca^{2+}-ATPase, HCO_3^{-}-ATPase and Na^{+}/K^{+}-ATPase in the epidermal cells are up-regulated (Mangum et al., 1985; Cameron, 1989; Kubella and Elizur, 2007). The enzyme Ca^{2+}-ATPase is involved in calcification of the cuticle, and HCO_3^{-}-ATPase is for water

uptake. Calcification of the new endocuticle began on the second day following molt. By the end of postmolt, it was completely calcified (Travis, 1957). Because of the requirement of calcium to harden the exoskeleton, calcium uptake into the body is highest at this stage, and it could be from water or food intake (Greenaway, 1983; Neufeld and Cameron, 1993; Ziegler et al., 2007). For animals living in seawater, calcium uptake from seawater is not a problem since seawater contains high level of calcium. In freshwater crustaceans, calcium uptake from the environment is limited; therefore calcium is reabsorbed from the old exoskeleton before molting and stored as gastrolith, a calcification inside the stomach. It is during postmolt that calcium is brought back to the cuticle by degradation of gastrolith (Skinner, 1962; Willig and Keller, 1973). In freshwater crabs, *Gecarcinus lateralis* and *Orconectes limosus,* gastrolith formation began during early premolt and reached its largest size during late premolt (Skinner, 1962; Willig and Keller, 1973).

Besides increasing calcium uptake, water uptake is also increased and the uptake until after molting. In *H. americanus,* the highest rate of water uptake occurred in the midgut at one hour before ecdysis and was completed within two hours (Mykles, 1980). In *P. argus*, the water content was increased around the time of ecdysis before decreasing during late postmolt (Travis, 1954). In *Callinectes sapidus*, water uptake occurred primarily in the gills, and during premolt; the activities of HCO_3^--ATPase and Na^+/K^+-ATPase were increased dramatically, preceded the water uptake (Mangum, 1985). The increases in synthesis of DNA, protein and other substances in the body, especially in the muscle, in couple with water uptake, cause an expansion of the body.

During intermolt, the endocuticle reaches "mature" stage, with continuous increasing levels of DNA and protein synthesis from the epidermis (Stevenson, 1972; Wittig and Stevenson, 1975), as well as from the muscle, which signifies somatic growth (El Haj and Houlihan**,** 1987; De Oliveira Cesar et al., 2006). The activities of enzymes HCO_3^--ATPase, Ca^{2+}-ATPase and carbonic anhydrase in the epidermis are lowest at this stage (Mangum, 1985; Cameron, 1989).

Beginning at early premolt, the old exoskeleton is reabsorbed (Skinner, 1962; Willig and Keller, 1973). The membranous layer is digested and detached from the epidermis. The formation of new cuticle begins at early premolt (Skinner, 1962;

Willig and Keller, 1973) and is completed at late premolt (Charmantier-Daures and Vernet, 2004; Promwikorn et al., 2007), accompanied by an increase chitin synthesis (Stevenson, 1972).

In the epidermis, DNA and protein contents, as well as their synthesis, are declined to a basal level during early premolt, peaked at mid-premolt before dropping rapidly during late premolt (Stevenson, 1972; Wittig and Stevenson, 1975).

To prepare for molting, glycogen was accumulated in the cells of Leydig and lipoprotein cells in *G. lateralis* (Skinner, 1962). Total RNA in the muscles of *Carcinus maenas* and *P. vannamei* were abundant (Whiteley et al., 1992; De Oliveira Cesar et al., 2006). Rate of protein synthesis in leg muscle of *C. maenas* (El Haj and Houlihan, 1987) was lowest during early premolt, before peaked during late premolt; this peak was similar to the finding in *H. americanus* (El Haj et al., 1996).

The molt cycle, including periods of each molting stages, is believed to be modulated by both internal and external factors. The internal factors include several hormones, of which molt-inhibiting hormone (MIH) and ecdysteroids have been mostly referred to, and the external factors include photoperiods, water qualities, and others. As name implies, MIH acts as a suppressor to the molting process. It is synthesized and released from a group of neurosecretory cells in the eyestalk optic lobe called X organ. These cells send their long axons toward a neurohemal organ, which is a collection of their axon terminals called the sinus gland, which is located on the ventrolateral side of the eyestalk between medulla externa (ME) and medulla interna (MI) of the optic lobe (see below) (Bell and Lightner, 1988).

Together, the X-organ and sinus gland is conventionally termed X-organ-sinus gland complex (XOSG). MIH is believed to suppress the synthesis and release of ecdysteroids, the molting hormone, from the Y-organs (YOs), which is located in the cephalothorax closed to the gill chamber (Mattson and Spaziani, 1986).

3.2 The X-organ-Sinus Gland System (XOSG)

Several neurosecretory cells are located in the MT and MI of the eyestalk optic lobe, which also includes medulla externa (ME) and lamina ganglionaris (LG) (Fig. 3-2). The XOSG is known as the principal source of neurohormones controlling of the molting, reproduction and metabolism. The neurosecretory cells in the X-organ

and brain of crayfish *O. virilis* have been classified into four types (Fig. 3-3), according to their size and shape (Durand, 1956). Secretory granules of certain cell types and within the axon terminals in the SG are variable in the amount according to molt cycle; it is thus assumed that some of these cell types are MIH-producing cells (Pyle, 1943; Durand, 1956).
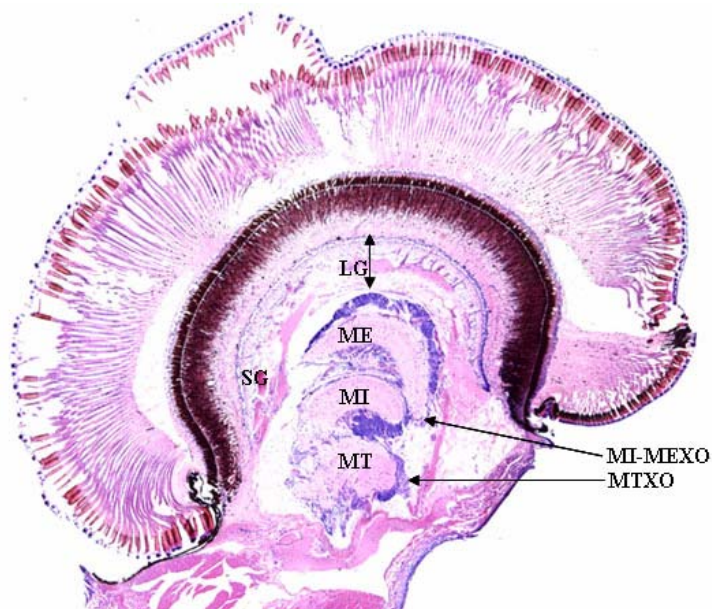
Figure 3-2   Light micrograph showing of the compound eye in *Penaeus monodon* stained with hematoxylin and eosin (based on Bell and Lightner, 1988)

Abbreviations: LG, lamina ganglionaris; ME, medulla externa; MI, medulla interna; MT, medulla terminalis; MI-MEXO, medulla interna-externa X organ ; MTXO, medulla terminalis X organ ; SG, sinus gland
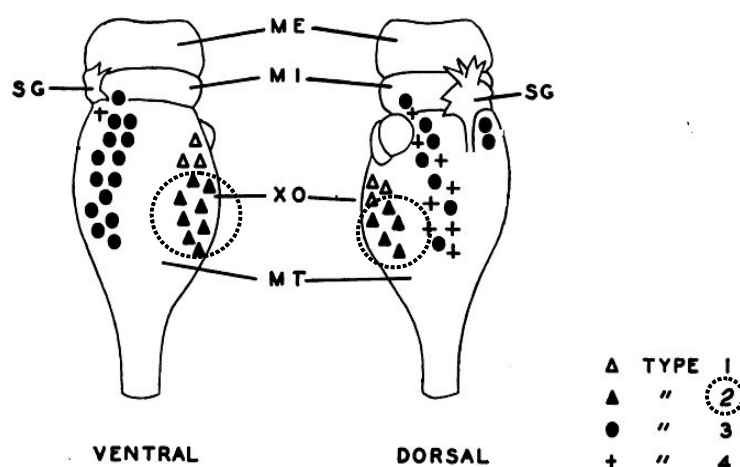
Figure 3-3   Schematic diagram shows the distribution of neurosecretory cells of the eyestalk of crayfish *Orconectes virilis,* only type 2 cells (in circles) which restricted in the medulla terminalis X organ are correlation with the molt cycle (modified from Durand, 1956).

Abbreviations: ME, medulla externa; MI, medullar interna; XO, X-organ; MT, medulla terminalis; SG, sinus gland

Each type of neurosecretory cells may contain one or more types of neurohormones (Dircksen and Webster, 1988). In lobsters, *Jasus lalandii* and *Panulirus homarus*, and crab *C. maenas*, certain neurosecretory cells and their axon terminals in the SG contain MIH, crustacean hyperglycemic hormone (CHH) and gonad-inhibitory hormone (GIH) (Macro and Gäde, 1999). In the Kuruma shrimp, *Penaeus japonicus*, co-localization of CHH and MIH was observed in a neurosecretory cell in the optic lobe (Shih et al., 1998). Since the neurohormones were detected by immunohistochemistry, there was a possibility that the antibody might have cross-reacted with more than one hormone. In *P. monodon*, amino acid sequences of *Pem-MIH1* and *Pem-MIH2* were 60% identity (Yodmuang et al., 2004) and of *Pem-MIH1* and *Pem-GIH* were 65% identity (Treerattrakool et al., 2008). In *C. maenas*, MIH and CHH amino acid sequences had only 28% homology. In *H. americanus,*

CHH and GIH had 28% homology. Surprisingly, *C. maenas* MIH and *H. americanus* GIH had amino acid sequences that shared 48% homology (Keller, 1992). These data suggested that the amino acid sequences of MIH, CHH and GIH are not very closed and thus cross-reactivity to other hormones by a specific antibody to a particular hormone may not be high, if any. In brachyuran crustaceans, it was reported that the numbers of CHH-immunoreactive cells were twice that of the MIH cells (Dircksen et al, 1988).

Besides receiving axon terminals from MI and MT, SG also received terminals from the brain and probably thoracic ganglia. If SG is the site of MIH release into the circulation, then removal of SG should induce molting; however, experimental remove of SG in the land crab, *G. lateralis*, does not induce molt (Bliss et al, 1954). It is thus possible that MIH, and other neurohormones, could be released at other sites, besides SG, or MIH may not directly suppress ecdysteroid synthesis in YO.

3.3 Y-organs

Y-organs (YOs) are paired slender tissue of ectodermal derivatives lying just beneath the epidermis, in the junction of prebranchial and the branchial chambers. The organs extend antero-horizontally from the posterior end of the prebranchial chamber, just beneath the inner wall of branchiostegite. The posterior part is located between the lateral end of the posterior dorso-ventral muscle where it is attached to the cuticle and the anterior dorsal roof of the branchial chamber forming a slender crescent (Bell and Lightner, 1988). The organs synthesize and release molting hormone or ecdysteroids and thus have histological changes regarding the sizes of cytoplasm, nuclei, and inter-lobular spaces, during the molt cycle. At intermolt, the cytoplasm was scant with intensely stained nucleus, suggesting low activity. During early premolt, the cell size was increased and reached maximum, twice as much as that of intermolt. The amount of cytoplasm was dropped again during postmolt (Aoto et al., 1974; Birkenbeil and Gersch, 1979).

Cells of YOs contain organelles that are similar to steroid-secreting cells in mammals, which have abundant smooth endoplasmic reticulum (SER) and a great number of mitochondria (Buchholz and Adelung, 1980). The mitochondria changed in

shape according to molt cycle; they were small and had rod-shape in late premolt and postmolt and became round and large in intermolt and early premolt. The SER had tubular form during mid to late premolt and postmolt, but became vesiculated during intermolt and early premolt (Aoto et al., 1974). The significance of these findings awaits further studies.

3.4 Molt-inhibiting hormone (MIH)

The belief that MIH inhibit YO synthesis of ecdysteroids came from an *in vitro* study by Mattson and Spaziani (1986). The optic lobe extract of the crab *Cancer antennarius* was incubated with YO culture and the levels of ecdysteroid releasing *in vitro* were measured by radioimmunoassay technique. The eyestalk extract inhibited the ecdysteroidogenesis in dose-dependent manner, and the effect was reversible. It is thus possible that the optic lobe contains MIH, but whether as a single entity or as a group of compounds is not known. The mechanism of action of MIH on ecdysteroid synthesis was also tested in the crayfish, *O. limosus* by incubating the crayfish YOs with SG extract, and significant inhibition of protein synthesis was found within 3 hours (Dauphin-Villemant et al., 1995). This suggests that the extract from SG, presumably MIH, could suppress ecdysteroid synthesis by at least one mechanism, i.e., inhibition of protein synthesis in the YO.

MIH as a peptide has been discovered in several crustacean species. Its amino acid sequence is very close among species. The amino acid sequence of *P. monodon* MIH-1 (*Pem-MIH-1*) showed 95% identical to MIH of *Marsupenaeus japonicus* (Maj-MIH; GenBank acc. no. P55847). The tertiary structure of Pem-MIH-1 and Maj-MIH (Katayama et al., 2003) was also similar, being comprised of five α-helices and the N- and C-termini (Fig. 3.4). Maj-MIH was similar to Maj-CHH, the latter peptide lacked α1 helix and it was therefore presumed that the region containing α1 and the C terminus was important for molt-inhibiting activity (Katayama et al., 2003). These regions were conserved among penaeid MIHs (Chen et al., 2007).
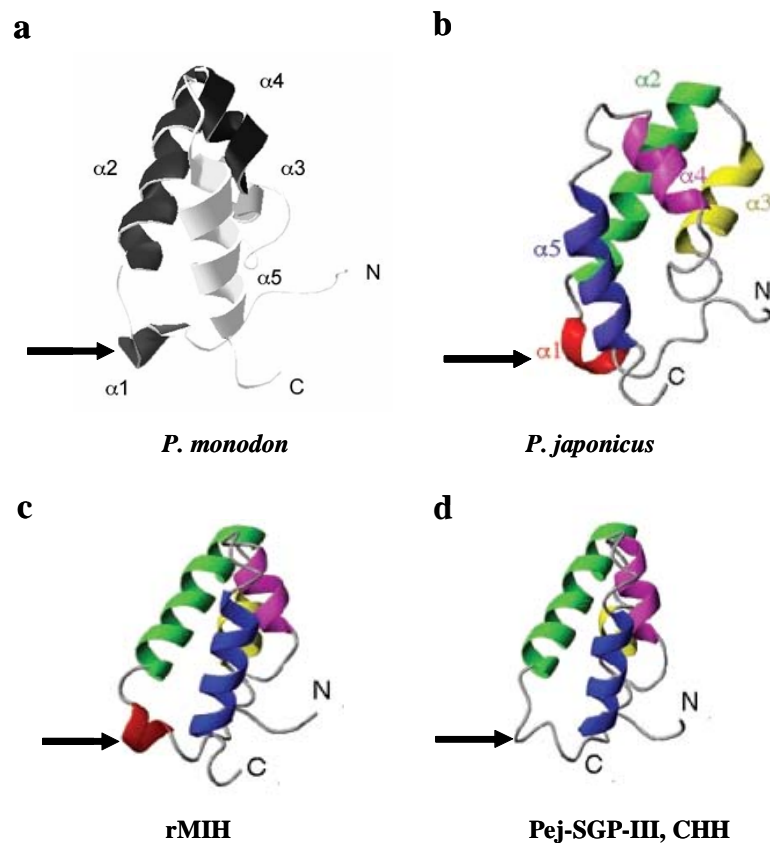
Figure 3-4   Tertiary structure of MIH and CHH peptides derived from *Penaeus monodon* (modified from Yodmuang et al., 2004) and *Penaeus japonicus* (Chen et al., 2007). The amino acids in the α1-helix region (arrowheads, **a**, **b**, and **c**) were conserved among the MIH from penaeids. While in CHH peptide, it absented (**d**).

A recombinant MIH from *P. monodon* produced by *E. coli* suggests a molecular weight of 6 kDa (Treerattrakool, 2008), but if the peptide could not be detected from the optic lobe of *P. monodon* by Western blot analysis, probably being due to low concentration of the extracted protein.

Since MIH is believed to suppress the synthesis and/or release of ecdysteroids from YO, it is logically assumed that MIH levels should be high during

postmolt and intermolt, to suppress ecdysteroid levels, and becomes low during premolt, to allow the surge of ecdysteroids. With the advance of methods to identify MIH in crustacean circulation throughout the molt cycle, the traditional concept has now been challenged. By using time-resolved fluoroimmunoassay to determine the levels of MIH in the hemolymph during the molt cycle of the crayfish *Procambarus clarkii*, it was found that MIH was at its basal level at early premolt, increased at middle premolt stages, and maintained at high levels from late premolt through intermolt stages (Nakatsuji and Sonobe, 2004). The findings in SGs, levels were high from early premolt to middle premolt and dropped at late premolt, before slightly increased at postmolt to intermolt stages (Nakatsuji et al., 2000). Similarly in the crab *C. maenas*, the basal MIH level in the hemolymph was observed at intermolt, gradually increased during early and mid premolt, with significantly peaked at late premolt (D_{3-4}), and dropped just 1 day prior to ecdysis, whereas the levels in SGs were maintained rather high throughout the molt cycle, except rapidly emptied at late premolt (Chung and Webster, 2005). Interestingly, the common findings dictate that the storing of MIH in SGs is low prior to molt, whereas the circulating hormone is rather high. As MIH was increase, instead of decrease, at the mid to late premolts, it suggests that YO became unresponsive to MIH during premolt.

At gene level, the findings on *MIH* genes in the optic lobe are rather inconclusive. The cDNA encoding MIH gene in *P. monodon* was classified into two types, MIH-1 and MIH-2 (GenBank acc. nos.<u>AY496454</u> and <u>AY496455</u>), being composed of 1,146 and 1,079 bp, respectively (Yodmuang et al., 2004). The two transcripts shared 60% identity in their nucleotide sequences (ClustalW2 analysis). However, only Pem-MIH-1 peptide showed molt-inhibiting activity. The nucleotide sequences of *Pem-MIH-1* were closed to the MIH from *L. vannamei* (*Liv-MIH-1*) (Chen et al., 2007) (Fig. 3-5). However, the tissue expression of both genes was slightly different, *Liv-MIH-1* was found in only in the eyestalk but *Pem-MIH-1* was found in both eyestalk and thoracic ganglia (Yodmuang et al, 2004). Both *Liv-MIH-1* and *Liv-MIH-2* were up-regulated during intermolt to early premolt and down-regulated during late premolt. The hemolymph ecdysteroid levels were inversely correlated to the MIH transcripts; peaked elevation was reached during late premolt and declined to the basal at late postmolt (Chen et al., 2007).

By using semi-quantitative, Northern blot analysis to determine *MIH* mRNA in the eyestalk of crab *Callinectes sapidus*, the peak was observed at postmolt and then gradually dropped during intermolt to the basal level at late premolt stages, by 10-fold, before ecdysis (Lee et al, 1998). This result seemed to be conformed to the traditional concept. On the other hand, in *C. maenas*, *MIH* mRNA expression remained the same throughout the molt cycle (Chung and Webster, 2005).
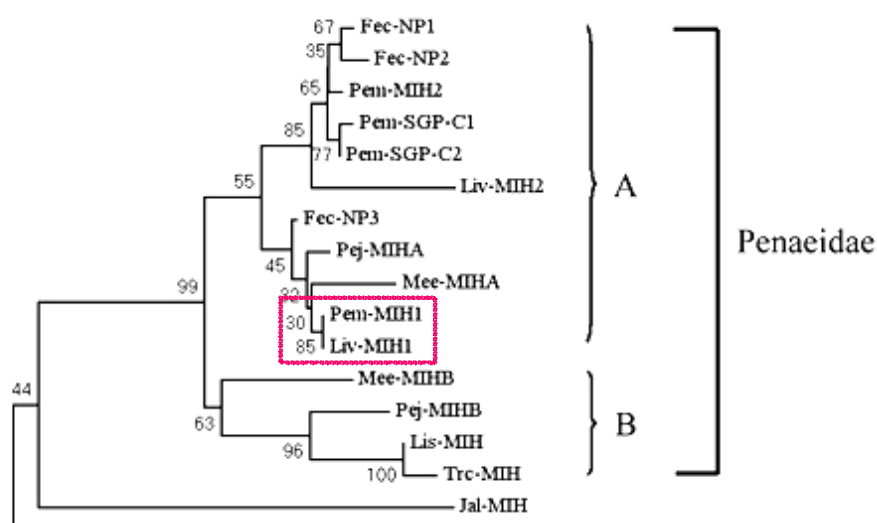
Figure 3-5   Phylogenetic analysis of the peptides of CHH family (modified from Chen et al., 2007). The highest identity was found between the *MIH* genes obtained from *Penaeus monodon*, *Pem-MIH-1* and *Litopenaeus vannamei*, *Liv-MIH-1* (as shown in rectangle).

3.5 Ecdysteroids

Ecdysteroids occur in more than one form; there are 20-hydroxyecdysone (20E), ecdysone, 3-hydroxyecdysone and some other unknown forms (Baldalia et al, 1984; Blais et al, 1994). The most prominent derivative circulating in hemolymph is 20E, which could be detected by radioimmunoassay (RIA) and a combined high-performance liquid chromatography/enzyme immunoassay (HPLC/EIA) (Graf and Delbecque, 1987; Snyder and Chang, 1991; Blais et al, 1994). The formation of YO and ecdysteroid synthesis occur as early as during the embryogenesis, since

ecdysteroids concentrations were increased with the appearance of organ (Spindler et al., 1987).

The ecdysteroid titers during the molt cycle showed similar pattern whether the measurements were from whole body, integument, or hemolymph. Several species also showed similar profile of the titers throughout the molt cycle, i.e., it is low during postmolt stage, gradually decreased to low basal level at intermolt stage, then increased during early premolt stages, reached peak at late premolt, and sharply declined just before ecdysis. This pattern has been reasonably well established in *P. serratus* (Baldalia et al., 1984), *L. vannamei* (Chan et al., 1988; Blais et at., 1994), *M. rosenbergii* (Harpaz et al., 1987; Okumura and Aida, 2000), and *Libinia emarginata* (Laufer et al., 2002).

The mechanism of action of ecdysteroids is far from a complete understanding. Evidence from studies in the insect *Drosophila melanogaster* and the crab *Portunis pelagicus* suggested that ecdysteroids may be involved in up-regulation of ACP-20, a gene for cuticle formation in the epidermal cells (Braquart et al., 1997; Kuballa and Elizur, 2007). There is a possibility that several ecdysteroid derivatives may act concertedly to complete the molting process since it was found that removing of YO resulted in inhibition of molting process in the terrestrial crab, *Sesarma haematocheir*, and the inhibition could not be converted by ecdysterone injection (Suzuki, 1985).

It is believed that ecdysteroids are negatively regulated by MIH from the eyestalk (Mattson and Spaziani, 1986; Dauphin-Villemant et al, 1995). This belief is rather empirical. Mattson and Spaziani (1986) reported that when Y-organs of the crayfish *O. limosus* at early premolt stage were incubated *in vitro* with sinus gland extracts, significant inhibition of protein synthesis were found in the sinus gland. It is not known whether the sinus gland extract contained MIH, and/or other neurohormones from the XOSG, therefore the experiment did not show that MIH inhibited protein synthesis in YO.

3.6 Does MIH Inhibit Ecdysteroid Synthesis?

It has been postulated, and generally believed, that steroidogenesis from Y-organs was negatively regulated by MIH thus the hemolymph levels of both

hormones should be in reciprocal to each other during the molt cycle. This relationship, however, has not been advocated. In the blue crab, *C. sapidus*, both *MIH* mRNA and ecdysteroids levels were low at late premolt (D_4); this, however, could mean that gene transcription may not be unrelated to the peptide synthesis and regulation of MIH might be at post-transcriptional level (Lee et al, 1998). On the contrary, the hemolymph levels of MIH and ecdysteroids peaked during mid premolt in the crayfish *P. clarkii* (Nakatsuji and Sonobe, 2004) or late premolt in the crab *C. maenas* (Chung and Webster, 2005). The data suggest that the reciprocal relationship between MIH and ecdysteroids may not be true.

Another line of evidence suggesting that MIH may not directly inhibit ecdysteroid synthesis from YOs came from the study by Nakatsuji and Sonobe (2004). The Y-organs of de-eyestalked crayfish *P. clarkii* from various stages of the molt cycle were incubated *in vitro* with Prc-MIH and the percentage of inhibition of ecdysteroid synthesis was determined. As relative to the maximum inhibition at intermolt, which was assigned as 100%, the responsiveness of Y-organ to Prc-MIH declined gradually at the early premolt (51.8%) and reached a low level at the middle and late premolt (3.7 and 10.8%, respectively). At postmolt, the responsiveness of Y-organ to Prc-MIH increased again (61.4%). Similarly, responsiveness of YOs of *C. maenas* to MIH was highest during late postmolt and intermolt, and gradually declined during premolt (Chung and Webster, 2003).

MIH have been known negatively regulating Y-organ (YO) ecdysteroidogenesis, but the mechanisms in which how it interacts with other peptides, signaling the hormone synthesis in YO, at transcriptional or post- transcriptional levels are still not well defined. However the MIH mechanisms action on YO ecdysteroidogenesis that have ever been elucidated are being concluded as following schematic diagram (Fig. 3-6).

Recently MIH receptor was characterized in *C. sapidus*, CsGC-YO1, and categorized as the receptor guanylyl cyclase (rGC) which is the membrane-associated protein. The receptor is comprised of five domains: extracellular, transmembrane, kinase-like, dimerization, and cyclase catalytic (Zheng et al., 2008). MIH bound to its receptor on YO cell membrane; the guanylyl cyclase enzyme domain activated, and catalyzed the synthesis of the second messengers, 3',5'-cyclic adenosine

monophosphate (cAMP) or 3′,5′-cyclic guanosine monophosphate (cGMP) from adenosine triphosphate (ATP) and guanosine triphosphate (GTP), respectively (Spaziani et al., 1999; Lucas et al., 2000). MIH mediated through the second messenger, cGMP were detected in *O. limosus* (Gliscynski and Sedlmeier, 1993), *C. maenas* (Saïdi et al., 1994; Chung and Webster, 2003), and *P. clarkii* (Nakatsuji et al., 2006). Cyclic GMP mediated the protein phosphorylation through binding with protein kinases in the cytosol of Y-organ cells, MIH treatment prior incubation with cyclic nucleotides or analogs, exhibited the increasing of cGMP-dependent kinase (PKG) activity more than cAMP-dependent kinase (PKA). The phosphorylated proteins by cGMP were found increasing during intermolt more than premolt, whereas by cAMP, only premolt YO showed the phosphorylated proteins (Baghdassarian et al., 1996).

The responsiveness of *P. clarkii* YO to MIH was regulated by the phosphodiesterases (particularly PDE1), enzymes that hydrolyzed the second messengers, cAMP and cGMP. PDE activity measured by using [^{3}H]cGMP as substrate was low during intermolt, rose to a peak at mid premolt and declined during late premolt, which were contrast to the responsiveness of YO to MIH during a molt cycle (Nakatsuji et al., 2006). Thus in *P. clarkii*, MIH controls YO ecdysteroidogensis through cGMP-mediated PDE activity. The PDE1 found in *C. sapidus* YO was known as calcium/calmodulin dependent (Nakatsuji et al., 2009), therefore calcium may regulate ecdysteroidogensis through the activation of PDE.

In *C. antennarius*, calcium was found stimulating YO ecdysteroidogenesis and enhanced PDE activity *in vitro*, whereas the calmodulin inhibitor, trifluoperazine enhanced the inhibitory effects of MIH that counteracted with the actions of calcium. Thus, calcium stimulates ecdysteroidogenesis by activating a calcium/calmodulin-dependent PDE, a cAMP-PDE in this specie (Mattson and Spaziani, 1986), by which MIH counters the mechanism by increasing intracellular cAMP, which consequently causes Ca^{2+} efflux (Spaziani et al., 1999). Extracellular Ca^{2+} influxes into YO cells through the L-type voltage-gated channels (LTC), when blocking with calcium channel's blockers, nifedipine and verapamil, they inhibited ecdysteroid synthesis with dose-dependent action, as evidenced in crabs *C. antennarius*, *Menippe mercenaria* and crayfishes *Orconectes immunis*, *O. rusticus*. However the influxes of calcium

influence ecdysteroidogenesis in different ways, small amounts of Ca^{2+} influx from extracellular or intracellular (by blocking of Ca^{2+}-pump channels at membrane of smooth endoplasmic reticulum or SER) are stimulatory, whereas excess amount of intracellular Ca^{2+} depresses ecdysteroidogenesis. Additionally, accumulation of intracellular Ca^{2+} (Spaziani et al., 2001) and diacylglycerol (DAG) also activated the protein kinase C (PKC), and resulted in increase of ecdysteroidogenesis. Interestingly, the activation of PKC was not interacting with cAMP or Ca^{2+}-calmodulin system (Mattson and Spaziani, 1987; Seinsche and Sedlmeier, 1998). As shown during the molt cycle of crab *Scylla serrata*, PKC protein found in YO only during premolt (Imayavaramban et al., 2007).

Otherwise the activation of MIH was possibly through the nitric oxide synthase (NOS), as established in *G. lateralis* (Kim et al., 2004). NOS, enzyme synthesizes nitric oxide (NO), the ligand that binds to soluble guanylyl cyclase (sGC). Apart from the membrane-associated guanylyl cyclase receptor, sGC receptor was also detected in the YO using real-time PCR (Lee et al., 2007). Thus it was presumed that the regulation of YO ecdysteroidogenesis by MIH through NOS could involve the Ca^{2+}/calmodulin-dependent nitric oxide synthase (Covi et al., 2009).

The synthesis of YO ecdysteroids was begun from uptake of cholesterol binding to high-density lipoprotein (HDL) by endocytosis of the entire HDL-cholesterol complex (Kang and Spaziani, 1995), particularly during intact premolt and even more in activated eyestalkless YOs (Watson and Spaziani, 1985); its uptake was inhibited by MIH from the eyestalk (Spaziani and Wang, 1993). The major ecdysteroid synthesis and secretion from YOs of crustacean is β-ecdysone (Chang and O'Conner, 1977), whereas its metabolites occurred in the peripheral tissues, the predominant type was 20-hydroxyecdysone (α-ecdysone) (20E), conversed by 20-monooxygenase (Soumoff and Skinner, 1988) by C-20 hydroxylation of ecdysone. Rates of conversion were highest during late premolt D_3, in the epidermis, midgut gland, and hindgut (McCarthy, 1982). 20-hydroxyecdysone was typically loss from exoskeleton, carcass, during late premolt, in the meantime that it was principal in the circulation (Chang and O'Conner, 1978). By which high circulating level, it also did feedback inhibition on its synthesis at YO, during intermolt, *in vivo* and perhaps activated premolt, *in vitro*, as had been reported in *O. limosus* (Dell et al., 1999).

In short, MIH regulates YO through the activation of second messengers, Ca^{2+} and various kinds of protein kinases including the uptake of hormone precursor, HDL-cholesterol. Their interaction influences synthesis of ecdysteroids in one way or another. To date, at least two kinds of cyclic nucleotides, cAMP and cGMP are known involving in the signal transduction. However it is not clear if there is the cross-talk relationship between these signaling pathways.
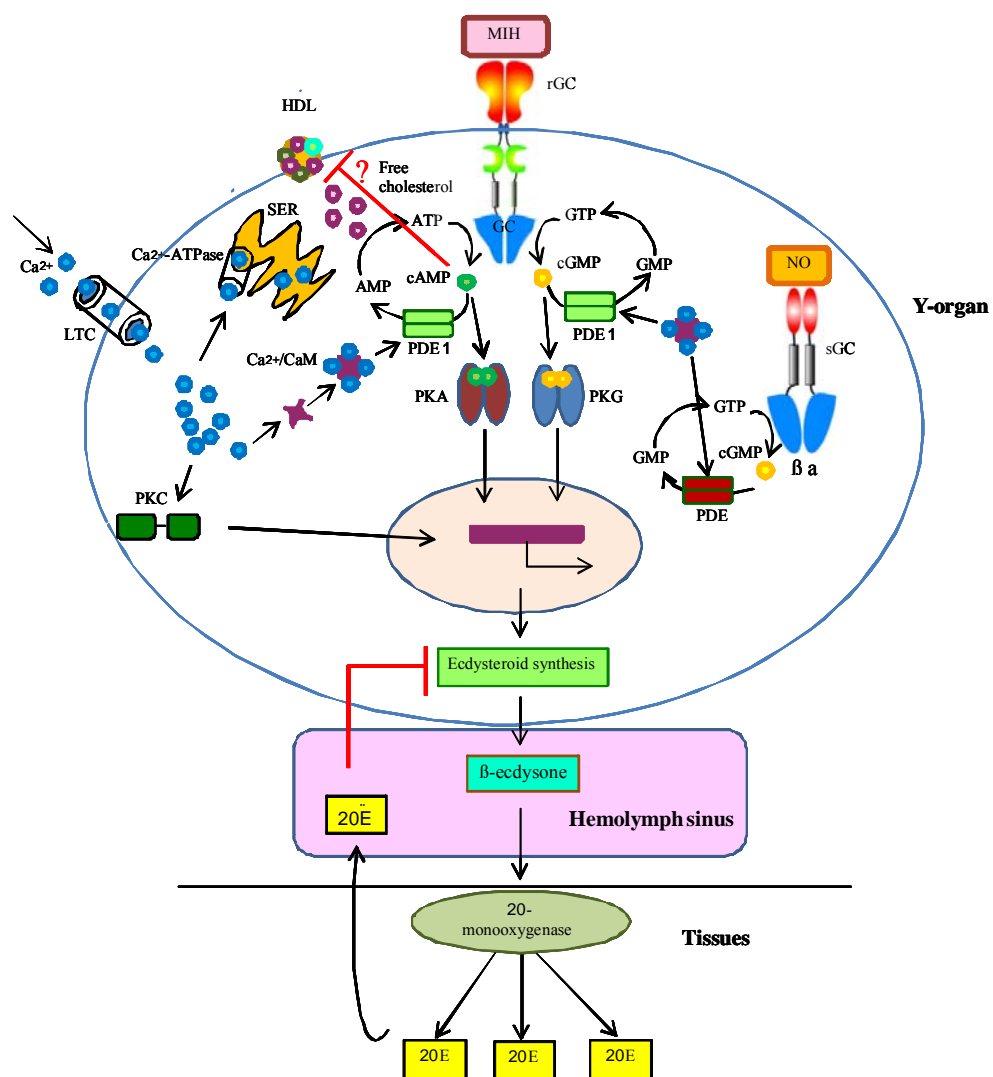
Figure 3-6   Schematic diagrams representing the signaling transductions in which MIH regulation of Y-organ ecdysteroidogenesis

3.7 Other Hormones and Neurotransmitters that may be Involved in Molt Cycle

Crustacean hyperglycemic hormone (*CHH*). This neurohormone increases glucose levels in the hemolymph and it seems also to affect the molting process as well. In *C. maenas*, both CHH and MIH inhibited *in vitro* ecdysteroids synthesis in the YO (Webster and Keller, 1986); the inhibition of MIH was even higher than that of CHH, about 10-folds (Chung and Webster, 2003). The CHH levels in the green crab *C. maenas* were significantly increased during late premolt (which was the only period detected) and drastically declined just prior to ecdysis, and evidence suggests that the hormone induces water uptake during ecdysis (Chung et al., 1999).

Methyl farnesoate (*MF*). The hormone, a homologue of insect juvenile hormone, is produced in the mandibular organs (MOs). The action of MF is mainly on metamorphosis during larval development and also on reproductive function. In an experiment where YOs and MOs were co-cultured, it was found that MF directly stimulated ecdysteroid synthesis in YOs. This finding was support by another finding that sizes of the MOs were increased as the development progressed toward the ecdysis, and the MF contents in organ itself were correlated with the increasing sizes of the organs (Chang et al., 1993). Likewise, when MOs of the crab *C. sapidus* were implanted into the abdominal region of the shrimp *Penaeus setiferus* during the intermolt, the molt intervals were significantly shortened (Yudin et al, 1980). MF levels in the MOs and hemolymph of the crab *Oziotelphusa senex senex* were elevated as the animals approached ecdysis, or reached ovarian maturation (Nagaraju et al., 2006).

The hormone MF is inhibited by mandibular organ-inhibiting hormones (MOIH), a neurohormone produced and secreted from the XOSG, at least in the crab *Cancer pagurus* (Tang et al., 1999). The study was done under MOs culture, in which the MF produced in the eyestalk-ablated animals was higher than the intact animals. Likewise, MF produced by MOs culture was decreased by SG homogenate in dose-related manner. By chromatographic purification of SG homogenate, MOIH-1 and MOIH-2 were characterized (Wainwright et al, 1996). The amino acid composition of MOIH-1 and MOIH-2 differed on only one amino acid; both could inhibit MO

synthesis of MF with an equal strength. In SG, MOIH-1 was more abundant than MOIH-2.

3.8 Molting-Reproduction Relationship

Interestingly, molting and reproductive function in crustaceans are interrelated. In the sand crab *Emerita asiatica,* both ovarian index and total ovarian proteins were gradually increased from the intermolt stage to premolt, which was coincident to the active vitellogenic phases. Meanwhile the hemolymph protein level was also high during the entire intermolt period, but increased sharply during premolt stage with a drastic decline just before ecdysis (Gunamalai and Subramoniam, 2002). However, it is not exactly known what hormones are responsible for the synchrony of the two processes. What is known is that ecdysteroids are unlikely to be the ones. Injection of 20E augmented protein synthesis in the ovary. Ecdysteroid level in the ovary peaked at intermolt stage C_3 and was declined drastically to the lowest level at D_{3-4} stage. The decline was inversely related to rising hemolymph ecdysteroids during premolt. The hatching of the embryos, attached to the pleopods of the ovigerous females also occurs under a high titer of hemolymph ecdysteroids (Gunamalai and Subramoniam, 2004). In the crab *Metograpsus messor*, high concentration of hemolymph ecdysteroids was found at premolt, accompanied by spermatogonial proliferation. However, during the intermolt, the spermatogenesis also occurs normally in the consistent low level of ecdysteroids (Suganthi and Anilkumar et al, 1999). Likewise, in *M. rosenbergii*, ecdysteroids levels in the reproductive and non-reproductive molt cycle did not show any significant difference, but the reproductive function between the two cycles was markedly different (Okumura and Aida, 2000).

In *P. monodon*, eyestalk-ablated females either undergo molting or ovarian maturation, followed by spawning. It is not known what mechanism(s) causes the shrimp to go in one direction or the other. It is conventionally believed that a drop in GIH following eyestalk ablation causes ovarian maturation, but it is also noticed that not all the eyestalk-ablated shrimp undergo ovarian maturation; some just go to a regular molting process.

3.9 Environmental Factors that May Influence Molting

Environmental factors that may influence molting are photoperiods, salinity, temperature, dissolved oxygen, pH, and nutrition. The effects of photoperiods are species-specific. There are species that short-day photoperiod (e.g., 6L:18D) stimulates molting and results in increased molting frequency, and species that long-day photoperiod (e.g., 18L:6D) has that effect, compared to the animals that stay in the equal light:dark (12L:12D) photoperiod. And yet there are species that any regime of photoperiods does not seem to affect molting (Table 3.1). The increased or decreased molting by different photoperiod regimes may or may not affect growth rate; it is true that crustacean growth requires molting, however, molting may not result in growth. In certain species photoperiods have a strong effect on survival rate, and this may be related to conflicting effects of photoperiods on different parts of the internal milieu that control molting (e.g., hormonal profiles).

Table 3.1 Photoperiods and molting in different crustaceans

Photoperiod	Affects on Molting	Species	References
Constant dark	induce	*Gecarcinus lateralis* (juvenile)	Bliss, 1964
		Uca pugilator (juvenile)	Weis, 1976
Short-day	induce	*Panulirus argus* (adult)	Quackenbush and Herrnkind, 1983
		Pseudocarcinus gigas (larvae)	Gardner and Maguire, 1998
Long-day	induce	*Palaemonetes argentinus* (juvenile)	Díaz et al., 2003
		Cambarus (Orconectes) virilis (juvenile)	Stephens, 1955; Aiken, 1969
		Sicyonia ingentis (juvenile)	unpublished data
Any regimen	no effect	*Pacifastacus leniusculus* (juvenile)	Sáez-Royuela et al., 1996
		Penaeus merguiensis (juvenile)	Hoang et al., 2003
		Hyalella azteca (adult)	Kruschwitz, 1978

Regarding survival rate, constant light causes high mortality in *C. virilis* (Stephens, 1955), and constant darkness promote survival rate of *M. rosenbergii* (Withyachumnarnkul et al., 1990). Light intensity also affects growth of crustaceans. In *P. merguiensis*, the percent weight gain was higher under the intensity of 750 lux than at 75 lux, and *F. chinensis*, the most favorite was at 300 luk (Hoang et al, 2003; Wang et al, 2004b).

Water temperature also affects molting. In *H. americanus*, molting of the adult lobsters was blocked if the water temperature dropped to 5 °C (Palma et al., 1998). The adult amphipods, *Hyalella azteca*, high temperatures (27 °C) shortened the intervals between oviposition, molting interval, and molting and oviposition (Kruschwitz, 1978).

Limbs loss or autotomy of appendages also affects molting. In *Palaemonetes kadiakensis*; limb loss at stage A and B accelerated the first molt following the limb loss; at stage C, two successive molts following limb loss were accelerated; at stage D, the first molt cycle was not affected but the second one was shortened significantly (Stoffel and Hubschman, 1974).

CHAPTER IV
MATERIALS AND METHODS

4.1 Experimental Setup

Penaeus monodon juveniles were reared in light control chambers, and were divided into three groups: those reared under normal-day, short-day and long-day photoperiods. The animals were reared for two succeeding molt cycle, during which they were determined for length of each molting stages, molting frequency and molting intervals. At each stage, 6-10 animals were sacrificed: their hemolymph was determined for levels of ecdysteroids, their optic lobes for *MIH* transcript by qRT PCR, and MIH-1-producing cells by immunohistochemistry.

4.2 Animals and Photoperiod Regimen

Juvenile domesticated *P. monodon*, males and females, of 10-18 g body weight were obtained from the Shrimp Genetic Improvement Center, Chaiya District, Surat Thani, Thailand. The center functions as a nucleus breeding center for the selective breeding program of specific pathogen-free *P. monodon* and is under the auspice of the National Center of Genetic Engineering and Biotechnology, National Science and Technology Development Agency, the Ministry of Science and Technology, Thailand.

The animals were reared individually in separate 30 cm x 25 cm x 30 cm (width x length x water depth) compartments of fiber-glass tanks located in a light-proved chambers. There were three chambers, each was under different lighting regimen: normal day (12L (h of light or photophase):12D (h of darkness or scotophase)) which mimics the ambient photoperiod in the tropical zone, short day (6L:18D) and long day (18L:6D). Each chamber contained two fiber-glass tanks and each tank contained 10 compartments. Therefore there were 20 animals per chamber. The compartments of the tank were separated by a 0.5 cm fiberglass wall with several 0.5 cm holes to allow free flow of water between compartments. All the tanks in the

three chambers were also connected to allow the same water to flow through all the tanks in a re-circulatory manner (Fig. 4-1). The water passed through mechanical and polyvinyl alcohol bead filters, which had been proven to control the levels of total ammonia and nitrite at the levels not exceeding 1 ppm, without water exchange. Natural seawater, being diluted to 15 ppt, was used throughout the experiment. The water temperature was kept at 28 ± 1 °C by aquarium heaters, aeration was provided to keep dissolved oxygen >6 ppm. The water alkalinity was at 130-150 ppm and pH at 8.4-8.6. All the water qualities were considered optimum for *P. monodon* rearing.

Before experiment, all the three chambers were kept under darkness condition for ten days to acclimatize the animals, before being shifted to individual lighting regimes. Feed pellets (Charoen Pokphand Foods Public Company) were provided at 3% body weight, two meals a day, at 07.00 h and 19.00 h. The shrimp body weights were determined individually at the beginning and at the end of the experiment and percentage of the mean body wet weight gain (%BWG) was calculated as: %BWG = $[(BW_f - BW_i)/ BW_i] \times 100$, where BW_I was the body weight at the start of the experiment and BW_f was the body weight at the end of the experiment. During the rearing, some shrimp died. Moribund and dead shrimp were taken away from the tank daily.

Light was provided through fluorescent lamps that generated light with the intensity at 3000-3200 lux on the water surface. Photoperiods were controlled by electrical timers to be normal day (12L:12D), short day (6L:18D) and long day (18L:6D).

a
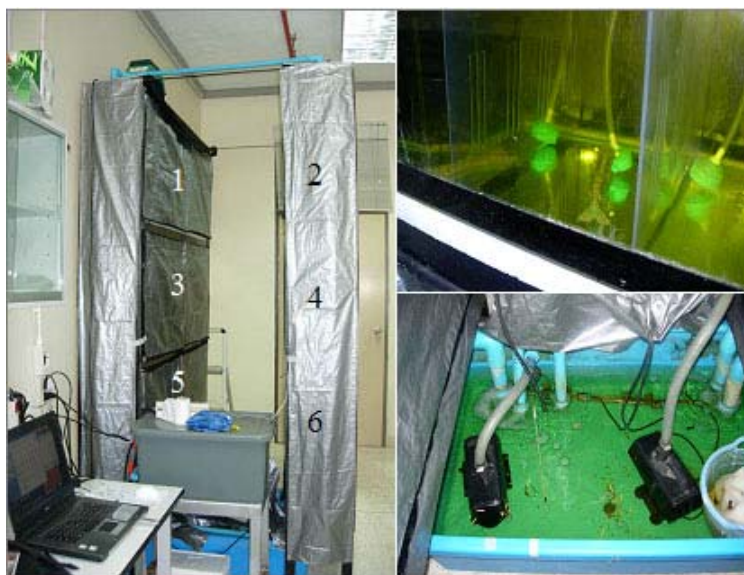
b
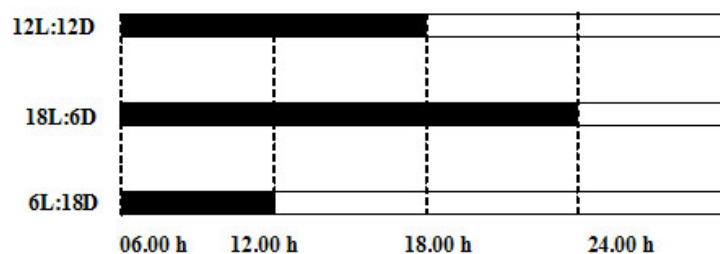
Figure 4-1   **a.** Six close-recirculated aquarium tanks (left panel). Within a tank, the clear flow-through partitions divided it into ten compartments; each was supplied with the individual air stone (right, upper panel). Two water pumps kept the water well circulation (right, lower panel). **b.** Diagram showing of the three photoperiods using in the experiments. Filled bars represent the scotophase.

4.3 Determination of Molt Stage

Molt stage of individual shrimp was determined daily by examination of the shrimp uropod under stereomicroscope according to the method described by Promwikorn et al (2007). The molt stages were categorized into postmolt (stages A & B), intermolt (stage C), early premolt (stage D_{0-2}), and late premolt (stage D_{3-4}). Two cycles of molt stage were recorded and lengths of individual molt stages, molting frequency and molt interval was calculated from means of the two cycles. At the end of the second molt cycle, shrimp were allowed to continue their molt cycle and sacrificed at postmolt, intermolt, early premolt and late premolt, 6-10 animals per stage. Since the number of animals was not adequate for all the molting stages, and some of them died during the experiment, therefore the experiment was repeated once, with 20 shrimp (10 x 2) per group. After the first molt, samples were collected according to the molt stages.

After determination of the molt stage, shrimp was chilled under iced-water for approximately 5 min before hemolymph was withdrawn (100 μL, for ecdysteroid determination), optic lobe (for *Pem-MIH-1* gene determination and Pem-MIH-1 immunohistochemitry) and Y-organs (using MIH-1 immunohistochemistry) were isolated.

4.4 Determinations of Ecdysteroids in the Hemolymph

Hemolymph Collection. Hemolymph, 100 μL, was withdrawn from underneath the arthropodial membrane at the abdominal portion with disposal insulin needle, then added into 300 μL of 95% methanol and placed in a 1.5 mL microcentrifuge tube. The tube was vigorously vortexed and kept at -20 °C.

Radioimmunoassay. Sample tubes were thawed to room temperature, vigorously vortexed, the microcentrifuge tubes were centrifuged at 14,000 x g, at 4 °C, for 20 min. The supernatant, 100 μL, in duplicate, was dried under vacuum. $[^3H]$-ecdysone (100 μL) was added to the sample and standard tubes containing a series concentrations of 20-hydroxyecdysone (Sigma), from 0 pg to 4.0 ng (0, 25, 50, 125, 250, 500, 1000, 2000, and 4000 pg). All the tubes were then added with ecdysteroid antisera, M-20 ecdysone antiserum (Chang and O'Connor, 1978). Non-specific binding tube contained $[^3H]$-ecdysone (100 μL), buffer and normal rabbit serum. All tubes

were incubated overnight at 4 °C. The antigen-antibody complex was precipitated with cold, saturated ammonium sulfate. The precipitate was then dissolved in 25 μL of distilled water and analyzed for radioactivity with 600 μL of scintillation fluor (Cytoscint) in a Packard 1500 TriCarb liquid scintillation spectrophotometer. Amounts of ecdysteroids were determined from the standard curve and expressed as ng/mL hemolymph of edysteroids equivalent.

4.5 Determinations of *Pem-MIH-1* Transcript

Total RNA Extraction. The optic lobe was dissected out from the eyestalk in diethyl pyrocarbonate (DEPC)-treated saline on cold sterile plate, immediately added to cold (4 °C) TRIzol reagent, and stored at -80 °C. RNA was extracted using TRIzol reagent (Invitrogen) as follows:

(1) *Homogenization*. The optic lobe was placed in 200 μL of TRIzol reagent and homogenized using a glass-Teflon®. The lysate was thoroughly mixed and centrifuged at 12,000 x g for 10 min, at 4 °C. The cleared supernatant containing RNA was transferred to a fresh tube.

(2) *Phase separation*. Chloroform 200 μL, was added into the supernatant and the tube was shaken vigorously by hand for 15 sec and incubated at room temperature for 3 min. The tube was then centrifuged at 12,000 x g for 15 min at 4 °C, after which the mixture was separated into a lower red phenol-chloroform phase (phenol was contained in TRIzol), an interphase, and a colorless upper aqueous phase containing RNA.

(3) *RNA precipitation*. The aqueous phase was transferred into a fresh tube and total RNA was precipitated by mixing with isopropyl alcohol, 500 μL. The mixture was incubated at room temperature for 10 min and centrifuged at 12,000 x g for 10 min at 4 °C. The RNA precipitate formed gel-like pellets.

(4) *RNA wash*. The RNA pellets were added with 500 μL of 75% ethanol, vortexed and centrifuged at 7,500 x g for 5 min at 4 °C. The pellets were isolated.

(5) *Redissolving the RNA*. The RNA pellets were air-dried, resuspended in 30 μL of DEPC-treated water, and determined for total RNA, using a spectrophotometer at OD_{260}.

DNase I Treatment. Protocol for the removal of contaminated DNA from the extracted RNA (Qiagen) was as follows. The extracted RNA, 1-2 μg, was added to 2 μL of 10x DNase buffer (500 mM Tris·HCl, pH 8.0; 50 mM $MgCl_2$; 10 mM DTT), 1 μL of DNase I, and RNase-free water to make the total volume of 20 μL. The solution was mixed in the RNase-free microcentrifuge tubes, and incubated at 37 °C, for 30 min. The mixture was added with 2 μL of 25 mM EDTA, and total RNA was re-extracted as the above procedure. The purified total RNA was then determined for the concentration, and stored at -80 °C.

Primer Design. By using Primer 3 software, specific primers for *P. monodon MIH* gene were designed based on a complete sequence of MIH-1 (GenBank acc. no. <u>AY496454</u>), and a partial sequence of the control gene, elongation factor (*EF-1α*) (GenBank acc. no. <u>DQ021452</u>); the expected amplicon sizes were 172 bp and 140 bp, respectively. Sequences of the primers for *Pem-MIH-1* (GenBank acc. no. <u>AY496454</u>, nt. 6-118), were Mat-F: 5′-CATAGACGGCACTTGTCGAG-3 and Mat-R: 5′-CCTGTTGGCAGCCTTTAGAC-3′; and for *EF-1α* were EF-F: 5′-GAACTGCTGACCAAGATCGACAGG-3′, and EF-R: 5′ GAGCATACTGTTGGAAGGTCTCCA-3′.

RT-PCR. The screening test of *Pem-MIH-1* mRNA expression from purified total RNA was conducted by RT-PCR (Biometra Cycler, Lab Focus) using the above primers. PCR reaction, 25 μL, was composed of 10.75 μL DEPC-H_2O, 12.5 μL 2X buffer, 0.5 μL of 10 μM *Mat-F* or *EF-1α-F*, 0.5 μL of 10 μM of *Mat-R* or *EF-1α-R*, 0.25 μL RT *Taq* polymerase (SuperScript™ One-Step RT-PCR, Invitrogen) and 1 μL of the extracted RNA (100 ng/μL). The amplification was carried out for 30 cycles, consisting of heating at 50 °C for 30 min, denaturation at 94 °C for 2.45 min, annealing at 55 °C for 45 sec, extension at 72 °C for 30 sec, and terminating with final extension at 72 °C for 5 min. The PCR product was then analyzed by 1.2% ethidium bromide agarose gel electrophoresis. The PCR products were purified by QIAquick PCR purification kit (Qiagen) and the DNA concentration determined by spectrophotometry with the absorption at OD_{260}.

Plasmid DNA Preparation. The purified PCR product was then ligated to pGEM®-T easy vector system (Promega) (Fig. 4-2). The mixture, 10 μL of total volume (1 μL of 200 ng DNA fragment, 3 μL of 50 ng pGEM®-T easy vector, 5 μL of

2x ligation buffer, and 1 μL of T4 DNA ligase) was incubated at 4 °C overnight. The content was then transformed into the competent cells, *E. coli* XL1 blue. Briefly, 50 μL of prepared competent cells (stored at -80 °C) was added with the ligation mixture, incubated on ice, 30 min in the microcentrifuge tube. The reaction tube was heated in the water bath at 42 °C for 2 min and placed on ice for 2 min. The LB medium (10 g Bacto-Tryptone, (Difco 0123-01-1), 5 g Bacto-yeast extract (Difco 0127-05-3), 10 g NaCl, ddH$_2$O to 1 L), 500 μL was added to the ligation tube, and mixed before incubated on the shaker at 37 °C for 1 h. The transformed reaction of 200 μL was plated on the LB/amplicilin/X-gal plate (10 g Bacto-Tryptone (Difco 0123-01-1), 5 g Bacto-yeast extract (Difco 0127-05-3), 10 g NaCl, 15 g Bacto-agar (Difco 0140-01), ddH$_2$O to 1 L) containing 100 μg/mL ampicilin, and 80 μg/mL X-gal. The plate was incubated overnight, at 37 °C, for 16 h.

PCR on colonies of bacteria, *E. coli* was conducted to analyze the transformants. PCR reaction (25 μL total volume consisting of 18 μL ddH$_2$O, 2.5 μL 10x buffer, 0.75 μL MgCl$_2$, 0. 5 μL dNTP, 1 μL sense primer, 1 μL antisense primer, 0.25 μL *Taq* DNA polymerase (Invitrogen), and *E. coli* cells) was done for 25 cycles (denaturation at 94 °C for 5 min 30 sec, annealing at 55 °C for 30 sec, extension at 72 °C for 30 sec, and terminating with final extension at 72 °C for 5 min) using primers, SP6 and T7 promoter. The products were separated on 1.2% agarose gel, and visualized with an ethidium bromide. Single colony was subcloned in LB medium containing ampicilin overnight at 37 °C on shaker. Cells containing inserted plasmid DNA were then extracted using HiYield^{TM} Plasmid Mini Kit (Real Genomics). PCR was done to confirm the insertion using gene specific primers before DNA sequencing. The sequences of a single colony were then compared with the mature *Pem-MIH-1* sequences using ClustalW (http://www.ebi.ac.uk/Tools/ clustalw2/index.html).
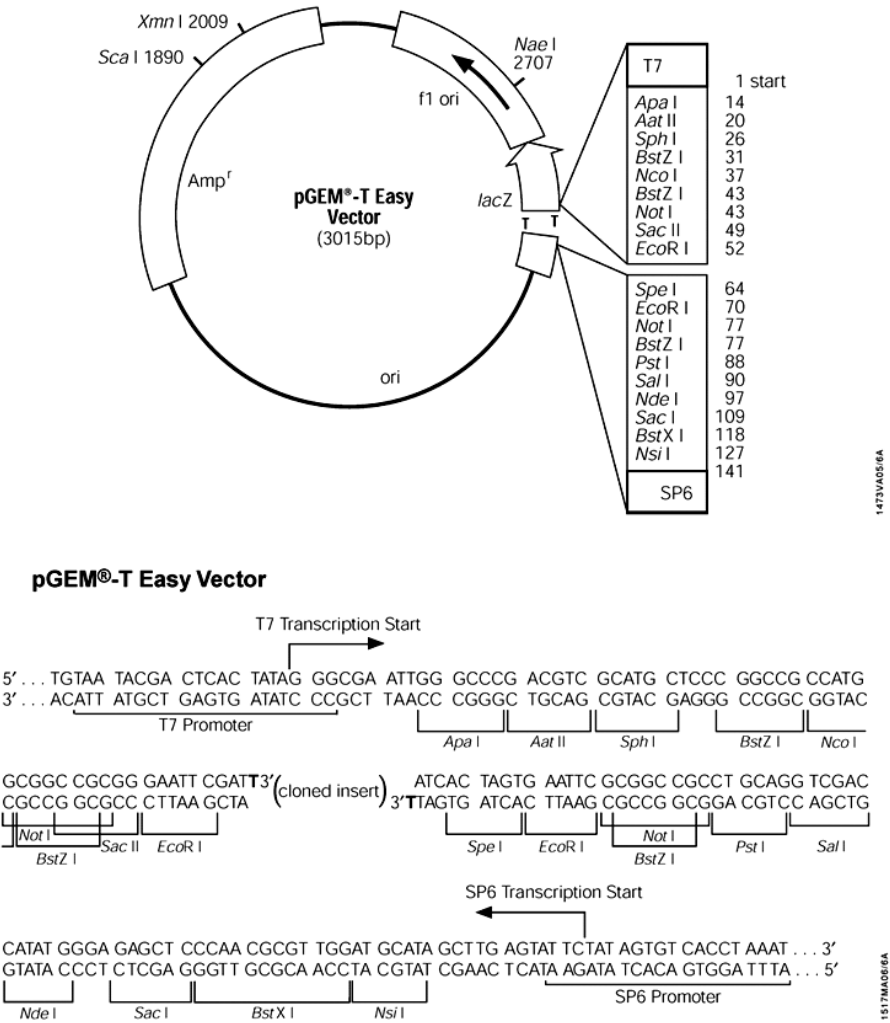
Figure 4-2   pGEM® T easy vector circle map and its priming regions of the primers, SP6 and T7 promoter.

The plasmid DNA of clone that was 100% identical to MIH-1 sequence was used for construction of standard curve of qRT PCR. The plasmid DNA was purified from the cells cultured in LB medium by GeneJET^{TM} Plasmid Miniprep kit (Fermentas), determined concentration, aliquoted, diluted into serial dilutions, before stored at -20 °C. The plasmid DNA standard curve was calculated as the copy number (molecules/μL) by the following the equation (QuantiTect SYBR Green PCR Handbook).

Y molecules/μL= (Xg/μL DNA / [plasmid length in basepairs x 660]) x 6.022 x 10^{23}

In the study, the plasmid vector, pGEM$^{®}$-T easy length at 3015 bp was used for MIH-1 plasmid DNA. While the EF-1α plasmid DNA was a gift from Molthathong et al., (2008) using pDrive vector with the length of 8900 bp.

qRT PCR. Two-step qRT-PCR was used. For RT step, the first-strand cDNA was synthesized; total RNA of 500 ng was reverse transcribed with SuperScript^{TM} III reverse transcriptase (Invitrogen). The reverse transcription conditions were as manufacturer's instructions. Briefly, the contents were added into RNase-free microcentrifuge tubes (1 μL of 10 μM *Mat-R* or *EF-R* primers, 1 μL of total RNA (500 ng), 1 μL of 10 mM dNTP mix, 11 μL of DEPC-ddH$_2$O), heated to 65 °C for 5 min, then incubated on ice for 1 min. The tubes were brief centrifuged and added new mixture (4 μL of 5x First-strand buffer, 1 μL of 0.1 M DTT, 1 μL of SuperScript III RT), and mixed gently. The cDNA was synthesized with the following conditions; incubation at 55 °C for 30-60 min and heat at 70 °C for 15 min to inactivate the reaction, and stored at -80 °C.

For the PCR step, amplifications were conducted using QuantiTect^{TM}Syber$^{®}$ Green PCR Kit (Qiagen). Thermocycling was conducted using Applied Biosystems 7500 (Applied Biosystems). Combined both manufacturing's instructions, the cycling conditions were consisted of three stages as following; stage 1, PCR initial step at 95 °C, for 15 min; stage 2, the PCR step for 45 cycles (denaturation at 95 °C, 15 sec; annealing at 55 °C, 30 sec; extension at 72 °C, 33 sec; with a data acquisition at 78 °C, 31 sec); and stage 3, the dissociation step.

By using the absolute quantification method, the standard curves, the linear relationship between the threshold cycle (Ct) and the log copy number of standard plasmid DNA dilutions, were constructed. A linear regression analysis was conducted to obtain the percentage of PCR efficiency, which was calculated from the equation, $E = (10^{-1/slope}-1)$(Kubista et al., 2006). Ct values were determined by the ABI software using a fluorescence threshold value setting for all runs in order to limit the variations of the assays (Rutledge and Côté, 2003). In this study, the threshold used was at 0.02165234. The data of results were exported into the MS Excel worksheet (Microsoft) for calculation, and further analysis. By using EF-1α as an internal standard, it was found that the expression of EF-1α was variable between the light regimes (see Results). Therefore in subsequent experiments, the amount of total RNA which was subject to the reverse transcription was used to normalize the expression of *Pem-MIH-1* gene, as recommended by Šindelka et al (2006).

4.6 Immunohistochemistry of MIH-1-Producing Cells

Antibody Production. Polyclonal antibody was raised in the Swiss mice at the Department of Biology, Faculty of Science, Srinakharinwirot University. Recombinant MIH-1 (rMIH-1), which was in an inclusion form in *E. coli* (strain BL 21), was a gift from Dr. Apinunt Udomkit, Institute of Molecular Biology and Genetics, Mahidol University. The protein rMIH-1 in the inclusion form, 50 µg, at a total volume of 500 µL in distilled water was mixed 1:1 (V/V) with 500 µL of complete Freund's adjuvant. One hundred microliters of the mixture was intraperitoneally injected into four Swiss albino mice (ICR strain) at the age of six weeks. The injection was done every two weeks for three times as booster doses, using rMIH-1 inclusion peptide mixing with incomplete Freund's adjuvant. One week after the last injection, approximately 1 mL of blood was collected from each mouse through retrobulbar (sinus behind the eyeball) sinus bleeding, and placed into 1.5 mL microcentrifuge tube. The tubes were centrifuged at 5,000 x g for 10 min; and the serum was transferred into a new tube, aliquoted at 50 µL, and stored at -20 °C.

Partial Purification of the Antibody. Prior to use, the immunoadsorption was done in order to partially purify the polyclonal antibody (Sithigorngul et al., 1999). Cell lysate of *E. coli* was preincubated 9:1 (V/V) with the antibody at 4 °C

overnight. The mixture was then centrifuged at 12,000 x g, 4 °C for 10 min; the clear supernatant was subsequently applied for immunoblotting or immunohistochemical staining, and stored in aliquots at -20 °C. For the test of specificity, antiserum was also prior adsorbed with purified MIH-1 (1:4, V/V).

To determine specificity of the antibody, as well as its optimum titer, the anibody binding ability to rMIH-1 was carried out by Western blot analysis and by paraffin-sectioned immunohistochemical staining. Other recombinant proteins in the MIH-CHH-GIH family, GIH (Treerattrakool, 2008), CHH (Treerattrakool et al., 2003), and MIH-2 (Yodmuang et al., 2004) were employed for the specificity test. The Western blot was carried out by sodium dodecyl sulfate polyacrylamide gel electrophoresis (SDS-PAGE) and then by nitrocellulose membrane transferring.

The SDS-PAGE (Laemmli, 1970) was prepared by a single gel preparation being composed of 6 mL of 12.5% separating gel. The gel was composed of 2.5 mL of 30% acrylamide, 1.9 mL of distilled water, 1.5 mL of 1.5 M Tris-HCl pH 8.8, 60 μL of sodium dodecyl sulfate (SDS), 60 μL of 10% ammonium persulphate (APS), 6 μL of tetramethylethylenediamine (TEMED), and 3 mL of 4% stacking gel. The stacking gel was composed of 400 μL of 30% acrylamide, 2.15 mL of H_2O, 375 μL of 1.0 M Tris-HCl pH 6.8, 30 μL of 10% SDS, 30 μL of 10% APS, and 3 μL of TEMED. The polymerization of gels was allowed for at least 2 h or overnight. The separation was carried on the Hoefer mini vertical unit (Pharmacia Biotech).

Final concentration of proteins, ~ 0.3-0.5 μg/μL was mixed with the protein sample buffer, which were 2x and 6x preparations. The 2x preparation contained 0.5 M Tris-HCl pH 6.8, 4.4% (w/v) SDS, 20% (v/v) glycerol, 2% (v/v) 2-mercaptoethanol, and bromophenol blue in distilled/deionized water. The 6x preparation contained 125 mM Tris-HCl, pH 6.8, 2% (w/v) SDS, 20% (v/v) glycerol, 2% (v/v) 2-mercaptoethanol, and 2% bromophenol blue in distilled/deionized water. The mixture was incubated at 95 °C, for 5 min, and immediately placed on ice. The mixture was briefly centrifuged and each 1-2 μL of the mixture was loaded per well. Recombinant MIH-1 and cell lysate of BL 21 *E. coli* containing non-inserted pET 3a vector were loaded. The separation of proteins was electrophoresed under constant 100 V for 2 h. The gel was stained with Coomassie brilliant blue R-250 to visualize the

protein bands and another gel with identical preparation was transferred to a nitrocellulose membrane to be detected with anti- rMIH-1 antibody.

Western Blot Analysis. For Western blotting, protein gel was transferred to the nitrocellulose membrane using semi-dried blotter (Amersham Pharmacia Biotech, CA). Briefly, membrane and six pieces of Whatman filter paper no. 3 including gel were well soaked with the transferring buffer (20% methanol in 1x running buffer) for 5 min before using. The blotter was first sprayed until wet with the transferred buffer. Wet paper, membrane and gel were arranged in sheeted fashion as in order, three pieces of filter paper were placed on the bottommost layer, followed by the membrane, gel, and the uppermost layer was covered with other three pieces of filter paper. Transferring condition was conducted under constant current which was calculated from the membrane's size (width x length of membrane x 0.8 mA), and run for 4 h. Subsequently the membranes were processed for immunoblotting.

For screening of antibody and testing for its titers, the procedures used were modified from the protocol of Sithigorngul et al., (1999) and Abcam Immunohistochemistry protocol (http://www.abcam.com/index.html?pageconfig= resource&rid=10381). Briefly, the membrane containing transferred proteins was cut into strips, and incubated overnight at room temperature on gentle shaking in the blocking buffer (4% skim milk, 10% cell lysate of *E. coli*, 0.01% Triton X-100 in Tris buffer saline, TBS). The membranes were rinsed twice in TBST (20 mM Tris-HCL, 500 mM NaCl, 0.1% of Tween 20, pH 7.6), 5 min each, incubated with anti-rMIH-1 antibody at four dilutions, 1:2000, 1:4000, 1:8000, 1:16000 which was prepared in the 4% blotto solution (4% skim milk, 4% lysate, 0.01% triton X-100 in TBS) at room temperature on gentle shaker overnight. On the second day, the membranes were rinsed twice, 5 min each, in the washing solution (TBST). The membranes were later incubated with the secondary antibody, Goat Anti-Mouse IgG (Zymed) which was conjugated to horseradish peroxidase (GAM-HRP) at the dilution of 1:1000 or 1:500 for 2 h, washed twice in TBST for 5 min, and briefly visualized by AEC red (Zymed).

For specificity test, the recombinant proteins of CHH, GIH, and MIH-2 including rMIH-1 were run in the SDS gel, and transferred to nitrocellulose membrane, the procedures were as mentioned, except the dilution of primary antibody used was at 1:600.

4.7 Immunohistochemistry

Titer Test for Thin-Section Immunostaining. Protocol used for immunostaining was modified from Abcam (www.abcam.com). The procedures were as follows; the tissue sections were heated at 60 °C for 20 min to improve the attachment of tissue to the glass slide before deparaffinized process through three changes of xylene, 10 min each, retrograded EtOH series for 5 min each, three changes of 100% EtOH, and two changes of 95% EtOH, 80% EtOH, 70% EtOH, and 50% EtOH, for 5 min each. The sections were rinse in distilled water, and equilibrated in TBS for 5 min. Pieces of tissue were circle by the liquid-repellent slide marker pen before next steps.

The processes were taken for two days as follows. On day 1, the sections were exposed to antigen retrieval by submersion in the citrate buffer (10 mM tri-sodium citrate, 0.05% (V/V) Tween 20, pH 6), heated in microwave, for 5 min, and cooled down for 20 min. The sections were blocked in the 3% H_2O_2 (in TBS) for 30 min at room temperature (to stop the endogenous peroxidase reaction); then 1% triton X-100 was applied to the section, 10 min. The tissues were blocked with 10% normal goat serum, 1 h, finally those tissue sections were incubated with the primary antibody, anti-rMIH-1 antibody at three dilutions; 1:400, 1:600, and 1:800, overnight at room temperature. The processes were done in the moist chamber from the step of blocking. On day 2, the sections were washed with 0.025% triton X-100 in TBS, twice for 5 min each, the secondary antibody, GAM-HRP (Zymed) at the dilution of 1:500 were applied, 2 h at 37 °C, then they were washed twice, before developed with the DAB chromogen (Histostain®-SP Kit, Invitrogen), for 5 min, and briefly stained with eosin. Negative control sections were identically treated sections but omitting the primary or secondary antibody. The sections were then mounted with mounting media, before observing under the light microscope.

Specificity of antiserum was also conducted in the thin-section staining using the adsorbed primary anti-rMIH-1 pAb. Immunoreactivity was detected both with the peroxidase system and under the confocal laser microscope. For immunostaining, secondary antibody using was goat anti-mouse FITC (Sigma) at the dilution of 1:150, and counterstained with TO-PRO-3 iodide (Molcular Probes). After three–timed rinsing, slides were mounted in VECTASHIELD mounting medium

(Vector Laboratories, Inc.), and captured photographs using a Leitz fluorescence microscope and a Leica DMIRBE inverted epifluorescence/Nomarski confocal microscope outfitted with Leica TCS NT SP1 Laser Confocal optics (Leica, Inc.; Exton, PA).

For control, tissue sections were either skipped adding of primary antibody or secondary antibody, while the other procedures were the same as the treatment sections.

MIH-1 Immunoreactivity of the Optic Lobe. Series of paraffin sections of the optic lobe cut at 10 μm, 10-30 glass slides were subject to the immunostaining. The dilution of anti-rMIH-1 used was 1:600, while the secondary antibody, GAM-HRP, 1:500 was applied to the staining.

All sections were analyzed in an Olympus BX-51 microscope connected to an Olympus DP-50 digital camera. Photomicrographs were captured using the Viewfinder.

4.8 Data Analysis

Statistical analysis was assessed by one way ANOVA and t-test (SigmaStat 3.5, Systat Software). The histograms were constructed by MS Excel (Microsoft). All of the numerical values and histograms are expressed as means ± standard deviations.

CHAPTER V
RESULTS

5.1 Survival, Growth and Molt

The shrimp reared under normal and long-day photoperiods survived at 95% and 90%, respectively, while those reared under short-day photoperiod survived only 65%. Most of the short-day shrimp died during the premolt stage of the fourth molt cycle, which was the cycle when shrimp were sampled for hormonal studies. The initial body weights of the shrimp were comparable: normal day shrimp at 13.2 ± 0.6 (n=20) g; long-day shrimp at 12.1 ± 0.4 (20) g; and short-day shrimp at 14.2 ± 0.7 (20) g. After the end of the third molt cycle, the shrimp had some increase in their body weights, which were 7.3 ± 2.7%, 7.7 ± 2.6% and 4.3 ± 4.8% for the normal, long- and short-day shrimp, respectively; the values did not differ statistically.

Molt intervals for the normal, long- and short-day shrimp did not differ statistically (Table 5-1). Durations of each molt stage were similar in all groups, with premolt stage (early and late) spanned more than 70% of the molt interval. However, the duration of the postmolt in the short-day shrimp was shorter than that of the long-day shrimp, and reached statistically significant level (P<0.05). The duration of the intermolt and premolts for the short-day shrimp was not significantly shorter than that of the normal- and long-day shrimp.

Table 5-1　　Durations of each molt stages and molt interval, in days, of juvenile *Penaeus monodon* reared under three photoperiod regime. N = 19, 18 and 13 for 12L:12D, 18L:6D and 6L:18D groups, respectively.

Photoperiod	Postmolt	Intermolt	Early Premolt	Late Premolt	Molt Interval
12L:12D	1.3 ± 0.3	2.2 ± 0.7	5.0 ± 1.1	5.5 ± 1.1	14.9 ± 2.1
18L:6D	1.4 ± 0.5	2.5 ± 0.8	5.2 ± 1.2	5.8 ± 0.7	15.3 ± 1.4
6L:18D	$1.0 \pm 0.2*$	2.0 ± 0.5	5.0 ± 1.1	5.8 ± 1.3	14.8 ± 2.0

*$P<0.05$, compared to the 18L:6D values

5.2 Ecdysteroid Profiles

Profiles of the hemolymph ecdysteroid levels in molt cycle were similar in the shrimp reared under the three photoperiod regime, with basal level, 1-12 ng/mL, at postmolt, intermolt and early premolt, and a sharp, significant ($P<0.001$, compared to the other three stages) rise to 90-124 ng/mL at late premolt (Fig. 5-1). When the levels of the same stage were compared among different lighting regime, no statistical significance was detected.

5.3 *MIH-1* Gene Expression Profiles

Screening for MIH-1 and EF-1α Expression of the Optic Lobe. Total RNA extracted from the shrimp optic lobe was screened for *MIH-1* and *EF-1α* expressions; both were visualized in agarose gel electrophoresis at 172 and 140 bp, respectively (Fig. 5-2).

PCR Products from Plasmid DNA. After cloning, clones that contained plasmids inserted with *MIH-1* and *EF-1α* were amplified and bands of 172 and 140 bp were revealed, respectively (Fig. 5-3), which was corresponded to the sizes of PCR products derived from total RNA. DNA sequencing of the product from one particular clone (Clone # 12) revealed 100% identity to the mature sequences of *Pem-MIH-1* (Yodmuang et al., 2004) (Fig. 5-4); it was then used for construction of the standard curve for real- time PCR of *MIH-1*.

Standard Curve for qRT PCR. In all runs, as the threshold fluorescence bar was set at 0.02165234, the PCR efficiency values were 93-100%, and the correlation coefficients at 0.96-0.99. The amplification plot showed the Ct values of the samples that were amplified covering the range of six magnitudes of serial standard plasmid DNA dilutions, 10^7 - 10^2 copies for *MIH-1* (Fig. 5-5a) and *EF-1α* (Fig. 5-6a). A melting curve analysis was applied to confirm the specificity of the reaction; a single curve was detected for *MIH-1* (Fig. 5-5b) and *EF-1α* (Fig. 5-6b). The standard curve was a plot between the threshold cycle (Ct) and log of the starting copy number of *MIH-1* and *EF-1α* plasmid DNA, which showed linear lines (Fig. 5-7).
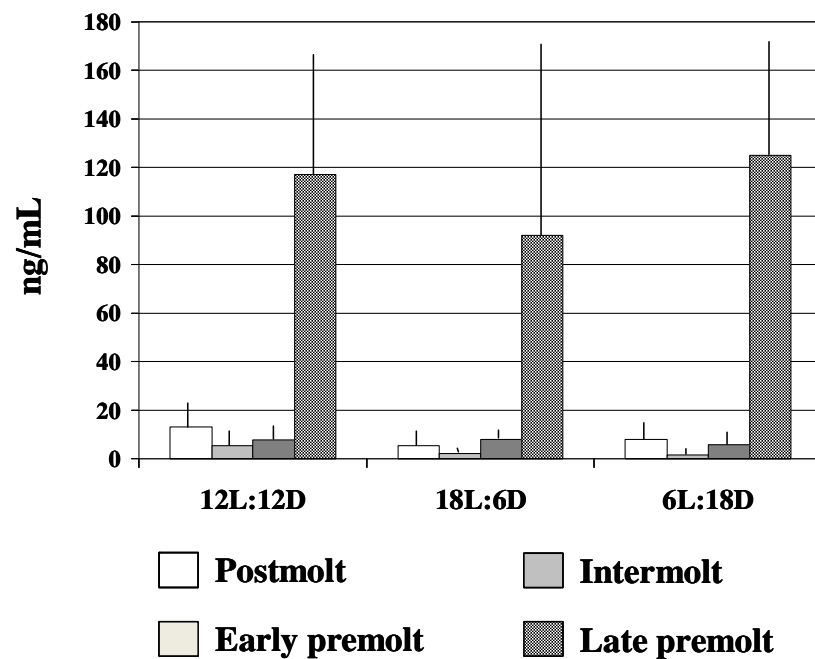
Figure 5-1 Histograms showing levels of hemolymph ecdysteroids of *Penaeus monodon* during the molt cycle from three photoperiod regimes. In all photoperiods, hemolymph ecdysteroids at the late premolt stages were significantly higher than that of other stages ($P<0.001$). Values of each histogram were from 7-21 shrimp.
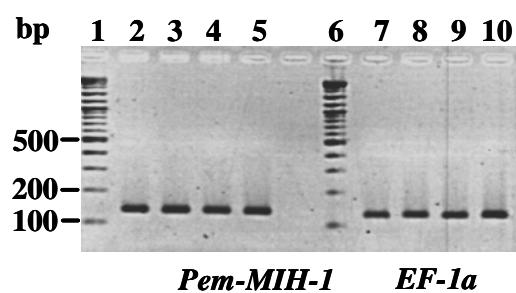
Figure 5-2   Gel electrophoresis of RT-PCR products of *MIH-1* (172 bp, lanes 2-5) and *EF-1α* (140 bp, lanes 7-10) from *Penaeus monodon* optic lobe. Lanes 1&6, DNA markers.

a

b
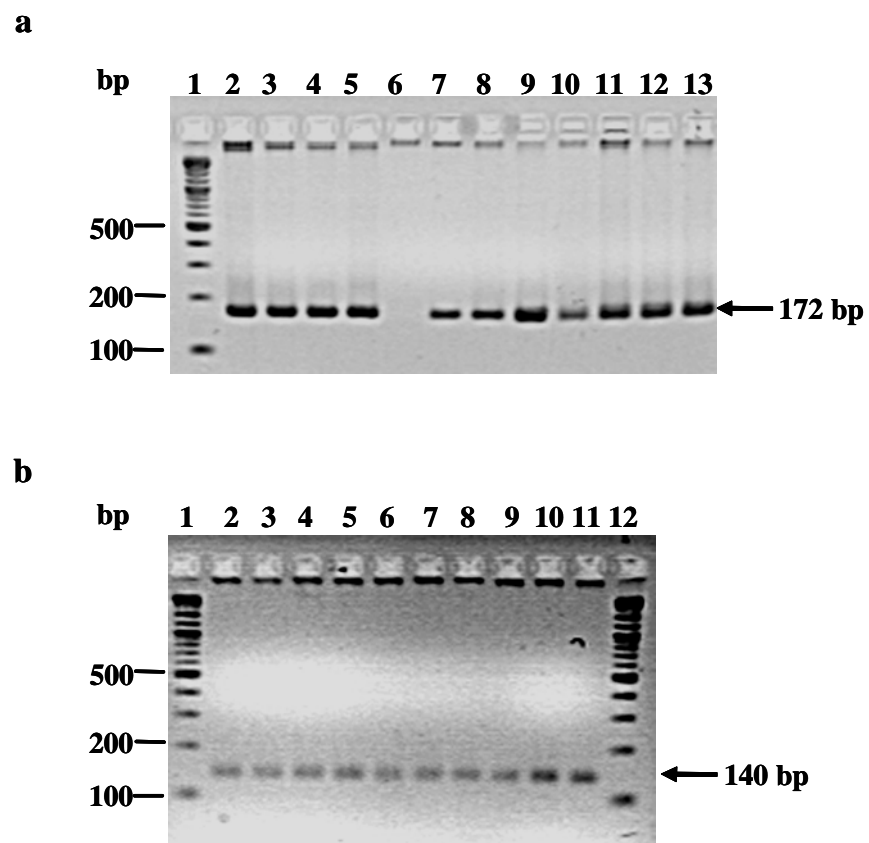
Figure 5-3   Gel electrophoreses showing the insertion of plasmid DNA with the fractions of *MIH-1* (**a**) and *EF-1α* (**b**)

a

```
Mature       AGTTTCATAGACGGCACTTGTCGAGGCGTAATGGGCAATCGTGACATTTACAAGAAGGTA 60
Clone12-Rev  -----CATAGACGGCACTTGTCGAGGCGTAATGGGCAATCGTGACATTTACAAGAAGGTA 55
                  ********************************************************

Mature       GTGCGTGTGTGTGAGGATTGCACCAATATCTTCCGACTTCCAGGCTTGGACGGCATGTGC 120
Clone12-Rev  GTGCGTGTGTGTGAGGATTGCACCAATATCTTCCGACTTCCAGGCTTGGACGGCATGTGC 115
             ************************************************************

Mature       AGAGATCGGTGCTTCTACAACGAATGGTTCCTGATTTGTCTAAAGGCTGCCAACAGGGAG 180
Clone12-Rev  AGAGATCGGTGCTTCTACAACGAATGGTTCCTGATTTGTCTAAAGGCTGCCAACAGG--- 172
             *********************************************************

Mature       GACGAGATCGAAAAATTCAAAGTTTGGATCAGCATCCTGAACGCCGGTCAGTGA 234
Clone12-Rev  ------------------------------------------------------
```

b

```
Clone12-Rev  --IDGTCRGVMGNRDIYKKVVRVCEDCTNIFRLPGLDGMCRDRCFYNEWFLICLKAANR- 57
Mature       SFIDGTCRGVMGNRDIYKKVVRVCEDCTNIFRLPGLDGMCRDRCFYNEWFLICLKAANRE 60
               ********************************************************

Clone12-Rev  --------------------
Mature       DEIEKFKVWISILNAGQ-XX 79
```

Figure 5-4   The homology of sequences of MIH-1 plasmid DNA of *Penaeus monodon* obtained from clone #12 were 100% identical to mature Pem-MIH-1 (Yodmuang et al., 2004), using ClustalW sequence alignment. **a**. Nucleotide sequence. **b**. Amino acid sequence.

a

Selected Detector: All
Well(s): A1-H12
Document: 6L-18D-27Feb2008-copy (Absolute Quantification)

b

Detector = MIH, Tm = 60.0 °C
Well(s): A1-H12
Document: 6L-18D-27Feb2008-copy (Absolute Quantification)
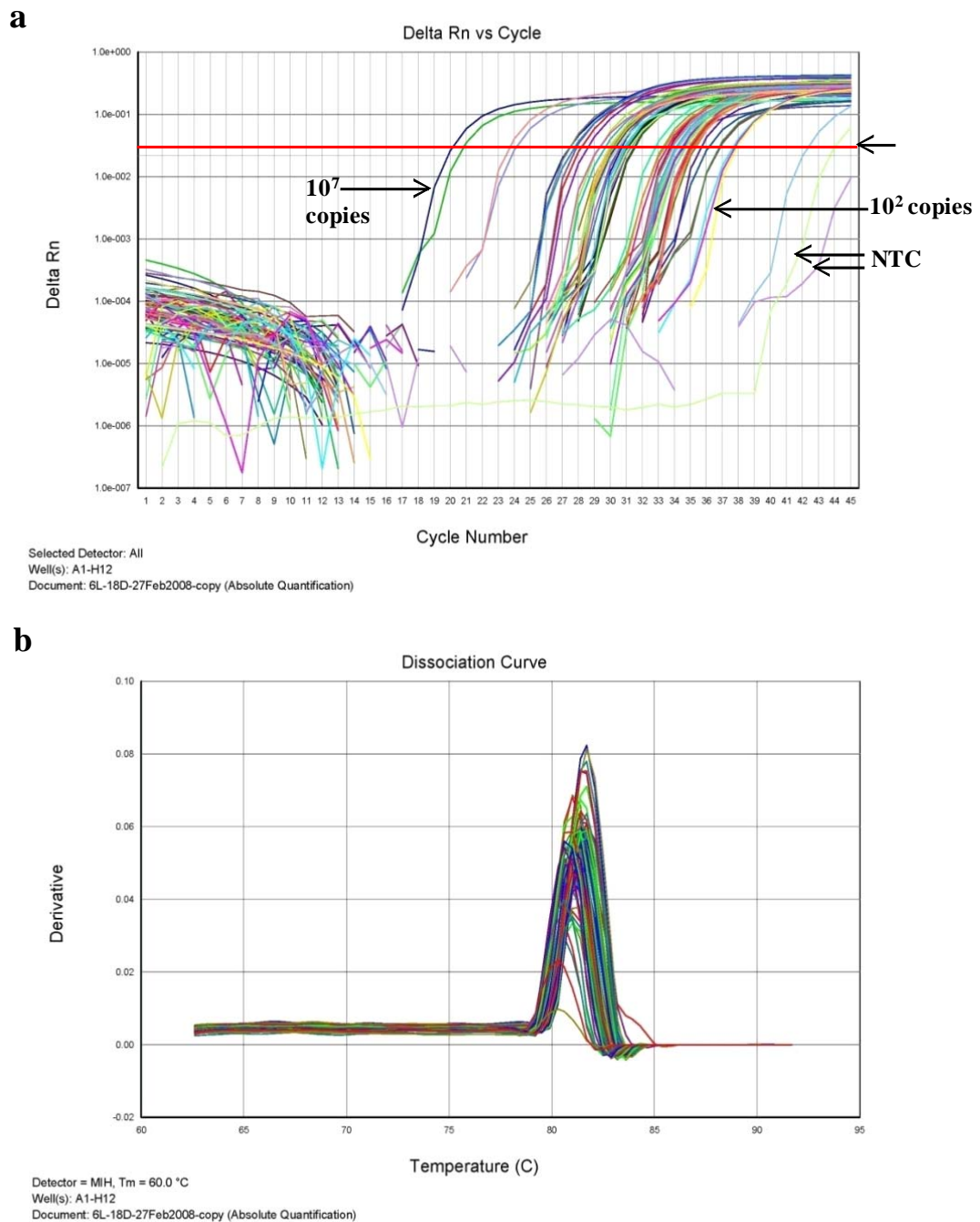
Figure 5-5   Amplification plot and melting curve analysis of the qPCR plate of MIH-1 plasmid DNA obtained from the samples in 6L:18D. **a.** The amplification plot in which the fluorescence threshold was set at 0.02165234. All replicates were amplified in the range of the standard curve. The non-template control (NTC) was unidentified. **b.** A melting curve showed a single curve of MIH-1 melting temperature, 80-82 °C with no primer-dimers.

a

Selected Detector: EF; Start: (Auto); End: (Auto); Threshold: 0.02165234
Well(s): A1-H12
Document: gr IV.sds (Standard Curve)

b

Detector = EF, Tm = 60.0 °C
Well(s): A1-H12
Document: gr IV.sds (Standard Curve)
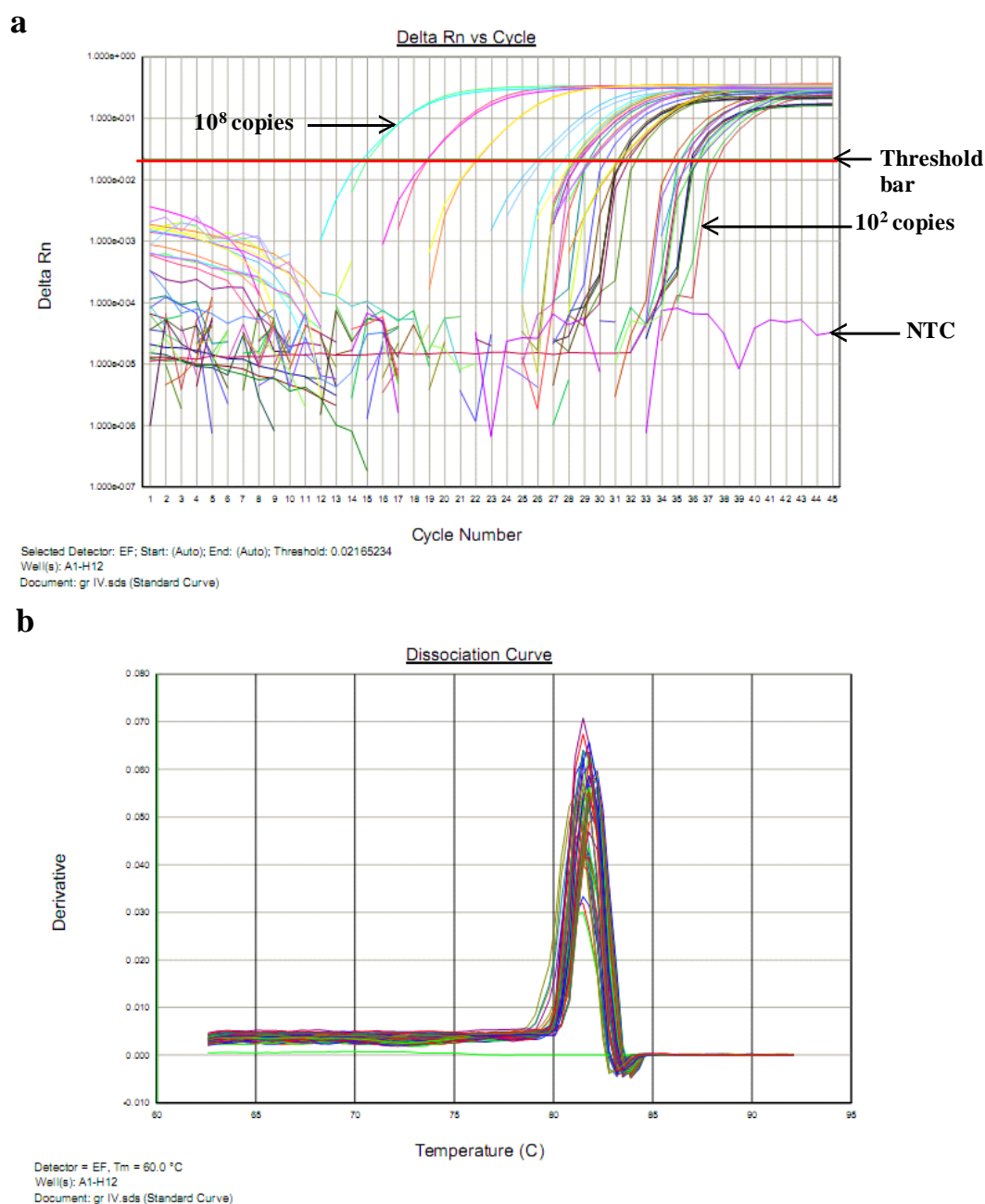
Figure 5-6   Amplification plot and melting curve analysis of the qPCR plate of EF-1α plasmid DNA obtained from *Penaeus monodon* in the late premolt group. **a**. The amplification plot in which the fluorescence threshold was set at 0.02165234. All replicates were amplified in the range of the standard curve. The non-template control (NTC) was unidentified. **b**. A melting curve showing a single curve of EF-1α melting temperature, 81-82.2 °C with no primer-dimers.

a
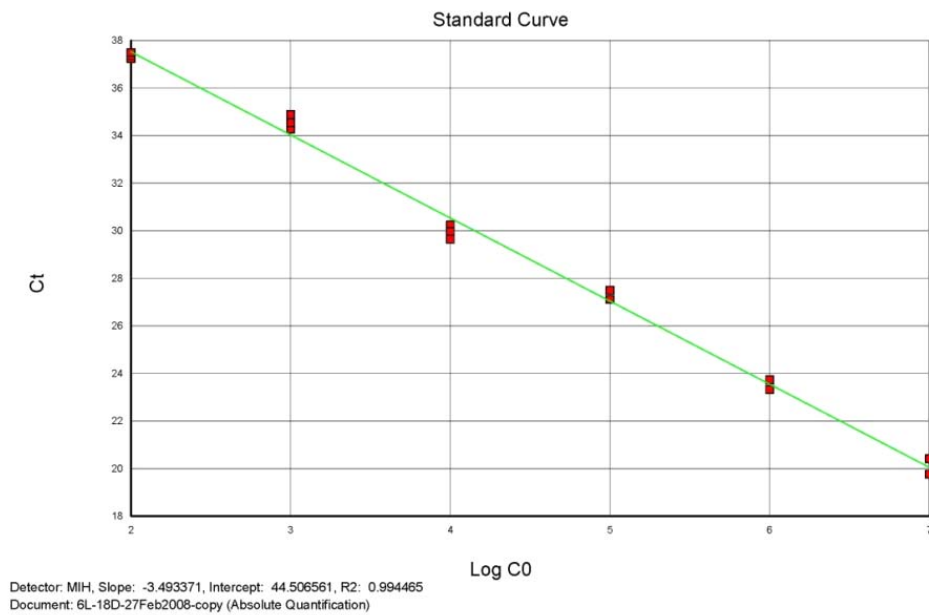
b
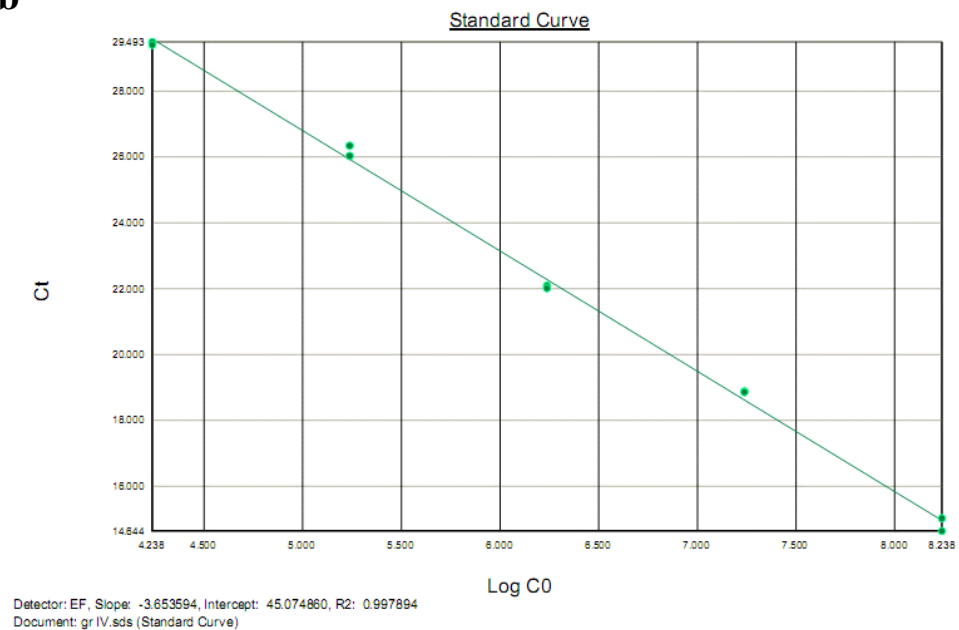
Figure 5-7 Real-time PCR standard curves of MIH-1 (**a**) and EF-1α (**b**) showing linear relationship between the threshold cycle (Ct) and log starting copy number (Log CO) of plasmid DNA. Three replicate amplification reactions were conducted for each concentration of DNA standard, covering six magnitudes of target DNA concentration, from 10^7 - 10^2 copies.

All plates in the experiments were run in duplicates and the amounts of copies were derived from the averages. It was found that the levels of the internal control gene, *EF-1α*, were unstable; the transcripts were increase significantly (P<0.05) at intermolt in long-day and decrease significantly at early premolt in short-day shrimp, compared to normal-day photoperiod (Fig. 5-8). Therefore it was decided that *EF-1α* transcript was not suitable to normalize the values of *MIH-1*, and thus they were normalized by the amount of total RNA input during the step of cDNA conversion and expressed as number of copies per ng total RNA. The use of total RNA to normalize the gene of interest has been suggested by many investigators (Bustin, 2000, 2002; Chung and Webster, 2003; Sindelka et al, 2006; Kubista et al., 2006).

MIH-1 Transcript Levels. Levels of *MIH-1* transcript in the optic lobe (Fig. 5-9) of the normal-day shrimp were gradually decreased from postmolt to late premolt stage; the value of the late premolt stage was significantly (P<0.05) lower than that of the postmolt stage. This decreasing pattern from postmolt to late premolt stage of *MIH-1*, however, was not found in the long- and short-day shrimp. In the long-day shrimp, the level peaked at intermolt and was significantly (P<0.05) higher than in other stages. Whereas in the short-day shrimp, the level peaked at postmolt, decreased at intermolt and early premolt but rose again at late premolt.

When comparing among the values of the same molting stage of different photoperiod regime, *MIH-1* transcripts in late premolt stage of the long- and short-day shrimp were significantly (P<0.001) higher than that of the normal-day shrimp. No significant difference was detected in other molting stages although high level of MIH-1 transcript was shown in the intermolt stage of the long-day shrimp; this was due to a high variation in individual values.
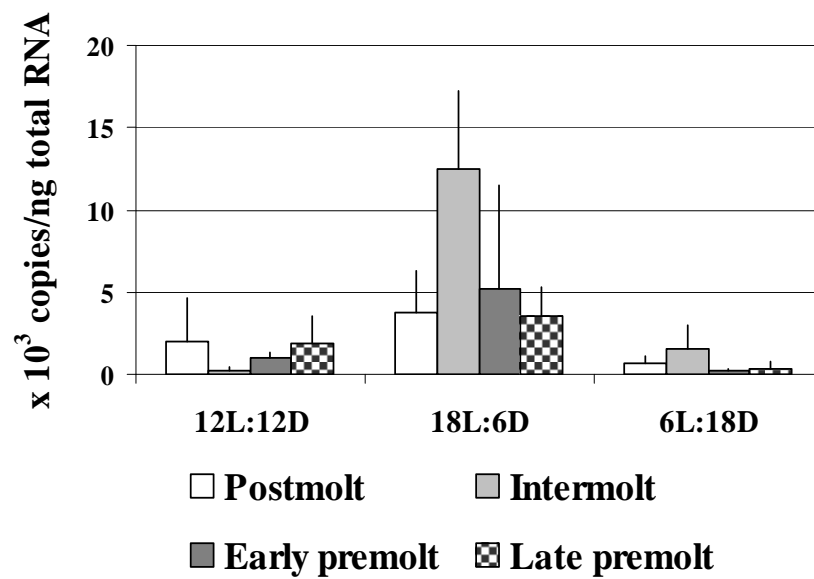
Figure 5-8   Histograms showing the expression of *EF-1α* gene during the molt cycle of *Penaeus monodon* in the three photoperiod regimes. Values at intermolt stage in 18L:6D and early premolt stage in 6L:18D were significantly differed compared to the values in 12L:12D (P<0.05). Each histogram was derived from three shrimp samples.
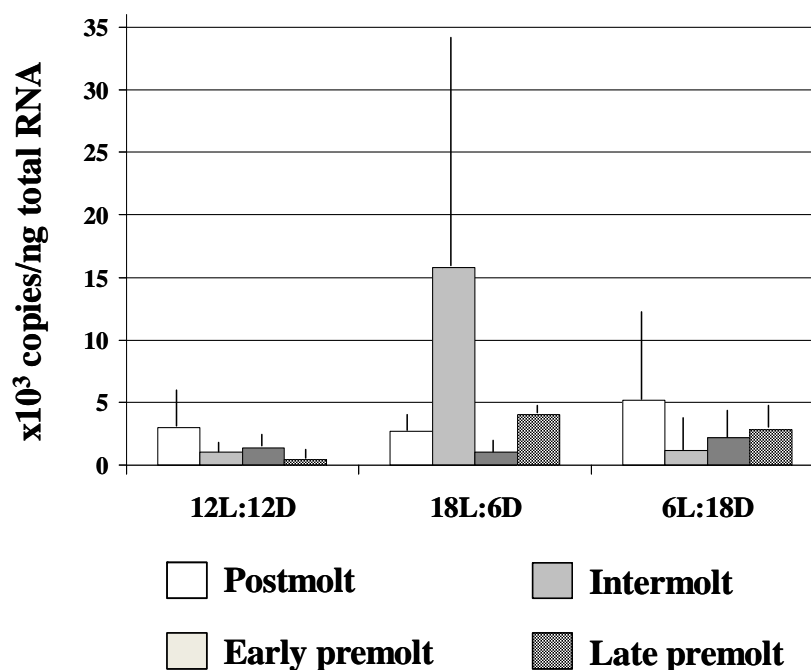
Figure 5-9   Histograms showing levels of *MIH-1* mRNA transcriptional levels of *Penaeus monodon* during molt cycle from three photoperiod regimes. In all photoperiods, levels of *MIH-1* in 12L:12D shrimp in the late premolt stages was significantly ($P<0.05$) lower than that of the postmolt stage. In 18L:6D shrimp, the value of the intermolt stage was significantly higher ($P<0.05$) than that of other stages. The values of the 6L:18D shrimp did not differ statistically. When comparing the values among photoperiods, the values of the late premolt stages of the 18L:6D and 6L:18 D animals were significantly ($P<0.001$) higher than that of the 12L:12D animals. Samples were collected from 4-10 shrimp per each molt stage.

5.4 Immunohistochemistry of MIH-1

MIH-1 Antibody. Specificity test using Western blot analysis, the polyclonal antibody (pAb) bound to two bands of rMIH-1 inclusions at the sizes of approximately 9 and 14 kDa. The larger size was also positive in the fractions of *E. coli*, whereas the smaller one was detected only in the purified rMIH-1 (Fig. 5-10a). The findings were consistent with all dilutions of the antiserum applied. The antiserum also bound to several faint bands of *E. coli* at the sizes of 14-34 kDa. In the eyestalk sinus gland extract, the antiserum reacted to a single band of peptide at the size of 17-18 kDa (Fig. 5-11a), but did not bind to MIH-2, CHH and GIH (Fig. 5-11b).

For the titer test, all strips of purified rMIH-1 were incubated with four dilutions of the pAb. The intensity of positive band at ~ 9 kDa was in the orders from strong to weak as follows: 1:2000>1:4000>1:8000>1:16000 (Fig. 5-10b). The pAb obtained from two mice (M_1 and M_2) showed similar strong titers; thus they were used for cross-reactive test and immunostaining.

Immunostaining. The pAb staining, with different dilutions, was applied to consecutive paraffin sections was as shown in Fig. 5-12**.** The positive immunoreactivity showing as reddish-brown stain was located at the SGs, and the intensity was strong with pAb dilutions of 1:400 and 1:600, but rather faint at 1:800; therefore the dilution at 1:600 was employed for the immunostaining.

Immunoreactivity of MIH-1 in the eyestalk tissues was observed in a group of cells in the medulla terminalis, in the SG, and unidentified groups of tissue in the fasciculate zone and around its base (Fig.5-13). In the medulla terminalis, a small group of hexagonal or round cells of 20-40 μm containing the positive reaction was observed (Fig. 5-13d); these cells were likely neurosecretory cells. The reaction was in the cytoplasm of the cells with different staining intensity. Positive reaction in the SG (Fig. 5-13e) was in small (3-10 μm) spherical appearance with different staining intensity, mixed with empty spaces; as SG is a group of terminal axons of the neurosecretory cells, especially from the medulla terminalis, surrounded by hemolymphatic sinus, it was likely that the staining represent cross sections of several terminal axons. In the fasciculated zone and connective tissue around its base, spherical groups of positive reaction (approximately 50-100 μm per group), were observed (Fig. 5-13f); they had a similar appearance to SG; thus could represent a group of axon traversing the fasciculated zone and around its base. In certain sections,

the group seemed to contain a bunch of donut-like structures or cells that stained positively in the nuclei and cytoplasm (Fig. 5-16a). This structure also stained positively with periodic-Schiff reagent (Fig. 5-16b), suggesting glycoprotein in nature. In certain area of the fasciculated zone, positive-reaction structures similar to small cells (clear zone at the center and intense staining at the periphery) at the size of 5-6 μm were observed (Fig. 5-13g).

Immunoadsorption with *E. coli* lysate (1:10, V/V), and purified MIH-1 (1:4, V/V) showed strong and quite weak reactivity in the eyestalk tissue detected under the peroxidase system, respectively (Fig. 5.14). Correspondingly with observation under the confocal laser microscopy which detected MIH-1 reactivity of the unidentified cells at the eyestalk fasciculated zone (Fig. 5-15, a, c and e). Meanwhile the MIH-1 reactivity was not seen in Y-organ (Fig. 5-15, b, d, and f; Fig. 5-17d).

Besides the neurosecretory cells of the medulla terminalis that contained MIH-1, the positive reaction was also observed in the axons sending out from the cells,   traversed to the SG (Figs. 5-17a, b). No MIH-1-reactive cells were present in medulla externa (Fig. 5-17c).
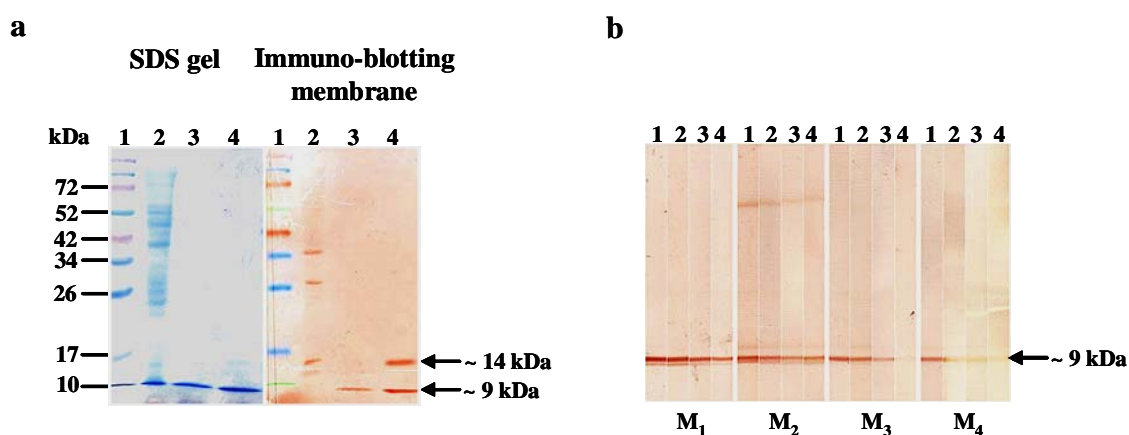
Figure 5-10　SDS-PAGE and Western blot analysis showing the specificity and titers of anti-rMIH-1 pAb. Antiserum reacted with the rMIH-1 peptides, which showed a reddish-brown color, at the size of approximately 9 and 14 kDa (**a**, immunoblotting membrane at lane 4). In left panel (**a**), lane 1, prestained marker (Fermentas, #SM1841); 2*, E. coli* fractions; 3, purified rMIH-1; 4, rMIH-1 inclusions. Protein loaded per lane was at ~ 0.3 μg. Antiserum dilution used was 1:600. Proteins on SDS-PAGE and membranes were visualized by Coomassie brilliant blue G-250 and peroxidase staining, respectively. For titer test (**b**), four serial dilutions of pAb, 1:2000 (1), 1:4000 (2), 1:8000 (3), and 1:16000 (4) obtained from four mice (M_1, M_2, M_3, M_4) were applied to the strips of purified rMIH-1 of ~ 0.5 μg, each.

a

SDS gel   Immuno-blotting membrane

kDa   1   2   3   4   1   2   3   4

72—
43—
34—
26—

17—   ← ~ 17 kDa
                                                 ← ~ 14 kDa

10—   ← ~ 9 kDa

1, marker; 2, rMIH-1 inclusions
3, eyestalk sinus gland; 4, *E. coli* fractions

b

SDS gel   Immuno-blotting membrane

kDa   1   2   3   4   5   1   2   3   4   5

15—   ← ~ 14 kDa
10—   ← ~ 9 kDa

1, marker; 2, rMIH-1 inclusions
3, purified CHH; 4, rGIH inclusions.
5, rMIH-2
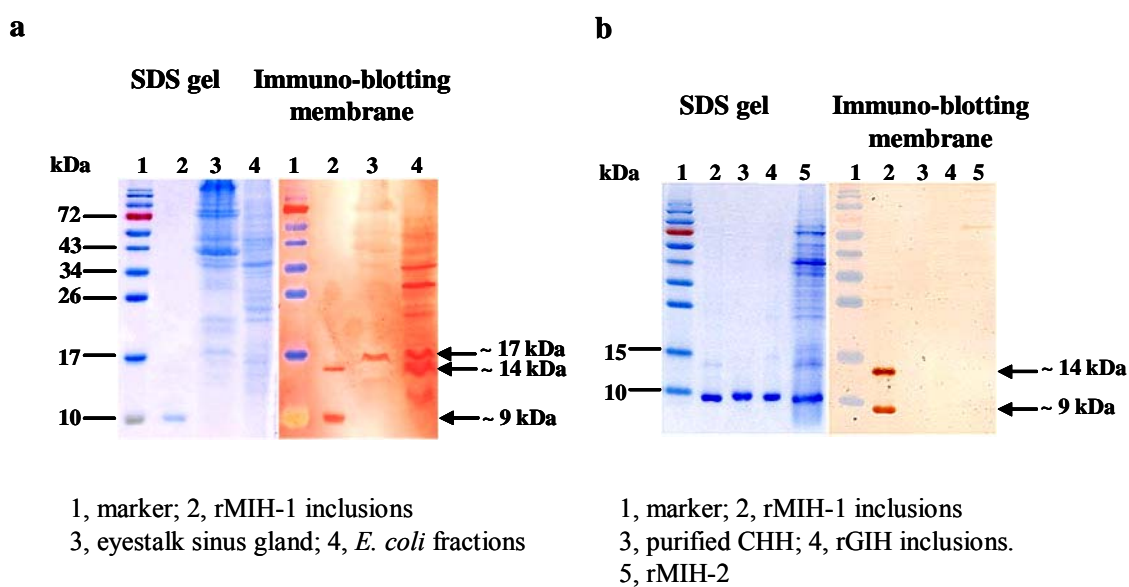
Figure 5-11 SDS-PAGE and Western blot analysis showing binding of anti-rMIH-1 antibody to different peptides and extracts. Positive reaction was observed at 9 and 14 kDa in the rMIH-1 inclusions (**a** & **b**, lane 2) and 17 kDa in the eyestalk sinus gland (**a**, lane 3). No reaction was observed in CHH, rGIH and rMIH-2 bands.
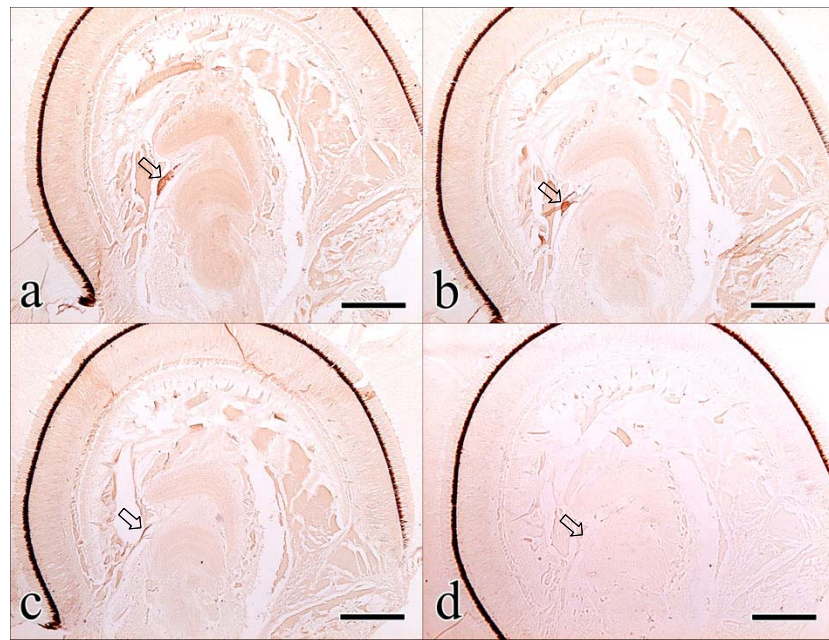
Figure 5-12   Titer test of polyclonal antibody against MIH-1, using immunostaining in the optic lobe and sinus gland (SG) of *Penaeus monodon* detected with the peroxidase system. Intense reddish-brown staining (arrows) was detected in the SGs at the dilutions of 1:400 (**a**) and 1:600 (**b**) (arrows), but weak staining was detected at the dilution of 1:800 (**c**). The primary antibody was omitted in the negative control (**d**). Sections were cut at 10 μm. Bars are 500 μm.
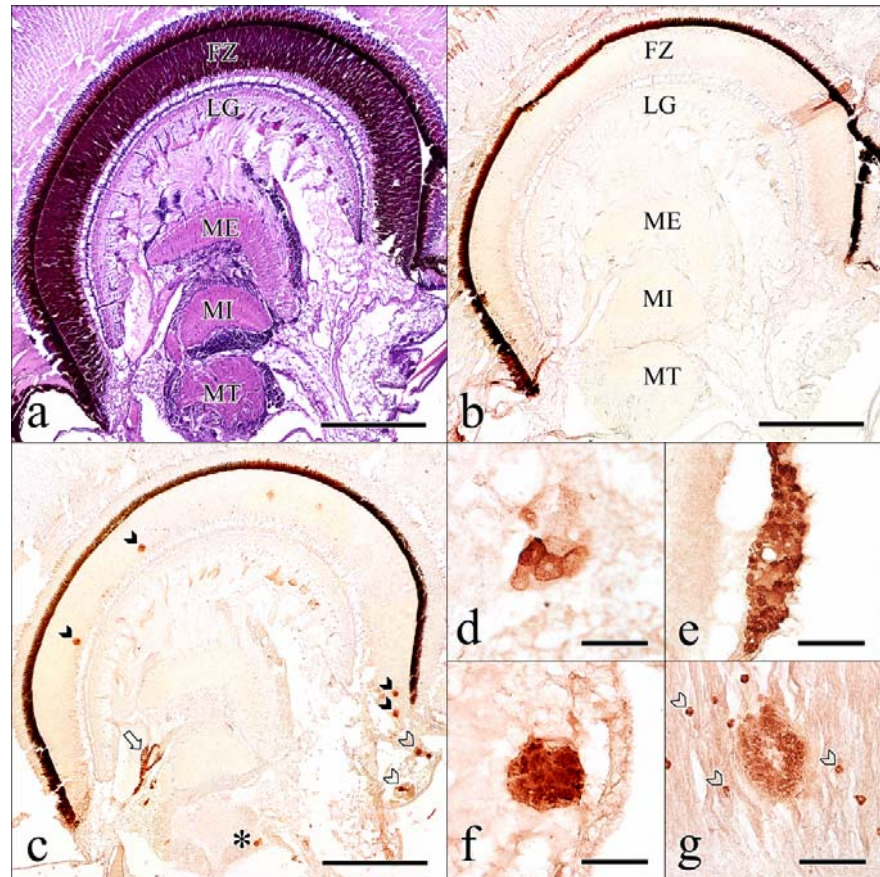
Figure 5-13   Light photomicrographs of the eyestalk tissue of *Penaeus monodon* at the postmolt stage kept under 6L:18D photoperiod and stained with H & E (**a**), and the MIH-1 polyclonal antibody (**b-g**). The MIH-1-immunoreactivity was detected in four areas (**c**); medulla terminals X-organ (MTXO) (asterisk in **c**, **d**), sinus gland (SG) (clear arrow in **c**, **e**), tegumental gland (TG) at the periphery of medulla terminalis (clear arrowheads in **c**, **f**), and unidentified groups of cells in the fasciculate zone (dark arrowheads in **c**, **g**). Negative control showed light brownish optic lobe (**b**). FZ, fasciculated zone; LG, lamina ganglionaris; ME, medulla externa; MI, medulla interna; MT, medulla terminalis. Sections were cut at 10 μm. Bars of 500 μm are applied to **a-c**; 50 μm to **d-g**.
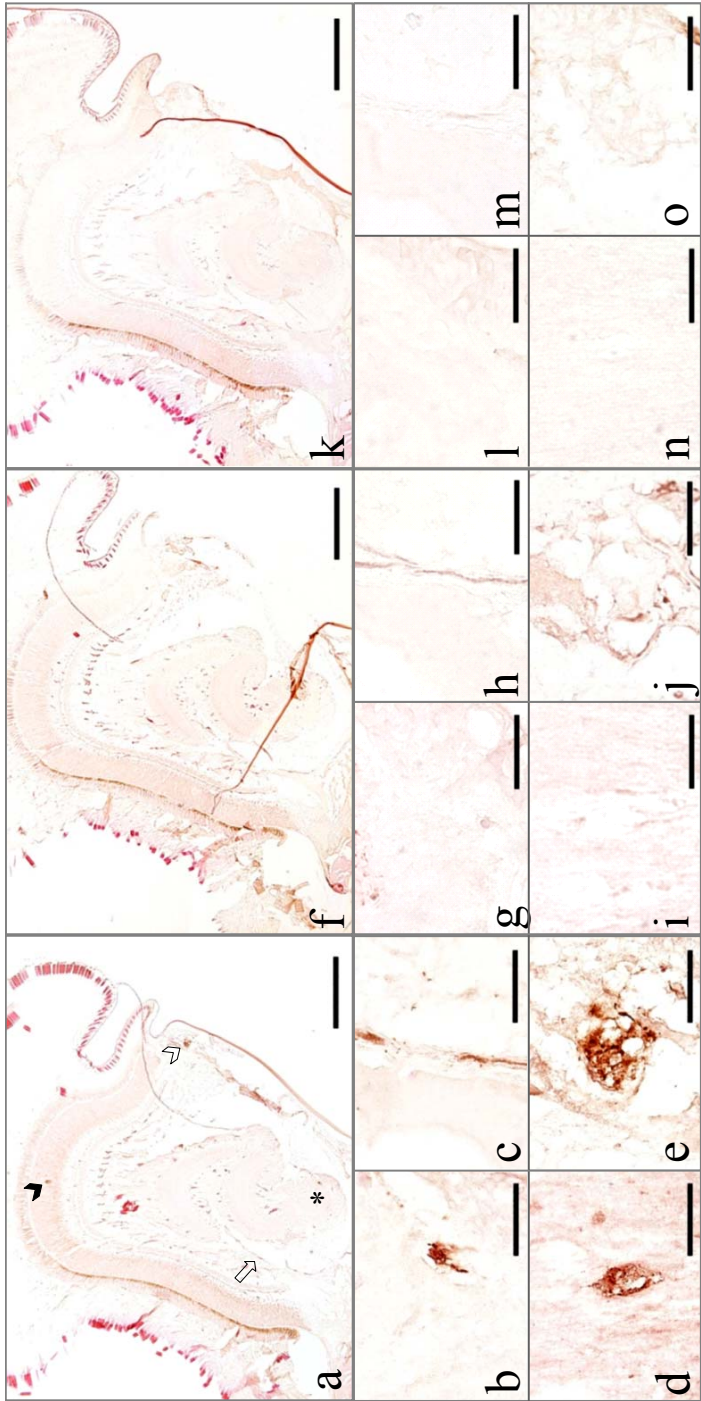
Figure 5.14 Light photomicrographs of MIH-1-immunoreactive cells in the eyestalk tissue of *Penaeus monodon* at the postmolt stage kept under 12L:12D photoperiod. Antiserum used for staining was adsorbed with *E. coli* lysate (a-e), purified MIH-1 (f-j), and negative control section (k-o). Note, the immunoreactivity revealed in MTXOs (asterisk in a, enlarged in b, g, l), SGs (arrow in a, enlarged in c, h, m), TGs (clear arrowhead in a, enlarged in e, j, o), and unidentified cells at FZ (dark arrowhead in a, enlarged in d, i, n) was faint or disappeared in the purified MIH-1 adsorption eyestalk. FZ, fasciculated zone; MTXO, medulla terminalis X-organ; TG, tegumental gland. Sections were cut at 10 μm. Bars of 500 μm are applied to a, f & k; 50 μm to other panels.
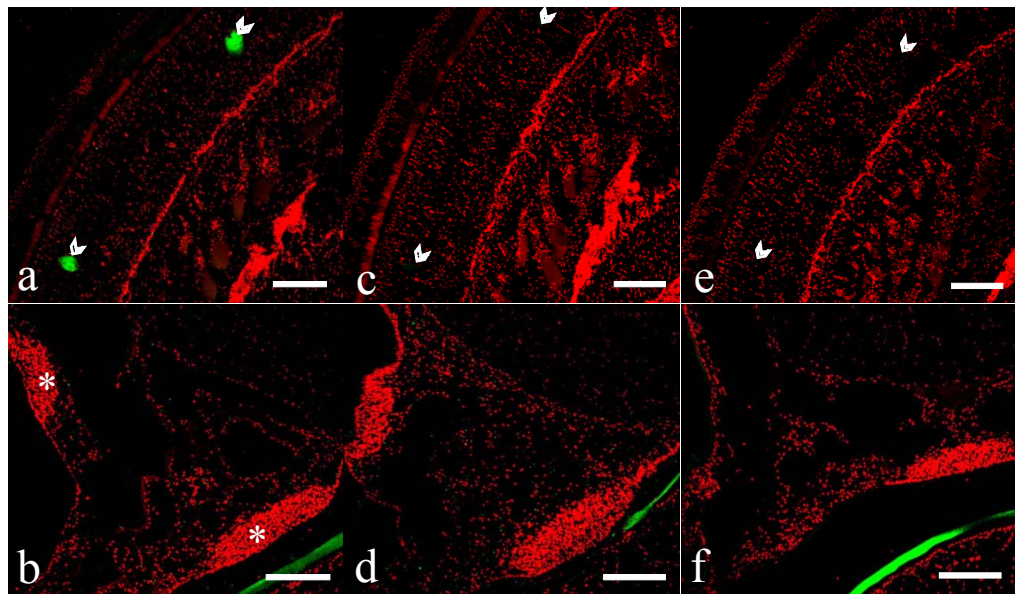
Figure 5-15   Light photomicrographs of the eyestalks (upper row) and Y-organs (lower row) of *Penaeus monodon* at intermolt stage of 6L:18D group captured under confocal laser microscope. The MIH-1 immunoreactivity of unidentified cells was detected at the fasciculated zone (arrowheads, a), the intensity was faint or hindered in immunoadsorption sections (arrowheads, c). The immunoreactivity was not found in Y-organs (asterisks in b). Sections were stained with anti-rMIH-1 polyclonal antibody adsorbed with *E. coli* lysate (a, b), purified MIH-1 (c, d), and control (e, f). Bars are 200 µm.
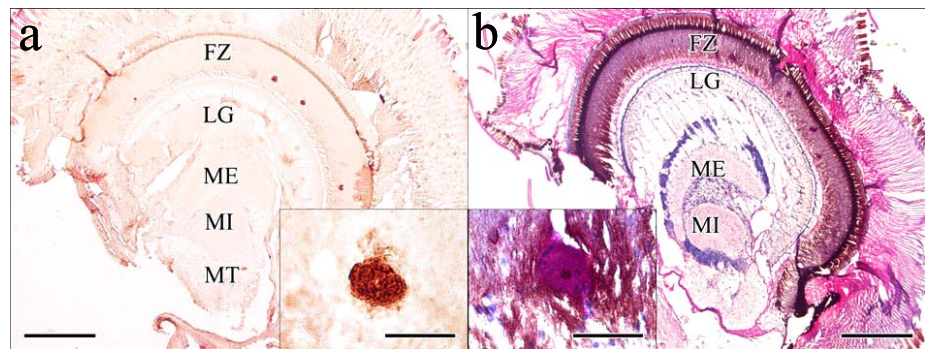
Figure 5-16   Light photomicrographs showing of MIH-1 immunoreactivity (**a**) and periodic acid-Schiff-positive (PAS) reaction (**b**) groups of structures in the fasciculated zone of the eyestalk of *Penaeus monodon*. The structures (enlarged in insets) showed reddish-brown reactivity to anti-rMIH-1 polyclonal antibody and purple-magenta to PAS. FZ, fasciculated zone; LG, lamina ganglionaris; ME, medulla externa; MI, medulla interna; MT, medulla terminalis. Sections were cut at 10 μm. Bars are 500 μm in large panels, and 50 μm in insets.
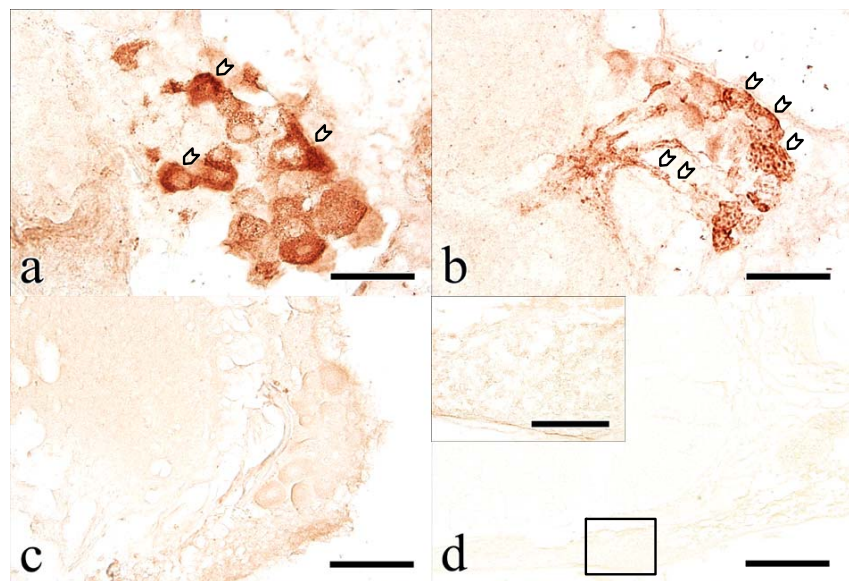
Figure 5-17   Light photomicrographs of MIH-1-immunoreactive cells of the medulla terminalis neurosecretory cells (**a** and **b**). Positive reaction was also found in the axons leading out from the cells (arrow heads, **b**). Negative reaction was found in the cells located in the medulla externa (**c**) and in Y-organ (**d**). Sections were cut at 10 μm. Bars at 50 μm were in **a** and **b**, 100 μm in **c** and inset in **d**, and 200 μm in **d**.

5.5 Intensity of MIH-1-Reactivity during Molt Cycle

In the MIH-1 immunohistochemistry, the number of reactive cells and the intensity of immuno-staining were arbitrarily graded into four levels, from weak (+) to very strong (++++) reactions (Table 5-2). In the medulla terminalis (Fig. 5-18) of the 12L:12D shrimp, strong reaction was observed at postmolt and intermolt, and moderate reaction at early premolt; weak to moderate reaction was observed in the late premolt. In the long-day shrimp, the reaction was rather weak at postmolt and became moderate at other stages; no strong reaction was observed in any of the molting stages. In short-day shrimp, moderate reaction was observed in the postmolt stage, and the reaction became stronger toward the late molt stage, which was registered as having a very strong reaction.
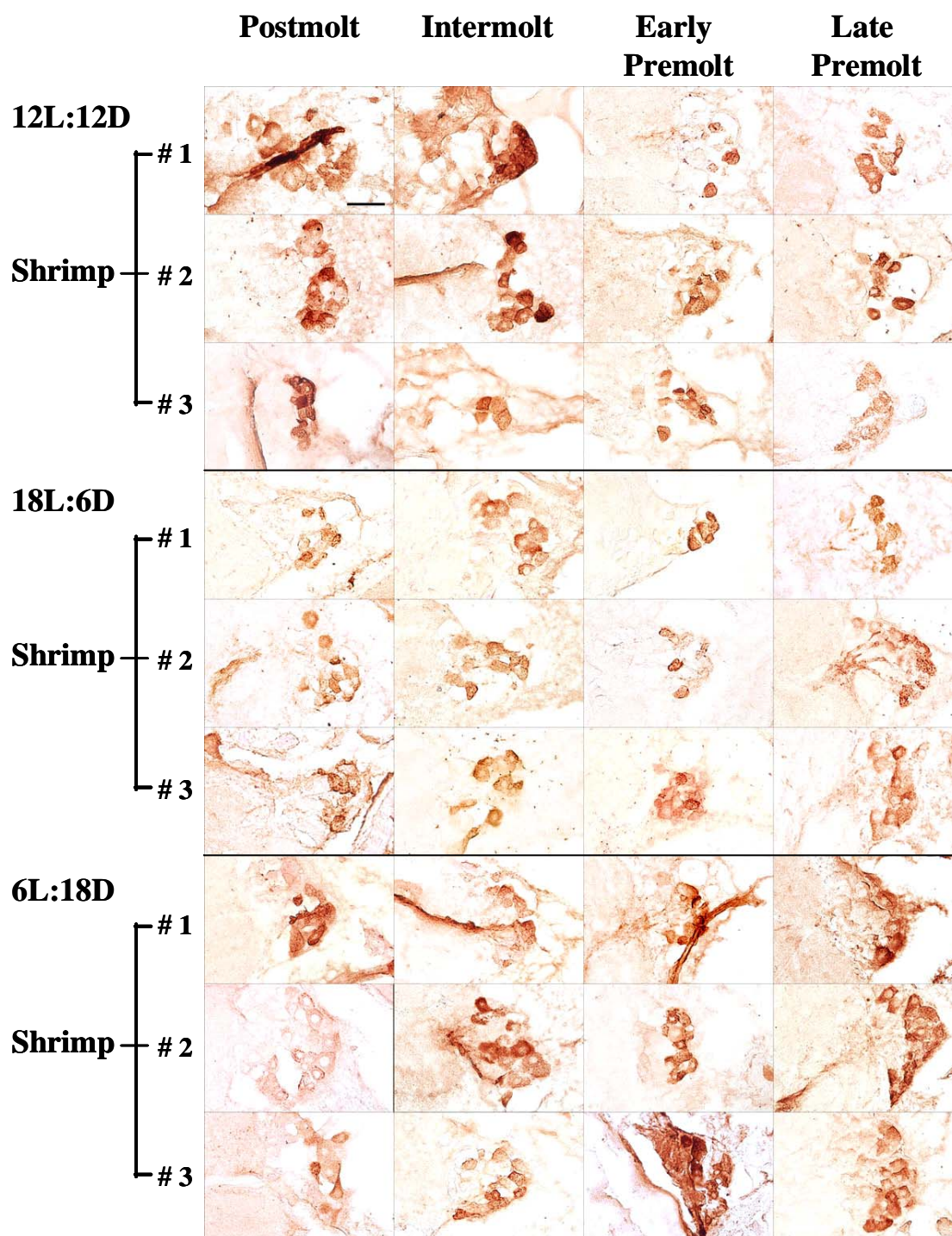
Figure 5-18 MIH-1 immunoreactive cells in the medulla terminalis of the eyestalk optic lobe of *Penaeus monodon* reared under normal (12L:12D), long (18L:6D) and short (6L:18D) photoperiods**.** Bar at 50 μm, applied to all sections

Table 5.2 Grading of MIH-1-immunoreacitity of the neurosecretory cells of the medulla terminalis in the optic lobe and in the sinus gland of *Penaeus monodon* reared under different photoperiod regimes. The levels of intensity were recorded as weak (+), moderate (++), strong (+++) and very strong (++++). Three shrimp were used per each molting stage.

The neurosecretory cells

Photoperiod Regimen	Molt Stage			
	Postmolt	Intermolt	Early Premolt	Late Premolt
12L:12D	+++	+++	++	++
18L:6D	+	++	++	++
6L:18D	++	++	+++	++++

In the sinus gland

Photoperiod Regimen	Molt Stage			
	Postmolt	Intermolt	Early Premolt	Late Premolt
12L:12D	+++	++++	++++	++++
18L:6D	+++	+++	++++	+++
6L:18D	+++	++++	++++	++++

In the SGs (Fig. 5-19), the immunoreaction in the normal- and short-day shrimp was rather strong in all molting stages, and tended to be very strong toward the late premolt stage. In the long-day shrimp, however, the reaction was rather variable, toward the moderate and strong sides, and was not much different among different stages.

Taking together, amount of MIH-1 storing in the SGs was rather consistently high, whereas the amount containing in the neurosecretory cells was more variable.
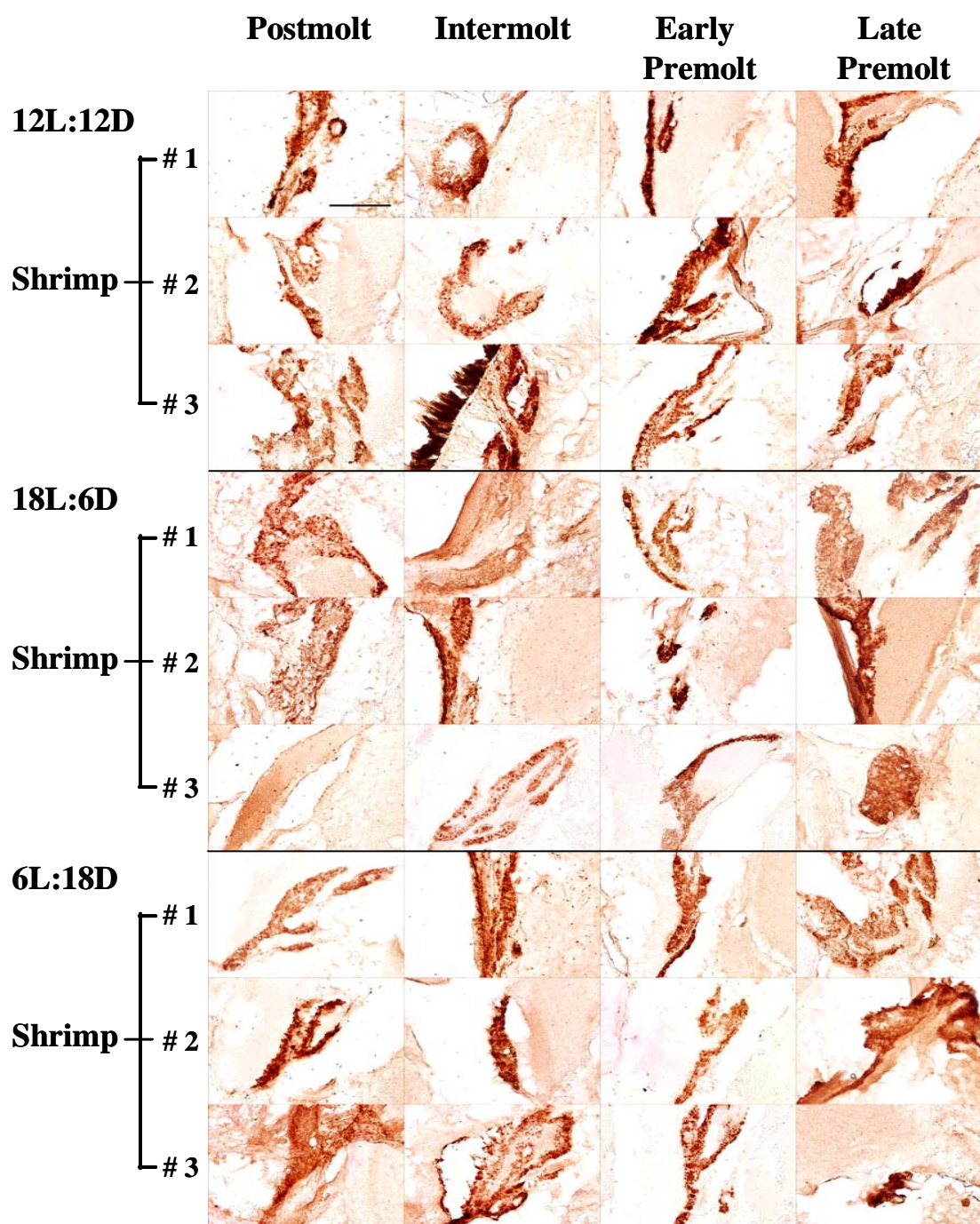
Figure 5-19 MIH-1 immunoreactive cells in the sinus gland of *Penaeus monodon* reared under normal (12L:12D), long (18L:6D) and short (6L:18D) photoperiods. Bar 100 μm, applied to all sections

CHAPTER VI

DISCUSSION

6.1 Survival, Growth and Molt

The results of this study showed that survival of *P. monodon* exposed to short-day photoperiod was lowest, and mortality occurred at the last cycle of molting, after staying in captivity for more than one month. The cause of death is unknown at present but it was not likely from unsuitable water qualities since the water was shared by the shrimp of the other two groups (normal- and long-day shrimp) and those shrimp survived normally. Infectious disease as a cause of death is also unlikely as the disease should spread to the other two groups since they were in the same water. It was most likely due to the effect of photoperiod that the shrimp were exposed to. Since most mortality occurred during premolt, it is likely that the cause of death was molt-related, probably hormonal imbalance caused by non-suitable lighting regimen.

Very few reports in literature mentioned about mortality in crustaceans exposed to short- or long-days. In the shrimp *P. argentinus*, it was long-day that caused high mortality (Díaz et al., 2003). It was also suggested that changes in hormonal levels induced by abnormal photoperiods was responsible for the mortality. In this study, ecdysteroid levels in the three groups of shrimp did not differ, therefore it is unlikely that abnormal ecdysteroid level was the cause of death in the shrimp. Injection of ecdysteroids into crustacean was reported to induce crustacean to enter premolt stage and resulted in high mortality (Hubschman and Armstrong, 1972; Rao et al., 1973; Chan et al., 1990). In this study, however, it is not the case since ecdysteroid levels in the short-day shrimp were normal. The level of MIH-1 peptides, as observed indirectly through immunohistochemistry, showed high intensity in the neurosecretory cells of the medulla terminalis, which may suggest either high (because of high synthesis) or low (because of the inhibition of release from the neurosecretory cells) level in the hemolymph; both may induce mortality. This hypothesis obviously cannot be proven in this study and thus needs further tests.

In this study, different photoperiod regimes did not seem to affect growth of *P. monodon*, although short-day had a tendency to slow down its growth rate. The difference may be there but not enough to reach statistically significant level. This is probably due to the fact that the animals that were kept in clear seawater, with small space (as in lab experiment), grow much slower than the shrimp in earthen ponds; thus the difference may not be high enough to become significant. It is interesting to see if the shrimp grow in earthen pond, but being exposed to short-day photoperiod, would have slow growth. Again, very few reports concerning the effects of photoperiod on growth appeared in literature. Similar to this study, in *P. indicus* (Vijayan and Diwan, 1995) and the crayfish *P. leniusculus* (Sáez-Royuela et al., 1996), photoperiods did not have any influence on survival and growth.

In this study, if the growth rate was lower in the short-day shrimp, it would be similar to what happened in juvenile lobster *Jasus edwardsii* (Crear et al., 2003); but how short-day brings about retarded growth was still unknown. It is possible that MIH-1 peptide level, either high or low, may play role in growth abnormality as well.

Others reported that light intensity was regarded as a stronger influence on growth rate than photoperiod. In juvenile *P. merguiensis*, light intensity of 750 lux promoted better growth with two imposing light/dark cycles, 7L:5D than at 75 lux in 12L:12D (Hoang et al., 2003). In *F. chiensis*, the specific growth rate was highest at 300 lux, and lowest at 5500 lux (Wang et al., 2004b). Light source was shown to affect growth rate as well. In *L. vannamei*, the metal halide lamp was recommended for indoor rearing since it provided higher growth rate than the fluorescent lamp (You et al., 2006). All these, however, are not relevant to this study since the light intensity and quality of light were the same in the three groups of shrimp.

Except for a shorter postmolt duration in the short-day shrimp, photoperiods did not affect the molting cycle of *P. monodon*. The result was similar to that of *P. indicus* (Vijayan and Diwan, 1995), but different from that of *P. argentinus,* when long-day shortened molt cycle (Díaz et al., 2003). The basis on this species-specific response to photoperiods is not known. And what accounts for the decrease postmolt duration in *P. monodon* is not known either; it could be due to the abnormal synthesis/release of MIH-1 as mentioned earlier. Moreover, the time of molting in relation to the onset of light or darkness seemed to play an important role in the

molting activity. The lobsters *Thenus orientalis* (Mikami and Greenwood, 1997) and *H. americanus* (Waddy and Aiken, 1999) molted synchronously after sunset. In *P. monodon*, it is observed in cultured pond that molting occurs mainly at night. Therefore it is possible that molting occurred during the dark period, and, for short-day shrimp, chance of molting would be more since darkness spanned for 18 hours. A slight non-significant decrease in the molting interval in the short-day shrimp may be the result of the molting stimulation by prolonged darkness.

6.2 Hemolymph Ecdysteroids

The profile of hemolymph ecdysteroids in *P. monodon* exposed to normal-day photoperiod during the molt cycle is similar to that of the crayfish *P. clarkii* (Nakatsuji et al, 2004), the crabs *C. maenas*, *C. sapidus*, and *M. messor* (Soumoff and Skinner, 1983; Lee et al., 1998; Suganthi and Anilkumar, 1999; Styrishave et al., 2004), the freshwater prawn *M. rosenbergii* (Okumura and Aida, 2000; Okumura, 2004), and the shrimp *P. vannamei* (Chan et al., 1988; Chen et al., 2007). The hormone was at basal level during the intermolt, gradually increased during early premolt and peaked at the late premolt. Administration of ecdysteroids, both *in vivo* and *in vitro*, induced an increase in protein production in the muscle and cuticle of the animals (Paulson and Skinner, 1991; El Haj et al., 1996), as well as an up-regulation of certain genes, such as *ACP-20*, in some animal (Braquart et al., 1996). In the shrimp *P. vannamei*, the synthesis of actin and myosin of the abdominal muscle was highest during the postmolt stage (de Oliveira Cesar et al., 2006). It is possible that peak of ecdysteroids at late premolt stage functions as a stimulator of protein synthesis during molt and postmolt, at the level of transcription.

This pattern of ecdysteroids in the hemolymph remained the same even *P. monodon* were exposed to long- and short-day photoperiods, while *MIH-1* pattern and MIH-1 immunoreactivity were noticeably changed by changes in the photoperiods. These results suggest that the synthesis/release of ecdysteroids in this species may not directly under influence of MIH-1. It was found that intracellular mechanisms of Y-organ play role in addition to MIH-1 action, which is semi-independent to MIH-1 (Baghdassarian et al., 1996; Nakatsuji et al., 2006; Nakatsuji et al., 2009).

6.3 *MIH-1* Transcription

A gradual decrease of *MIH-1* from postmolt to late premolt in normal-day *P. monodon* was similar to the findings in crab *C. sapidus* and in *P. vannamei* (Lee et al., 1998; Chen et al., 2007). In the Kuruma prawn *Penaeus japonicus* and the crab *Charybdis feriatus*, the peak was found in the intermolt (Ohira et al., 1997; Chan et al., 1998). On the contrary, *MIH* transcripts in the crab *C. maenas* tended to increase from intermolt toward premolt (Chung and Webster, 2003).

The gradual decrease toward late premolt of *MIH-1* in *P. monodon* is corresponded to a traditional concept that MIH inhibit the synthesis/release of ecdysteroids; the low level of *MIH* transcript and subsequently MIH allows ecdysteroids to reach peak at late premolt. This does not seem to be the case in the long- and short-day *P. monodon* as the premolt *MIH-1* was increased. The duration of light/dark perceived by the animals may send signals to neurosecretory cells of the medulla terminalis, resulting in changes in *MIH-1* transcript levels.

6.4 Specificity of MIH-1 Polyclonal Antibody

By Western blot analysis, anti-rMIH-1 pAb showed no cross-reactivity to other peptides in the CHH/MIH/GIH family at the dilution of 1:600. The binding of antibody to sinus gland extract on the membrane was at the size of ~ 17-18 kDa, which was approximately two-fold of the predicted size (~ 9 kDa) of the mature MIH-1 (Yodmuang et al., 2004). It is possible be the dimers of protein. However, antiserum was occasionally found binding to the suspected prohormone at the size of ~ 12 kDa as had been reported in *C. sapidus* (Lee and Watson, 2002). Note, the expected size at ~ 9 kDa could not be detected may be due to the low amount containing in the shrimp eyestalk.

By immunoadsorption with purified MIH-1, immunolocalization demonstrated very weak intensity at SG, MTXO, TG and unidentified cells. It could be verified that antiserum used was bound specific to the MIH-1 antigen on the target tissue.

6.5 MIH-1 Immunohistochemistry

The intensity of MIH-1 immunoreactivity in the neurosecretory cells of the medulla terminalis of the normal-day *P. monodon*, which was decreasing from postmolt to late premolt, is corresponded to the *MIH-1* transcript levels. The intensity in the SG, however, was not corresponded to the levels in the neurosecretory cells, remaining more or less the same throughout the molt cycle or showing a slight increase from postmolt toward late premolt. Or, at least, it did not show low MIH-1 intensity at late premolt MIH-1. As SG is the site of release of MIH-1, and other neurohormones, into hemolymph, it is possible that the increase intensity is due to the inhibition of MIH-1 release at SG.

MIH-immunoreactive cells were detected in the optic lobe of the crabs *C. sapidus* and *C. maenas* at intermolt stage, using fluorescent immunostaining; the immunoreactivity in the cells sized ~ 30 µm, and in their axons toward SG (Watson et al., 2001). In *C. maenas*, the staining was intense at the postmolt and intermolt but faint at premolt, and SG showed similar staining intensity in all molt stages. On the contrary, a study of MIH content in SG of crayfish *P. clarkii* and the crab *C. maenas* revealed its peak during early premolt and at basal level during late and very late premolt stages (Nakatsuji et al., 2000; Chung and Webster, 2005). Imayavaramban et al., (2007) claimed that MIH-immunoreactivity in the swimming crab *Scylla serrata*, were detected in the optic lobe in postmolt and intermolt stages, and the positive reaction was also found on the membrane of Y-organ, with high intensity at postmolt and intermolt, but weakly at the premolt stages. Correspondingly, immunoblotting of protein from XOSG was strong from postmolt to intermolt and weak at premolt stages. Their findings suggest that MIH is synthesized and released mainly during the postmolt and intermolt stages. These findings were comparable to the MTXO immunoreactivity of *P. monodon* at normal day in this study, however MIH immunoreactivity on YO was not revealed.

In the lobsters *J. lalandii* and *P. homarus*, and crab *C. maenas,* co-localization of CHH and MIH were observed within the same cell (Marco and Gäde, 1999). In our study, we did not stain for CHH or other related peptides, it is thus not possible to know if the co-localization exists.

In the long-day shrimp, the MIH-1- immunoreactivity did not seem to correlate with *MIH-1* transcript; for instance, weak immuno-staining was observed in the late premolt but the transcript level was high. No explanation can be offered at present. It is possible that the abnormal exposure to light had influence on gene expression but not on peptide synthesis. In short-day shrimp, MIH-1-immunoreactivity was prominent in the late premolt, which was corresponded to high level of *MIH-1* transcript. Again, several postulates could be offered but it is better not to until being proven by further studies.

CHAPTER VII
CONCLUSIONS

1. Long (18L:6D)- or short (6L:18D)-day photoperiods did not change molt intervals and durations of each molting stage of *Penaeus monodon*, compared to those of the shrimp exposed to normal (12L:12D)-day photoperiod.

2. Both short-and long-day photoperiods did not change the growth of *P. monodon*, but short-day photoperiod caused significant mortality of the shrimp.

3. Both short-and long-day photoperiods did not change the pattern and levels of hemolymph ecdysteroids during the entire molt cycle.

4. *MIH-1* gene expression in the optic lobe of *P. monodon* exposed to normal-day photoperiod was gradually decreased from postmolt to late premolt stage. This pattern was not observed in the shrimp exposed to long- and short-day photoperiods. In general the expressions were variably higher than those in the normal-day shrimp.

5. MIH-1-immunoreactivity was observed in the neurosecretory cells of the medulla terminalis or MTXO and the intensity in the normal-day shrimp was gradually decreased from postmolt to late premolt, corresponding to the levels of *MIH-1* gene expression in the optic lobe. However, the level in the sinus gland was intense throughout the molt cycle. In the long-day shrimp the MIH-1 immunoreactivity in the neurosecretory cells was variably lower than that of the normal-day shrimp. In the short-day shrimp, the intensity was higher at late premolt than that at postmolt and intermolt, which was opposite to the pattern observed in the normal-day shrimp.

REFERENCES

1.   Aiken DE. Photoperiod, endocrinology and the crustacean molt cycle. Science. 1969 Apr 11;164(876):149-155.

2.   Aoto T, Kamiuchi Y, Hisano S. Histological and ultrastructural studies on the Y organ and mandibular organ of the freshwater prawn, *Palaemon paucidens* with special reference to their relation with the molting cycle. Journal of the Faculty of Science Hokkido University. Series VI. Zoology. 1974 Apr;19(2):295-308.

3.   Armitage KB, Buikema AL, William NJ. The effect of photoperiod on organic constituents and molting of the crayfish *Orconectes nais* (Faxon). Comp Biochem Physiol. 1973;44A:431-456.

4.   Baghdassarian D, de Bessé N, Saïdi B, Sommé G, Lachaise F. Neuropeptide-induced inhibition of steroidogenesis in crab molting glands: involvement of cGMP-dependent protein kinase. Gen Comp Endocrinol. 1996 Oct;104(1):41-51.

5.   Baldalia L, Porcheron P, Coimbra J, Cassier P. Ecdysteroids in the shrimp *Palaemon serratus;* relations with molt cycle. Gen Comp Endocrinol. 1984 Sep;55(3):437-443.

6.   Bell TA, Lightner DV. A Handbook of Normal Penaeid Shrimp Histology. Louisiana: World Aquaculture Society; 1988, 114 p.

7.   Birkenbeil H, Gersch M. Ultrastructure of the Y-organ of *Astacus astacus* (L.) (Crustacea) in relation to the moult cycle, Cell Tissue Res. 1979 Feb 28;196(3):519-524.

8.   Bliss DE, Durand JB, Welsh JH. Neurosecretory systems in decapod crustacean. Cell Tissue Res. 1954 Sep;39(5):520-536.

9.   Bliss DE. Environmental regulation of growth in the decapod crustacean *Gecarcinus lateralis*. Gen Comp Endocrinol. 1964 Feb;15:15-41.

10.   Braquart C, Bouhin H, Quennedey A, Delachambre J. Up-regulation of an adult cuticular gene by 20-hydroxyecdysone in insect metamorphosing epidermis cultured *in vitro*. Eur J Biochem. 1996 Sep 1;240(2):336-341.

11.   Buchholz C, Adelung D. The ultrastructural basis of steroid production in the Y-organ and the mandibular organ of the crabs *Hemigrapsus nudus* (Dana) and *Carcinus maenas* L. Cell Tissue Res. 1980;206(1):83-94.

12.   Buchholz F. Drach's molt staging system adapted for euphausiids. Mar Biol. 1982 Feb; 66(3);301-305.

13.   Cameron JN. Post-moult calcification in the blue crab, *Callinectes sapidus*: timing and mechanism. J Exp Biol. 1989;143(1):285-304.

14.   Castañon-Cervantes O, Lugo C, Aguilar M, Gonzalez-Moran G, Fanjul-Moles ML. Photoperiodic induction on the growth rate and gonads maturation in the crayfish *Procambarus clarkii* during ontogeny. Comp Biochem Physiol A Physiol. 1995 Feb;110(2):139-146.

15.   Chan SM, Rankin SM, Keeley LL. Characterization of the molt stages in *Penaeus vannamei:* setogenesis and hemolymph levels of total protein, ecdysteroids, and glucose. Biol Bull. 1988 Oct;175:185-192.

16.   Chan SM, Rankin SM, Keeley LL. Effects of 20-hydroxyecdysone injection and eyestalk ablation on the moulting cycle of the shrimp, *Penaeus vannamei*. Comp Biochem Physiol A Comp Physiol. 1990; 96(1) 205-209.

17.   Chan SM, Chen XG, Gu PL. PCR cloning and expression of the molt-inhibiting hormone gene for the crab (*Charybdis feriatu*s). Gene. 1998 Dec 11;224(1-2):23-33.

18.   Chang ES, O'Connor JD. Secretion of alpha-ecdysone by crab Y-organs *in vitro*. Proc Natl Acad Sci U S A. 1977 Feb;74(2):615-618.

19.   Chang ES, O'Connor JD. In vitro secretion and hydroxylation of alpha-ecdysone as a function of the crustacean molt cycle. Gen Comp Endocrinol. 1978 Sep;36(1):151-210.

20.   Chang ES, Bruce MJ, Tamone SL. Regulation of crustacean molting: a multi-hormonal system. Integr Comp Biol. 1993;33(3):324-329.

21. Charmantier-Daures M, Vernet G. Moulting, autotomy, and regenration. In : Forest J, von Vaupel Klein JC, editors. The crustacea. Leiden : Koninklijke Brill NV ; 2004. p. 161-255.

22. Chen HY, Watson RD, Chen JC, Liu HF, Lee CY. Molecular characterization and gene expression pattern of two putative molt-inhibiting hormones from *Litopenaeus vannamei*. Gen Comp Endocrinol. 2007 Mar;151(1):72-81.

23. Chockley BR, Mary CM. Effects of body size on growth, survivorship, and reproduction in the banded coral shrimp (*Stenopus hispidus*). J Crustac Biol. 2003 Dec; 23(4):836-848.

24. Chung JS, Dircksen H. Webster SG. A remarkable, precisely timed release of hyperglycemic hormone from endocrine cells in the gut is associated with ecdysis in the crab *Carcinus maenas*. Proc Natl Acad Sci U S A. 1999 Nov 9;96(23):13103-13107.

25. Chung JS, Webster SG. Moult cycle-related changes in biological activity of moult inhibiting hormone (MIH) and crustacean hyperglycaemic hormone (CHH) in the crab, *Carcinus maenas.* Eur J Biochem. 2003 Aug;270(15):3280-3288.

26. Chung JS, Webster SG. Dynamics of in vivo release of molt-inhibiting hormone and crustacean hyperglycemic hormone in the shore crab, *Carcinus maenas*. Endocrinology. 2005 Dec;146(12):5545-5551

27. Comeau M, Savoie F. Growth increment and molt frequency of the American lobster (*Homarus americanus*) in the southwestern Gulf of St. Lawrence. J Crustac Biol. 2001Nov;21(4):923-936.

28. Covi JA, Chang ES, Mykles DL. Conserved role of cyclic nucleotides in the regulation of ecdysteroidogenesis by the crustacean molting gland. Comp Biochem Physiol A Mol Integr Physiol. 2009 Apr;152(4):470-477.

29. Crear BJ, Hart PR, Thomas CW. The effect of photoperiod on growth, survival, colour and activity of juvenile southern rock lobster, *Jasus edwardsii*. Aquac Res. 2003 Apr;34(6):439-444.

30. De Oliveira Cesar JR, Zhao B, Malecha S, Ako H, Yang J. Morphological and biochemical changes in the muscle of the marine shrimp *Litopenaeus*

vannamei during the molt cycle. Aquaculture 2006 Nov 24;261(2):688–694.

31. Dell S, Sedlmeier D, Bocking D, Dauphin-Villemant C. Ecdysteroid biosynthesis in crayfish Y-organs: feedback regulation by circulating ecdysteroids. Arch Insect Biochem Physiol. 1999;41(3):148-155.

32. Díaz AC, Sousa LG, Cuartas EL, Petriella AM. Growth, molt and survival of *Palaemonetes argentinus* (Decapoda, Caridea) under different light-dark conditions. Iheringia Sér Zool. 2003;93:249-254.

33. Dircksen H, Webster SG, Keller R. Immunocytochemical demonstration of the neurosecretory systems containing putative moult-inhibiting hormone and hyperglycemic hormone in the eyestalk of brachyuran crustaceans. Cell Tissue Res. 1988 Jan;251(1):3-12.

34. Dauphin-Villemant C, Böcking D, Sedlmeier D. Regulation of steroidogenesis in crayfish molting glands: involvement of protein synthesis. Mol Cell Endocrinol. 1995 Mar;109(1):97-103.

35. Durand JB. Neurosecretory cell types and their secretory activity in the crayfish. Biol Bull. 1956 Aug;111:62-76.

36. El Haj AJ, Houlihan DF. *In vitro* and *in vivo* protein synthesis rates in a crustacean muscle during the moult cycle. J Exp Biol. 1987;127:413–426.

37. El Haj AJ, Clarke SR, Harrison P, Chang ES. *In vivo* muscle protein synthesis rates in the American lobster *Homarus americanus* during the moult cycle and in response to 20-hydroxyecdysone. J Exp Biol. 1996;199(Pt 3):579-585.

38. Gardner C, Maguire GB. Effects of photoperiod and light intensity on survival, development and cannibalism of larvae of the Australian giant crab *Pseudocarcinus gigas* (Lamarck). Aquaculture 1998;165:51-63.

39. Gliscynski UV, Sedlmeier D. Regulation of ecdysteroid biosynthesis in crayfish Y-organs: II. Role of cyclic nucleotide-dependent protein kinases. J Exp Zool. 1993;265 (4): 454-458

40. Graf F, Delbecque JP. Ecdysteroid titers during the molt cycle of *Orchestia cavimana* (Crustacea, Amphipoda). Gen Comp Endocrinol. 1987 Jan;65(1):23-33.

41.   Greenaway P. Uptake of calcium during the postmoult stage by the marine crabs *Callinectes sapidus* and *Carcinus maenas*. Comp Biochem Physiol. 1983;75A (2):181-184.

42.   Gunamalai V, Kirubagaran R, Subramoniam T. Hormonal coordination of molting and female reproduction by ecdysteroids in the mole crab *Emerita asiatica* (Milne Edwards). Gen Comp Endocrinol. 2004 Sep 1;138(2):128-138.

43.   Gunamalai V, Subramoniam T. Synchronisation of molting and oogenetic cycles in a continuously breeding population of the sand crab *Emerita asiatica* on the madras coast, South India. J Crustac Biol. 2002;22(2);398-410.

44.   Guyselman JB. An analysis of the molting process in the fiddler crab, *Uca pugilator*. Biol Bull. 1953 Apr;104(2):115-137.

45.   Harpaz S, Kahan D, Moriniere M, Porcheron P. Level of ecdysteroids in the hemolymph of the freshwater prawn, *Macrobrachium rosenbergii* (Crustacea: Decapoda) in relation to the phenomenon of cheliped autotomy in males. Cell Mol Life Sci. 1987 Aug;43(8):901-902.

46.   Hoang T, Barchiesis M, Lee SY, Keenan CP, Marsden GE. Influences of light intensity and photoperiod on moulting and growth of *Penaeus merguiensis* cultured under laboratory conditions. Aquaculture 2003 Feb;216(1):343-354.

47.   Hubschman JH, Armstrong PW. Influence of ecdysone on molting in *Palaemonetes*. Gen Com Endocrinol. 1972;18:435-438.

48.   Imayavaramban L, Dhayaparan D, Devaraj H. Molecular mechanism of molt-inhibiting hormone (MIH) induced suppression of ecdysteroidogenesis in the Y organ of mud crab: *Scylla serrata*. FEBS Lett. 2007 Nov 13;581(27):5167-5172.

49.   Kang BK, Spaziani E. Uptake of high-density lipoprotein by Y-organs of the crab Cancer antennarius: III. Evidence for adsorptive endocytosis and the absence of lysosomal processing. J Exp Zool. 1995 Dec 1;273(5):425-433.

50.   Katayama H, Nagata K, Ohira T, Yumoto F, Tanokura M, Nagasawa H. The solution structure of molt-inhibiting hormone from the Kuruma prawn *Marsupenaeus japonicus*. J Biol Chem. 2003 Mar 14;278(11):9620-9623.

51. Keller R. Crustacean neuropeptides: Structures, functions and comparative aspects. Experientia. 1992 May 15;48(5):439-448.

52. Kim HW, Batista LA, Hoppes JL, Lee KJ, Mykles DL. A crustacean nitric oxide synthase expressed in nerve ganglia, Y-organ, gill and gonad of the tropical land crab, *Gecarcinus lateralis*. J Exp Biol. 2004 Jul;207(Pt 16):2845-2857.

53. Kruschwitz LG. Environmental factors controlling reproduction of the amphipod *Hyalella azteca*. Proc Okla Acad Sci. 1978; 58: 16-21.

54. Kuo C-M, Lin W-W. Changes in morphological characteristics and ecdysteroids during the molting cycle of tiger shrimp, *Penaeus monodon* Fabricus. Zoolog Sci. 1996;35(2):118-127.

55. Kuballa A, Elizur A. Novel molecular approach to study moulting in crustaceans. Bull Fish Res Agen. 2007;no.23:53-57.

56. Kubista M, Andrade JM, Bengtsson M, Forootan A, Jonák J, Lind K, Sindelka R, Sjöback R, Sjögreen B, Strömbom L, Ståhlberg A, Zoric N. The real-time polymerase chain reaction. Mol Aspects Med. 2006 Apr-Jun;27(2-3):95-125. Epub 2006 Feb 3. Review.

57. Kurup NG. Effects of photoperiodism on moulting in *Hemigraphsus nudus* Dana. Curr Sci. 1970;39(7):149-151.

58. Laemmli UK. Cleavage of structural proteins during the assembly of the head of bacteriophage T4. Nature. 1970 Aug 15;227(5259):680-685.

59. Laufer H, Ahl J, Rotllant G, Baclaski B. Evidence that ecdysteroids and methyl farnesoate control allometric growth and differentiation in a crustacean. Insect Biochem Mol Biol. 2002 Feb;32(2):205-210.

60. Lee KJ, Watson RD, Rosr RD. Molt-inhibiting hormone mRNA levels and ecdysteroid titer during a molt cycle of the blue crab, *Callinectes sapidus*. Biochem Biophys Res Commun. 1998 Aug 28;249(3):624-627.

61. Lee KJ, Watson RD. Antipeptide antibodies for detecting crab (*Callinectes sapidus*) molt-inhibiting hormone. Peptides. 2002 May;23(5):853-862.

62. Lee SG, Bader BD, Chang ES, Mykles DL. Effects of elevated ecdysteroid on tissue expression of three guanylyl cyclases in the tropical land crab

Gecarcinus lateralis: possible roles of neuropeptide signaling in the molting gland. J Exp Biol. 2007 Sep;210(Pt 18):3245-3254.

63. Lucas KA, Pitari GM, Kazerounian S, Ruiz-Stewart I, Park J, Schulz S, Chepenik KP, Waldman SA. Guanylyl cyclases and signaling by cyclic GMP. Pharmacol Rev. 2000 Sep;52(3):375-414.

64. Lytle DA. Convergent growth regulation in arthropods: biological fact or statistical artifact? Oecologia 2001 Jun;128(1):56-61.

65. Mangum CP, deFur PL, Fields JHA, Henry RP, Kormanik GA, McMahon BR, Towle DW, Wheatly MG. Physiology of the blue crab *Callinectes sapidus* Rathbun during a molt. National Symposium of the Soft-Shelled Blue Crab Fishery 1985 Feb 12-13:1-12.

66. Marco HG, Gäde G. A comparative immunocytochemical study of the hyperglycaemic, moult-inhibiting and vitellogenesis-inhibiting neurohormone family in three species of decapod crustacea. Cell Tissue Res. 1999 Jan;295(1):171-182.

67. Mattson MP, Spaziani E. Evidence for ecdysteroid feedback on release of molt-inhibiting hormone from crab eyestalk ganglia. Biol Bull. 1986 Aug;171:264-273.

68. Mattson MP, Spaziani E. Demonstration of protein kinase C activity in crustacean Y-organs, and partial definition of its role in regulation of ecdysteroidogenesis. Mol Cell Endocrinol. 1987 Feb;49(2-3):159-171.

69. McCarthy JF. Ecdysone metabolism in premolt land crabs (*Gecarcinus lateralis*). Gen Comp Endocrinol. 1982 Jul;47(3):323-332.

70. Miller TW, Hankin DG. Descriptions and durations of premolt setal stages in female Dungeness crabs, *Cancer magister*. Mar Biol. 2004 Jan;144(1):101-110.

71. Mattson MP, Spaziani E. Evidence for ecdysteroid feedback on release of molt-inhibiting hormone from crab eyestalk ganglia. Biol Bull. 1986 Aug;171:264-273.

72. Mattson MP, Spaziani E. Demonstration of protein kinase C activity in crustacean Y-organs, and partial definition of its role in regulation of ecdysteroidogenesis. Mol Cell Endocrinol. 1987 Feb;49(2-3):159-171

73.   McCarthy JF. Ecdysone metabolism in premolt land crabs (*Gecarcinus lateralis*). Gen Comp Endocrinol. 1982 Jul;47(3):323-332

74.   Mikami S, Greenwood JG. Influence of light regimes on phyllosomal growth and timing of moulting in *Thenus orientalis* (Lund) (Decapoda: Scyllaridae). Mar Freshw Res. 1997;48(8):abstract.

75.   Molthathong S, Senapin S, Klinbunga S, Puanglarp N, Rojtinnakorn J, Flegel TW. Down-regulation of defender against apoptotic death (DAD1) after yellow head virus (YHV) challenge in black tiger shrimp *Penaeus monodon.* Fish Shellfish Immunol. 2008 Feb;24(2):173-179.

76.   Mykles DL. The mechanism of fluid absorption at ecdysis in the American lobster, *Homarus americanus*. J Exp Biol. 1980 Feb 1;84:89-102.

77.   Nagaraju GPC, Reddy PR, Reddy PS. Mandibular organ: it's relation to body weight, sex, molt and reproduction in the crab, *Oziotelphusa senex senex* Fabricius (1791). Aquaculture 2004;232(1-4):603-612.

78.   Nagaraju GPC, Reddy PR. Isolation and characterization of mandibular organ – inhibiting hormone from the eyestalks of freshwater crab, *Oziotelphusa Senex Senex.* Int J App Sci Eng. 2005;3:61-68.

79.   Nagaraju GPC, Reddy PR, Reddy PS. *In vitro* methyl farnesoate secretion by mandibular organs isolated from different molt and reproductive stages of the crab *Oziotelphusa senex senex*. Fish Sci. 2006 Apr;72(2):410-414.

80.   Nakatsuji T, Keino H, Tamura K, Yoshimura S, Kawakami T, Aimoto S, Sonobe S. Changes in the amounts of the molt-inhibiting hormone in sinus glands during the molt cycle of the American crayfish, *Procambarus clarkii*. Zoolog Sci. 2000 Nov 1;17(8):1129-1136.

81.   Nakatsuji T, Sonobe H. Measurement of molt-inhibiitng hormone titer in hemolymph of the American crayfish, *Procambarus clarkii*, by time-resolved flouroimmunoassay. Zoolog Sci. 2003;20:999-1001

82.   Nakatsuji T, Sonobe H. Regulation of ecdysteroid secretion from the Y-organ by molt-inhibiting hormone in the American crayfish, *Procambarus clarkii*. Gen Comp Endocrinol. 2004 Feb;135(3):358-364.

83.   Nakatsuji T, Han DW, Jablonsky MJ, Harville SR, Muccio DD, Watson RD. Expression of crustacean (*Callinectes sapidus*) molt-inhibiting hormone in

Escherichia coli: characterization of the recombinant peptide and assessment of its effects on cellular signaling pathways in Y-organs. Mol Cell Endocrinol. 2006 Jul 11;253(1-2):96-104.

84. Nakatsuji T, Lee CY, Watson RD. Crustacean molt-inhibiting hormone: structure, function, and cellular mode of action. Comp Biochem Physiol A Mol Integr Physiol. 2009 Feb;152(2):139-148.

85. Neufeld DS, Cameron JN. Transepithelial movement of calcium in crustaceans. J Exp Biol. 1993 Nov;184:1-16

86. Ohira T, Watanabe T, Nagasawa H, Aida K. Molecular cloning of a molt-inhibiting hormone cDNA from the kuruma prawn *Penaeus japonicus*. Zoolog Sci. 1997 Oct;14(5):785-789.

87. Okumura T, Aida K. Fluctuations in hemolymph ecdysteroid levels during the reproductive and non-reproductive molt cycles in the giant freshwater prawn *Macrobrachium rosenbergii*. Fish Sci. 2000;66(5):876-883.

88. Okumura T, Sakiyama K. Hemolymph levels of vertebrate-type steroid hormones in female kuruma prawn *Marsupenaeus japonicus* (crustacea: decapoda: penaeidae) during natural reproductive cycle and induced ovarian development by eyestalk ablation. Fish Sci 2004 June;70(3):372-380.

89. Paulson CR, Skinner DM. Effects of 20-hydroxyecdysone on protein synthesis in tissues of the land crab *Gecarcinus lateralis*. J Exp Zool. 1991;257(1):70-79.

90. Promwikorn W, Kirirat P, Intasaro P, Withyachumnarnkul B. Changes in integument histology and protein expression related to the molting cycle of the black tiger shrimp, *Penaeus monodon*. Comp Biochem Physiol B Biochem Mol Biol. 2007 Sep;148(1):20-31.

91. Pyle RW. The histogenesis and cyclic phenomena of the sinus gland and X-organ in crustacean. Biol Bull. 1943 Oct;85:87-102.

92. Quackenbush LS, Herrnkind WF. Regulation of the molt cycle of the spiny lobster, *Panulirus argus*: Effect of photoperiod. J Comp Physiol. 1983;76A:259-263.

93. Rao KR, Fingerman SW, Fingerman M. Effects of exogenous ecdysone on the molt cycles of fourth and fifth stage American lobster, *Homarus americanus*. Comp Biochem Physiol A Comp Physiol. 1973;44:1105-1120.

94. Rönnbäck P. Shrimp aquaculture - State of the art. Swedish EIA Centre, Report 1 Uppsala: Swedish University of Agricultural Sciences (SLU); 2001. Report no.: ISBN 91-576-6113-8,58 p.

95. Rutledge R, Côté C. Mathematics of quantitative kinetic PCR and the application of standard curves. Nucleic Acids Res. 2003 Aug 15;31(16):e93.

96. Sáez-Royuela M, Carral JM, Celada JD, Muñoz C, Pérez JR. Modified photoperiod and light intensity influence on survival and growth of stage 2 juvenile signal crayfish *Pacifastacus leniusculus*. Journal of Applied Aquaculture 1996, abstract

97. Seinsche A, Sedlmeier D. Ecdysteroid synthesis in crustacean Y-organs. Role of Ca^{2+}. Ann N Y Acad Sci.1998; 839: 594-595.

98. Sefiani M, Le Caer JP, Soyes D. Characterization of hyperglycemic and molt-inhibiting activity from sinus glands of the penaeid shrimp *Penaeus vannamei*. Gen Comp Endocrinol. 1996 Jul;103(1):41-53.

99. Shih TW, Suzuki Y, Nagasawa H, Aida K. Immunohistochemical identification of hyperglycemic hormone- and molt-inhibiting hormone-producing cells in the eyestalk of the kuruma prawn, *Penaeus japonicus*. Zoolog Sci. 1998 Jun 1;15(3):389-397.

100. Saïdi B, de Bessé N, Webster SG, Sedlmeier D, Lachaise F. Involvement of cAMP and cGMP in the mode of action of molt-inhibiting hormone (MIH) a neuropeptide which inhibits steroidogenesis in a crab. Mol Cell Endocrinol. 1994 Jun;102(1-2):53-61.

101. Šindelka R, Ferjentsik Z, Jonák J. Developmental expression profiles of *Xenopus laevis* reference genes. Dev Dyn. 2006 Mar;235(3):754-758.

102. Sithigorngul P, Panchan N, Vilaivan T, Sithigorngul W, Petsom A. Immunochemical analysis and immunocytochemical localization of crustacean hyperglycemic hormone from the eyestalk of *Macrobrachium*

rosenbergii. Comp Biochem Physiol B Biochem Mol Biol. 1999 Sep;124(1):73-80

103. Skinner DM. The structure and metabolism of a crustacean integumentary tissue during a molt cycle. Biol Bull. 1962 Dec;123(3):635-647.

104. Snyder MJ, Chang ES. Ecdysteroids in relation to the molt cycle of the American lobster, *Homarus americanus* : I. Hemolymph titers and metabolites. Gen Comp Endocrinol. 1991 Jan;81(1):133-145.

105. Soumoff C, Skinner DM. Ecdysteroid titers during the molt cycle of the blue crab resembles those of other crustacea. Biol Bull. 1983;165(1):321-329.

106. Soumoff C, Skinner DM. Ecdysone 20-monooxygenase activity in land crabs. Comp Biochem Physiol, Part C: Toxicol Pharmacol. 1988;91:139–141.

107. Spaziani E, Wang WL. Biosynthesis of ecdysteroid hormones by crustacean Y-organs: conversion of cholesterol to 7-dehydrocholesterol is suppressed by a steroid 5 alpha-reductase inhibitor. Mol Cell Endocrinol. 1993 Sep;95(1-2):111-114.

108. Spaziani E, Mattson MP, Wang WL, McDougall HE. Signaling pathways for ecdysteroid hormone synthesis in crustacean Y-organs. Amer Zool.1999 Jun 39 (3):496-512.

109. Spaziani E, Jegla TC, Wang WL, Booth JA, Connolly SM, Conrad CC, Dewall MJ, Sarno CM, Stone DK, Montgomery R. Further studies on signaling pathways for ecdysteroidogenesis in crustacean Y-Organs. Amer Zool. 2001 June 1;41(3): 418-429.

110. Spindler KD, Van Wormhoudt A, Sellos D, Spindler-Barth M. Ecdysteroid levels during embryogenesis in the shrimp, *Palaemon serratus* (crustacea, decapoda): quantitative and qualitative changes. Gen Comp Endocrinol. 1987 Apr;66(1):116-122.

111. Stephens GC. Induction of molting in the crayfish, *Cambarus*, by modification of daily photoperiod. Biol Bull. 1955 Apr;108:235-241.

112. Stevenson JR. Changing activities of the crustacean epidermis during the molting cycle. Am Zool. 1972;12(2):373-379.

113. Stoffel LA, Hubschman JH. Limb loss and the molt cycle in the fresh water shrimp, *Palaemonetes kadiakensis*. Biol Bull. 1974 Aug;147(1):203-212.

114. Styrishave B, Rewitz K, Lund T, Andersen O. Variations in ecdysteroid levels and Cytochrome p450 expression during moult and reproduction in male shore crabs *Carcinus maenas*. Mar Ecol Prog Ser. 2004;274:215–224.

115. Suganthi AS, Anikumar G. Moult-related fluctuation in ecdysteroid titre and spermatogenesis in the crab, *Metopographus messor* (brachura: decapoda). Zool Stud. 1999;38(3):314-321.

116. Suzuki S. Effect of Y-organ removal on limb regeneration and molting in the terrestrial crab, *Sesarma haematocheir*. Gen Comp Endocrinol. 1985 May;58(2):202-210.

117. Tang C, Lu W, Wainwright G, Webster SG, Rees HH, Turner PC. Molecular characterization and expression of mandibular organ-inhibiting hormone, a recently discovered neuropeptide involved in the regulation of growth and reproduction in the crab *Cancer pagurus*. Biochem J. 1999 Oct 15;343 Pt 2:355-360.

118. Travis DF. The molting cycle of the spiny lobster, *Panulirus argus* Latreille. I. Molting and growth in laboratory-maintained individuals. Biol Bull. 1954;107(3):433-450.

119. Travis DF. The molting cycle of the spiny lobster, *Panulirus argus* Latreille. IV. Post-ecdysial histological and histochemical changes in the hepatopancreas and integumental tissues. Biol Bull. 1957;113(3):451-479.

120. Treece GD. Shrimp maturation and spawning. Texas: Texas A&M University; 2000. Report No.: 28.14 p.

121. Treerattrakool S, Udomkit A, Sonthayanon B, Panyim S. Expression of biologically active crustacean hyperglycemic hormone (CHH) of *Penaeus monodon* in *Pichia pastoris*. Mar Biotechnol. 2003;5:373-379.

122. Treerattrakool S, Udomkit A, Panyim S. Anti-CHH antibody causes impaired hyperglycemia in *Penaeus monodon*. J Biochem Mol Biol. 2006 Jul 31;39(4):371-376.

123. Treerattrakool S. Molecular and functional characterization of gonad-inhibiting hormone (GIH) from the shrimp [dissertation]. (Salaya campus): Mahidol university, Institute of Molecular genetics and genetic engineering; 2008

Sep. Figure 66, Tricine SDS-PAGE of rPem-GIH protein eluted from polyacrylamide gel by electro-eluter; p. 136.

124. Treerattrakool S. Molecular and functional characterization of gonad-inhibiting hormone (GIH) from the shrimp [dissertation]. [Salaya campus): Mahidol university, Institute of Molecular genetics and genetic engineering; 2008 Sep. Figure 69, Sensitivity of anti-Pem-GIH antibody by western blot analysis; p. 139.

125. Treerattrakool S, Panyim S, Chan SM, Withyachumnarnkul B, Udomkit A. Molecular characterization of gonad-inhibiting hormone of *Penaeus monodon* and elucidation of its inhibitory role in vitellogenin expression by RNA interference. FEBS J. 2008 Mar;275(5):970-980.

126. Vanitchviriakit R, Khuevaisayawan H, Weerachatyanukul W, Tawipreeda P, Withyachumnarnkul B, Pratoomchat B, Chavadej J, Sobhon P. Molecular modification of *Penaeus monodon* sperm in female thelycum and its consequent responses. Mol Reprod Dev. 2004 Nov;69(3):356-363.

127. Vijayan K, Diwan A. Influence of temperature, salinity, pH and light on molting and growth in the Indian white prawn *Penaeus indicus* (Crustacea: Decapoda: Penaeidae) under laboratory conditions. Asian Fish Sci. 1995;8: 63-72.

128. Waddy SL, Aiken DE. Timing of metamorphosic molt of the American lobster (*Homarus americanus*) is governed by a population-based, photoperiodically entrained daily rhythm. Can J Fish Aquat Sci. 1999;56(12):2324-2330.

129. Wainwright G, Webster SG, Wilkinson MC, Chung JS, Rees HH. Structure and significance of mandibular organ-inhibiting hormone in the crab, *Cancer pagurus*. Involvement in multihormonal regulation of growth and reproduction. J Biol Chem. 1996 May 31;271(22):12749-12754.

130. Wang F, Dong S, Dong S, Huang G. Effects of photoperiod on the moulting and growth of juvenile Chinese shrimp *Fenneropenaeus chinensis*. Chinese Aqua Sci. 2004a, abstract.

131. Wang F, Dong S, Dong S, Huang G, Zhu C, Mu Y. The effect of light intensity on the growth of Chinese shrimp *Fenneropenaeus chinensis*. Aquaculture 2004b;234:475-483.

132. Wassenberg TJ, Hill BJ. Moulting behaviour of the tiger prawn *Penaeus esculentus* (Haswell). Mar Freshw Res. 1984;35(5):abstract.

133. Watson RD, Spaziani E. Biosynthesis of ecdysteroids from cholesterol by crab Y organs, and eyestalk suppression of cholesterol uptake and secretory activity, *in vitro*. Gen Comp Endocrinol. 1985 Jul;59(1):140-148.

134. Watson RD, Kee KL, Borders KJ, Dircksen H, Lilly KY. Molt-inhibiting hormone immunoreactive neurons in the eyestalk neuroendocrine system of the blue crab, *Callinectes sapidus*. Arthropod Struct Dev. 2001 Oct;30(1):69-76.

135. Webster SG, Keller R. Purification, characterisation and amino acid composition of the putative moult-inhibiting hormone (MIH) of *Carcinus maenas* (Crustacea, Decapoda). J Comp Physiol B Biochem Syst Environ Physiol. 1986 Sep;156(5):617-624.

136. Weis JS. Effect of environmental factors on regeneration and molting on fiddler crabs. Biol Bull. 1976 Feb;150:152-162.

137. Willig A, Keller R. Molting hormone content, cuticle growth and gastrolith growth in the molt cycle of the crayfish *Orconectes limosus*. J Comp Physiol A Neuroethol Sens Neural Behav Physiol. 1973 Dec;86(4):377-388.

138. Wittig K, Stevenson JR. DNA synthesis in the crayfish epidermis and its modification by ecdysterone. J Comp Physiol B Biochem Syst Environ Physiol. 1975 Dec;99(4):279-286.

139. Whiteley NM, Taylor EW, El Haj AJ. Short communication: actin gene expression during muscle growth in *Carcinus maenas*. J Exp Biol. 1992;167(1):277-284.

140. Withyachumnarnkul B, Poolsanguan W. Continuous darkness stimulates body growth of the juvenile giant freshwater prawn, *Macrobrachium rosenbergii* de Man. Chronobiol Int. 1990;7(2):93-97.

141. Withyachumnarnkul B, Plodphai P, Nash G, Fegan D, 2001. Growth rate and reproductive performance of F4 domesticated *Penaeus monodon* broodstock. In: The 3rd National Symposium of Marine Shrimp, November 8-9, Sirikit National Convention Center, Bangkok, Thailand, pp. 33-40

142. Yodmuang S, Udomkit A, Treerattrakool S, Panyim S. Molecular and biological characterization of molt-inhibiting hormone of *Penaeus monodon*. J Exp Mar Biol Ecol. 2004 Nov 25;312(1):101-114.

143. You K, Yang HS, Liu Y, Liu SL, Zhou Y, Zhang, T. Effects of different light sources and illumination methods on growth and body color of shrimp *Litopenaeus vannamei*. Aquaculture 2006; 252:557– 565.

144. Yudin AI, Diener RA, Clark WHJ, Chang ES. Mandibular gland of the blue crab, *Callinectes sapidus*. Biol Bull. 1980 Dec;159:760-772.

145. Ziegler A, Hagedorn M, Ahearn G, Carefoot T. Calcium translocations during the moulting cycle of the semiterrestrial isopod *Ligia hawaiiensis* (Oniscidea, Crustacea). J Comp Physiol B. 2007 Jan;177(1):99-108.

146. Zheng J, Nakatsuji T, Roer RD, Watson RD. Studies of a receptor guanylyl cyclase cloned from Y-organs of the blue crab (*Callinectes sapidus*), and its possible functional link to ecdysteroidogenesis. Gen Comp Endocrinol. 2008 Feb 1;155(3):780-788.

APPENDIX

Visual system and Molting

Compound eye and nervous system. The crustacean central nervous system is consisted of the ganglia and their nerve roots, located in the head, thorax, and abdomen. Dorsally, the brain or supraesophageal ganglia lies just posterior to the base of the anterior head appendages, which has the optic nerve, containing the interneurons and motorneurons to connect between the brain and optic ganglia. Adjacent to the brain is the subesophageal ganglia. Most distally is the ventral nerve cord, which constitutes thoracic and abdominal ganglia.

The optic lobe (Fig. 8-1, upper panel) of shrimps *P. monodon* based on Bell and Lightner (1988) and *Penaeus duorarum* (Elofsson, 1969), comprised of three ganglia, the most proximal medulla terminalis (MT), the medial medulla interna (MI), and the distal medulla externa (ME). The outermost of the eye is the photoreceptor zone called ommatidia (OM), composed of two zones, the proximally ganglionic portion separated by the basement membrane (Bas) from the distally dioptirc portion. The dioptric portion is composed of (proceeding distally); the rhabdoms and retinular cell bodies (Rha), the retinular cell nuclei (Ret), the crystalline tract (Crt), the crystalline cone (Crc), the cone cells (Con), and the outer lying cuticle (Cut). The axon tracts or neuropils organize relative to one another, the outermost is lamina ganglionaris (LG) lying between the ommatidia and ME, the innermost, optic tract connecting brain and MT; however between the medullae, there are the neuropils sending either distally or proximally. The axons of photoreceptor cells or retina terminate in the LG or partially at ME (Sandeman, 1988).

Photoreceptors and dark/light adaptation. A receptor structure comprises of seven retinularcells (Ret) and associated piment granules surround each rhabdom (Rha) (Bell and Lightner, 1988). Penaeid shrimps have a reflecting superposition eye, the rays of light will hit at the mirrors (crystalline cone); then the radial beams (reflect from the mirrors) form an image concentrating at a focus point (Fig. 8-1, lower left) (Land, 2004).
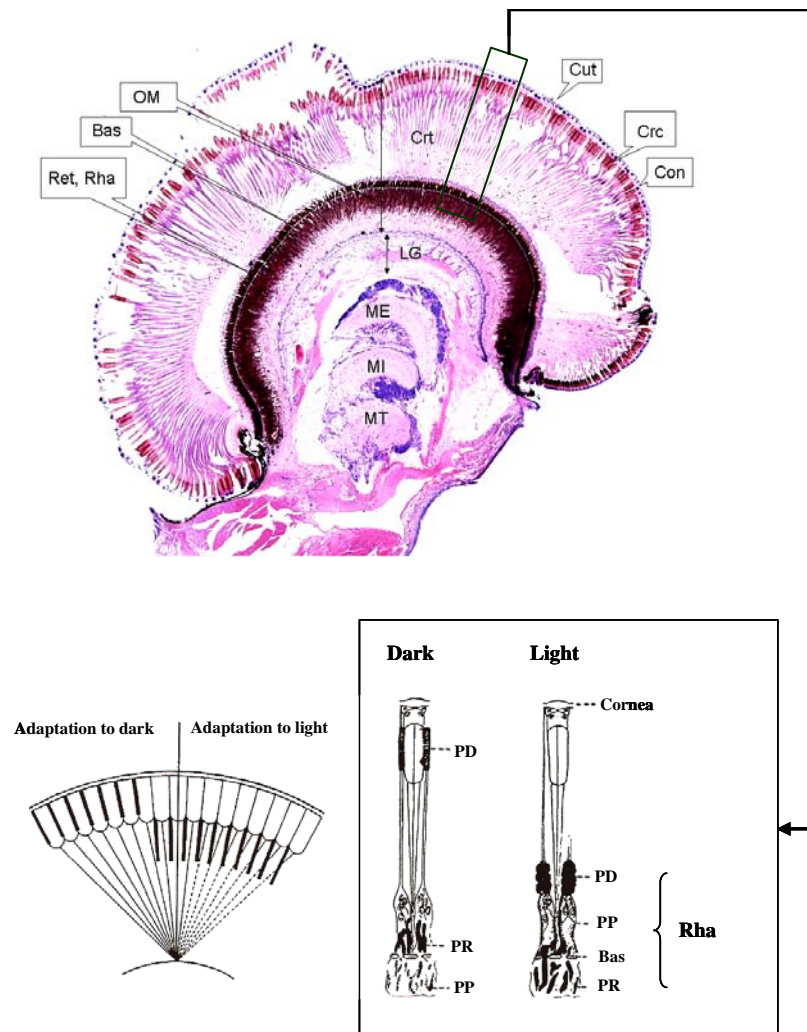
Figure 8-1   Light micrograph showing of the compound eye and photoreceptor portion in *Penaeus monodon* stained with hematoxylin and eosin (based on Bell and Lightner, 1988) (Upper panel). The schematic diagrams represent the mechanism of light/dark adaptation in the shrimp *Palaemonetes* (modified from Land, 2004) (Lower panels)

Abbreviations: PD, distal pigment; PP, proximal pigment; PR, reflecting pigment; Bas, Basement membrane; Rha, rhabdom

In the macruran eyes including the penaeid shrimp, the light/dark adaptation mechanisms are based on extensive pigment migrations. When *Palemonetes* eyes light-adapt, the distal pigment (PD) is withdrawn from a position of the mirror-boxes (crystalline cone) to a region of the clear zone (crystalline tract), distal to the rhabdoms, where it cuts off the oblique rays (Fig. 8-1, lower panel). At the same time, proximal pigment (PP) which believed functioned in visual acuity (de Bruin and Crisp, 1957) moves up from below the basement (Bas). Whereas at dark-adapt, the PD which consist of both reflecting and absorbing material, move out and becomes lining against the wall of the crystalline cone. The PP is retracted to beneath the basement membrane (Bas) and the reflecting pigment (PR) that forms the tapetum, moves into position around the rhabdoms (Land, 2004).

After three months kept in continuous darkness, the arrangement of rhabdom microvilli in crayfishes was markedly distress, and receptor potentials of retinular cells in the eye consisted only of the slow phase; the transmission of visual excitation from rhabdom to retinular cell soma must be possible inappropriate function (Eguchi, 1965). The comparable changes of this organ were also found in crab *Libinia* which exposed to either long periods of light (5h of dark) or dark (15h of dark) (Eguchi and Waterman, 1967). The implication of photoreceptor is not fundamental only for vision yet its function correlates to neurosecretion is quite crucial.

Neurosecretion and light. The secretion of X organ cell hormones is known to undergo spontaneous changes during the 24-hr cycle. The release of hormones or the electrical activity called electroretinogram (ERG), the massed electrical response of the retina to brief flashes of light (http://www.e-advisor.us/electrophysiology/erg.php) of X organ neurons is regulated by environmental and endogenous influences, such as light and darkness, stress, and circadian rhythms. These influences appear to be mediated by a host of neurotransmitters/modulators. These mediators acts upon a definite ionic substrate(s) and exerts specific regulatory effects on X organ cell activity. A given neuron may be under the control of more than one neurotransmitter, and a transmitter may mediate

different and even opposite influences on different neurons (Garćia and Aŕechiga 1998).

Nevertheless, there is no evidence that light can directly stimulates XO cells but it modulated the electrophysiological activities of these NSCs by illumination through the retina cells that subsequently followed the synaptic connection to the XOSG. As observed in the experiments of retinal illumination, the light of intensity ~100 lux with 0.5 ms pulse was applied to applied to the retina zone of crayfishes *Pacifastacus,* then moved along the proximal region toward the MTXO, the excitatory response of NSCs was seen only when exposed light to the retina. Light usually induced the burst action potential (at cell body of neuron) or slow with occasionally inhibitory response (hyperpolarization) obtained from the axon (Glantz et et al., 1983).

De Bruin GHP, Crisp DJ. The Influence of pigment migration on vision of higher crustacea. J Exp Biol. 1957;34(4):447-463.

Elofsson R. The development of the compound eyes of *Penaeus duorarum* (Crustacea: Decapoda) with remarks on the nervous system. Z Zellforsch Mikrosk Anat. 1969;97(3):323-50

Eguchi E. Rhabdom structure and receptor potentials in single crayfish retinular cells. J Cell Physiol. 1965 Dec;66(3):411-29.

Eguchi E, Waterman TH, Changes in retinal fine structure induced in the crab Libinia by light and dark adaptation. Z Zellforsch Mikrosk Anat. 1967;79(2):209-29

García U, Aréchiga H. Regulation of crustacean neurosecretory cell activity. Cell Mol Neurobiol. 1998 Feb;18(1):81-99. Review.

Glantz RM, Arechiga H. Light input to crustacean neurosecretory cells. Brain Res. 1983 Apr 18;265(2):307-11.

Land MF. Eyes and Vision. In: Forest J, von Vaupel Klein JC, editors. The Crustacea. Leiden: Brill Academic Publishers; 2004. p. 257-299.; 2004.

Sandeman DC. Atlas of serotonin-containing neurons in the optic lobes and brain of the crayfish, *Cherax destructor.* J Comp Neurol. 1988 Mar 22;269(4):465-78.

BIOGRAPHY

NAME	Miss Wisa Namwong
DATE OF BIRTH	October 15, 1970
PLACE OF BIRTH	Phichit, Thailand
INSTITUTIONS ATTENDED	Chiang Mai University, 1989-1992
	Bachelor of Associated Medical Science
	(Physical therapy)
	Mahidol University, 2000-2002
	Master of Science (Anatomy)
	Mahidol University, 2003-2009
	Doctor of Philosophy (Anatomy)
HOME ADDRESS	60 Moo 6 Wungwha, Taphanhin,
	Phichit, 66110, Thailand
E-MAIL ADDRESS	namwong2006@gmail.com
RESEARCH GRANT	The Ministry on Higher Education, Thailand.